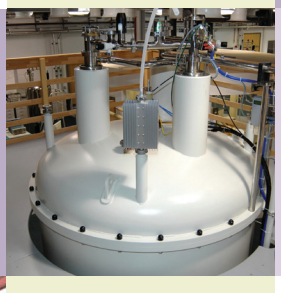

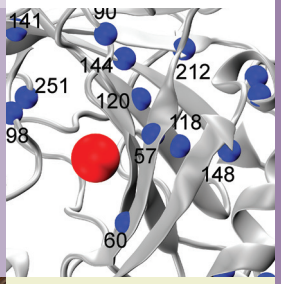

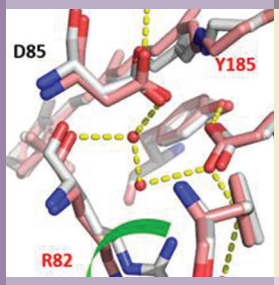

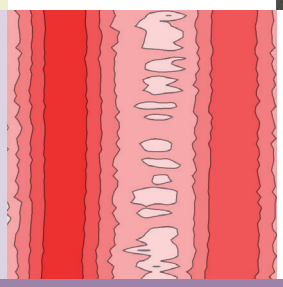

The UK 850 MHz Solid-State NMR Facility

Annual Report 2015

The UK 850 MHz Solid-State NMR Facility

In **6** years of operation:

1816 days have been allocated to

48 PIs from **23** different UK institutions

with **2666** days being requested.

Attendees at the 2015 Annual Symposium that took place at the University of Warwick on Thursday 26th March.

Contents

Introduction

This sixth annual report of the UK 850 MHz Solid-State NMR Facility corresponds to the start, as of January 2015, of new funding via a contract subject to a service level agreement signed with UKSBS (Shared Business Services). This contract is to operate a high-field solid-state NMR facility on behalf of the UK community for a period of three plus two years, with funding provided by EPSRC with a contribution from BBSRC. Under this new funding mechanism, we welcome Phil Williamson from the University of Southampton to the renamed Facility Executive, increasing expertise in biological solid-state NMR. The Facility Executive also now has a named Director and Deputy Director. In addition, as described on page 4, there is a new Oversight Committee that is an expansion of the International Advisory Board with the Chair from UK industry and two user representatives. The performance of the Facility is evaluated annually by EPSRC's Capital Equipment Strategic Advisory Team – in the 2015 evaluation, the Facility scored five out of six with an overall comment: "This is a high performing service, providing excellent support for their user base." Pages 57 to 61 of this report corresponds to content that will be submitted for this year's reporting procedure for EPSRC-funded mid-range facilities.

The use of high magnetic fields in NMR spectroscopy brings increases in both sensitivity and resolution, and so the 850 MHz Facility enables experiments to be performed that are impossible at lower fields. Since its inception, the Facility has proved a valuable shared resource for the UK science community, with visiting researchers from 23 different institutions using the 850 MHz spectrometer for solid-state NMR studies in a range of disciplines, including chemistry, material science, Earth sciences, biology and physics.

At the fifth annual symposium in 2015, there were over 60 registered participants with 10 talks by postgraduate students, postdoctoral researchers and principal investigators from 8 different institutions. This meeting provides an excellent opportunity for the user community to discuss new advances in solid-state NMR and its applications; we are pleased to see new collaborations being established in this way. The meeting is also well attended by graduate students in the field, thus giving them a forum to see the wider scope of solid-state NMR research and meet their peers.

We hope you enjoy reading about the new and exciting science taking place at the UK 850 MHz Solid-State NMR Facility, and we look forward to welcoming both new and experienced users during the next year.

Further details of the Facility can be found on our website:
http://go.warwick.ac.uk/850mhz/

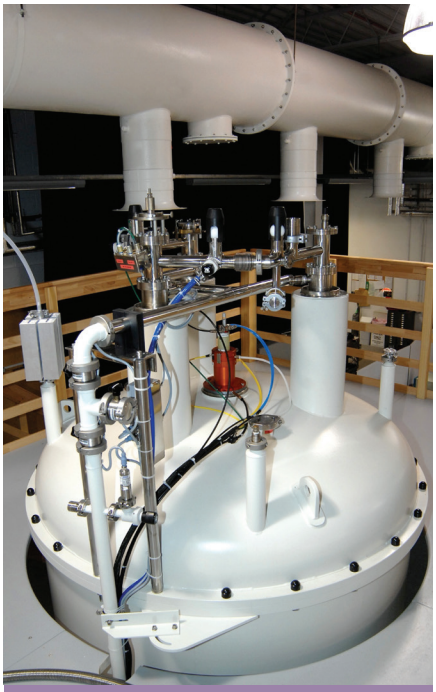

The Facility Executive

Sharon E Ashbrook
(St Andrews)

Steven P Brown
(Director, Warwick)

Melinda J Duer
(Cambridge)

Ray Dupree
(Warwick)

Mark E Smith
(Lancaster)

Jeremy J Titman
(Deputy Director, Nottingham)

Philip T F Williamson
(Southampton)

Stephen Wimperis
(Lancaster)

Organization and management of the Facility

The UK 850 MHz Solid-State NMR Facility is funded (from 2015 for three plus two years) via the award of a contract subject to a service level agreement. The eight investigators for whom PI time is funded by the contract comprise the Facility Executive (FE), which determines the strategic objectives for the Facility and the procedures by which these are to be achieved. The FE meets twice a year, communicating informally more frequently as the need arises. The operation of the Facility is the responsibility of the Local Management Team (LMT) comprising the Facility Manager (FM) who is an *ex-officio* member of the FE and the Warwick-based Facility Director. The duties of the Facility Manager include maintaining the instrumentation and assisting visitors with their experiments. The management of the Facility is overseen by an Oversight Committee (OC) which is chaired by an NMR spectroscopist from UK industry (Stephen Byard, Arcinova) and whose membership also comprises two eminent overseas solid-state NMR spectroscopists (Dominique Massiot, Orléans, and Beat Meier, Zurich) and two user representatives (Frédéric Blanc, Liverpool, and Daniel Dawson, St Andrews) as well as the Director and Deputy Director of the Facility. The terms of reference of the FE and OC, the remit of the LMT and the duties of the FM are available on the Facility website.

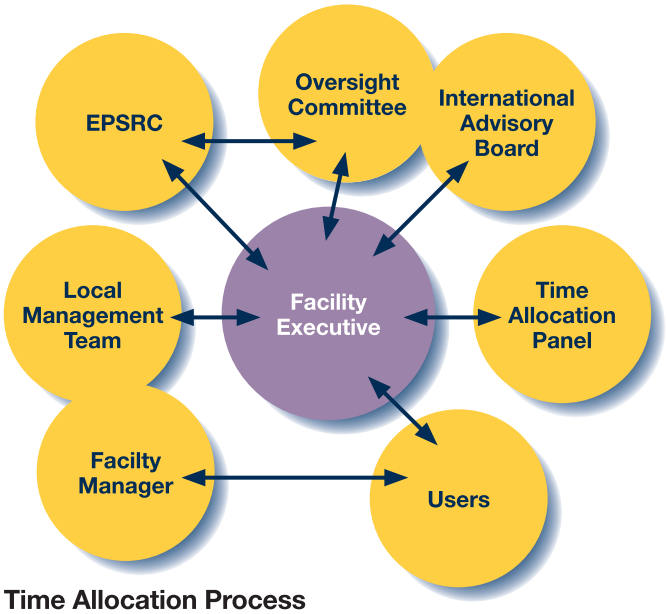

Time Allocation Process

All UK academics who are eligible to apply for Research Council funding, as well as UK researchers of similar standing in industry, may apply for an allocation of spectrometer time at the Facility. Users are expected to run their own experiments with the assistance of the Facility Manager, so personnel with previous solid-state NMR experience should be identified to visit the Facility and carry out the research (inexperienced users should contact the Facility Manager in advance, to agree a collaborative arrangement with the Facility Manager relating to the Facility Manager's role in carrying out the experiments). A minimum of 80% of the available time is allocated by an independent Time Allocation Panel (TAP) that comprises three UK scientists, including one member of the FE, as well as the Facility Manager in an *ex-officio* capacity. The balance is allocated by the FE and is used for fast-track applications, measurements referred from the EPSRC solid-state NMR service, the Facility Manager's designated research time, to compensate users who were unable to take up their allocated time because of instrument downtime, and a small number of maintenance days. Members of the TAP normally serve for a two-year term.

There are two allocation rounds each year for time, each covering a six-month period, starting in either January or July, corresponding to deadlines of October 31st and April 30th. Previous users of the Facility are notified of upcoming deadlines by email. Previous time allocations and instructions for applicants are given on the Facility website. The main criterion for allocating time is overall scientific merit, as well as the quality of the case made for high-field solid-state NMR. Where appropriate, the TAP will consider additional factors, such as the quality of publications arising from previous allocations of time and whether the research is supported by peer-reviewed grants or involves students funded by EPSRC or BBSRC. The TAP is charged with ensuring that the balance of the allocated time broadly reflects the research objectives of the Facility and with providing feedback for unsuccessful applicants. During the TAP meeting, the Facility Manager gives advice on the feasibility of the proposed experiments and the spectrometer time required.

The maximum time that can be requested by an individual applicant during any allocation round is 28 days, but this can be split between several applications. It is a condition that the Facility is mentioned in any publication arising wholly or partly from an allocation of time. Furthermore, a user report must be produced by the original applicant no later than the 7th of the month following the end of the specific six-month time-allocation period, i.e., January 7th and July 7th. Applications are not accepted from users who have outstanding reports from previous allocations of time. The code for all NMR pulse sequences implemented by users on the Facility's spectrometer must be deposited in a shared database. If the experiment is a new one, the code will only be made available to other users after the pulse sequence has been published. Reasonable travel costs associated with the use of the facility will be paid to academic users. The Facility rents accommodation on the University of Warwick campus for use by Facility visitors.

TAP membership (2015): Chair: Stephen Wimperis, Glasgow; non-FE members: Paul Hodgkinson, Durham (up to the first round of 2015), Yaroslav Khimyak, East Anglia (for the second round of 2015 onwards), Mark Pfuhl, King's College.

What is the Facility?

UK 850 MHz Solid-State NMR Facility Probes

No	Probe
1	1.3 mm probe HXY (+^{19}F) conventional insert design H13863
2	2.5 mm HXY DBB (double-broadband) H13856
3	2.5 mm HX (+^{19}F) H13889
4	2.5 mm HFX H13894
5	3.2 mm HXY DBB (double-broadband) H13857
6	3.2 mm HXY low E field for biosolids LLC H13900
7	3.2 mm HXY conventional insert design H13888
8	4 mm HXY conventional insert design (+^{19}F) H13694
9	4 mm HX (low gamma) H13892
10	7 mm X (low gamma) H13895
11	Static
12	1 mm HX (produced by JEOL)
13	DOR probe (produced by Samoson group, Tallinn, Estonia)

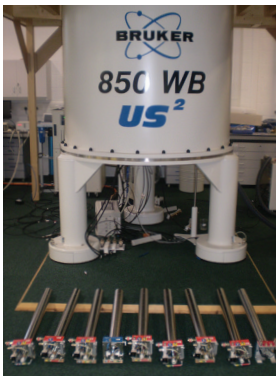

850 MHz spectrometer and probes. Probes 1 to 11 were supplied by Bruker. Maximum MAS frequencies: 4 mm probes 15 kHz; 3.2 mm probes 24 kHz, 2.5 mm probes 35 kHz; 1.3 mm probe 65 kHz. All 3.2 mm and 4 mm MAS probes are equipped with DVT stators and can operate between –140 °C and + 150 °C.

Probe usage 2010 to 2015

Year 1 to Year 6 (Round 1 to Round 12)

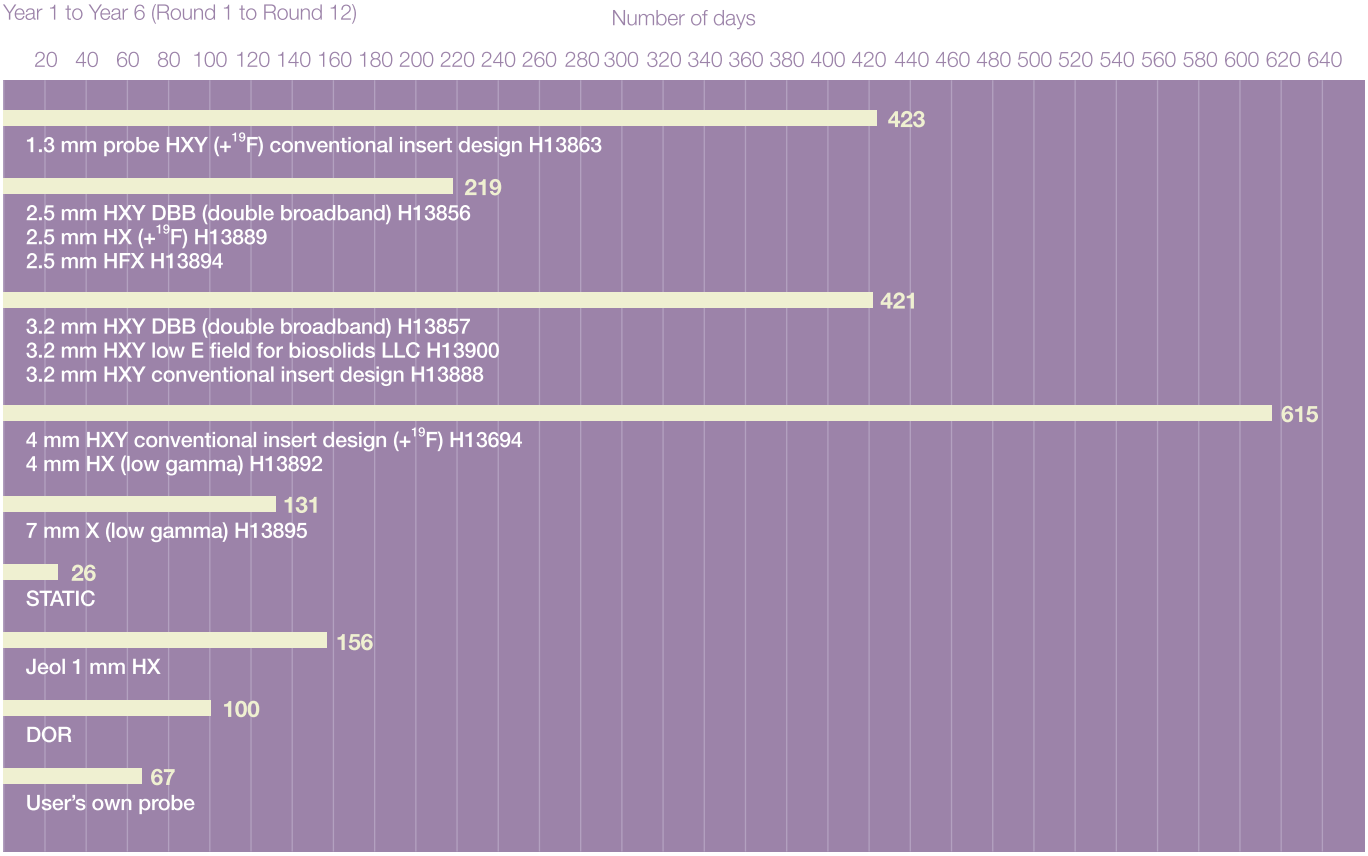

Nuclei tested in Double Resonance Mode

Probe in double Resonance mode	Mode	X-Nucleus: ^{31}P	^{7}Li	^{119}Sn	^{87}Rb	^{11}B	^{71}Ga	^{65}Cu	^{23}Na	^{27}Al	^{13}C	^{79}Br	^{93}Nb	^{45}Sc	^{69}Ga	^{59}Co	^{127}I	^{29}Si	^{77}Se	^{2}H	^{6}Li	^{139}La	^{17}O	^{133}Cs	^{137}Ba	^{15}N	^{35}Cl	^{91}Zr	^{33}S	^{14}N	^{43}Ca	^{95}Mo	^{67}Zn	^{25}Mg	^{89}Y	^{39}K	^{99}Ru	^{87}Sr	^{183}W	^{73}Ge
1.3 mm HXY (+^{19}F)	^{1}H-X ^{19}F-X ●	■	■	★	★	★	■	★	★	★ ■	■	■	■	■	■	★	★	★	★	★	★	★	■	★	★	■	★	★	★	■										
2.5 mm HX (+^{19}F) 2.5 mm HFX 2.5mm HXY DBB	^{1}H-X ^{19}F-X ●	■	★	★	■	★	■	★	★	■ ■	■ ■	■	★	■	■	★	★	★	■	■	★	★	■	★	★	■	★	★	★	■	★	★	★	■	★	■				
3.2 mm HXY low E field for biosolids LLC	^{1}H-X				★	★	★	★	★	★	■	■	★	★	★			★		★	★		★		★	■	★		★	■									
3.2 mm HXY 3.2mm HXY DBB	^{1}H-X				■	■	■	★	■	■	■	■	★	★	★	★	★	■	★	★	★	★	■	★	★	■	■	★	★	■									
4 mm HXY (+^{19}F)	^{1}H-X ^{19}F-X ●	■	★	■	★	★	★	★	■	■	■ ■	■	★	★	★	★	■	■	■	★	★	★	★	★	★	■ ■	★	★	★	★										
4 mm HX (low gamma)	^{1}H-X										■	■	■	★	■	■	★	■	★	■	■	★	■	■	★	■	★	★	■	■	■	★	■	■	■	■	■	■	★	★
7 mm X (low gamma)	X																						★	★	■	★	■	■	■	■	■	■	★	★	■	■	★	■	■	■
Static	X	■	★	★	★	■	■	■	★	★	■	★	■	★	■	★	★	★	★	■	★	■	★	★	★	★	■	★	★	■	★	★	★	★	★	■	★	★	★	★
DOR	X				■	■	■	★	■	■	★	★	★	★	★	★	★	★	★	★	★	★	■	★	★	★	★	★	★	■	■	★	★	★						
Jeol 1 mm HX	^{1}H-X		■	★	■	★	■	★	■	★	■	★	■	★	★	★	★	★	★	★	★	★	★	★	★	■	★	★	★	■									

■ *Experiments performed at the facility to date*

★ *Bench tests indicate should be possible*

● *Other ^{19}F-X DR combinations have not yet been investigated*

For triple-resonance capabilities, refer to the facility website

Time allocation

431 days requested by 25 PIs from 13 different institutions (Aberdeen, Cambridge, Cardiff, Glasgow, Keele, King's College London, Lancaster, Liverpool, Oxford, Southampton, St. Andrews, University College London and Warwick). 292 days allocated by the Time Allocation Panel.

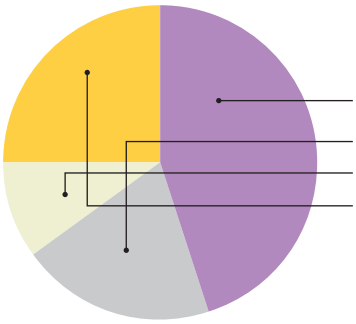

Requested time

Outside Warwick and non FE **45%**
FE outside Warwick **20%**
Warwick FE **10%**
Warwick non FE **25%**

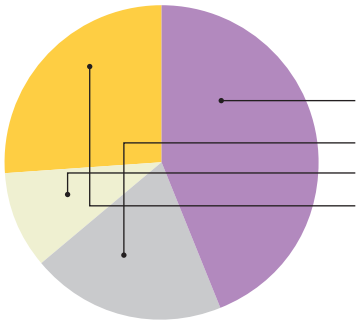

Allocated time

Outside Warwick and non FE **44%**
FE outside Warwick **20%**
Warwick FE **10%**
Warwick non FE **26%**

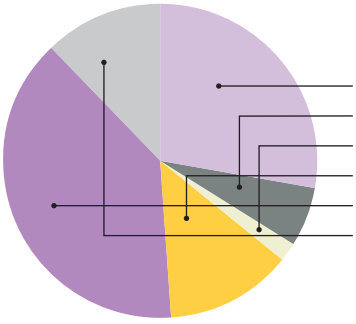

Requested time

Advanced materials **28%**
Bio-materials **6%**
Energy materials **2%**
Methods development **13%**
Proteins **39%**
Pharmaceuticals and self assembly **12%**

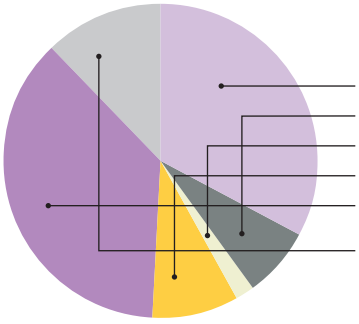

Allocated time

Advanced materials **33%**
Bio-materials **7%**
Energy materials **2%**
Methods development **9%**
Proteins **37%**
Pharmaceuticals and self assembly **12%**

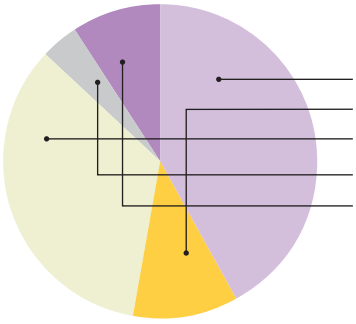

Requested time

EPSRC **42%**
BBSRC **11%**
Other agencies **34%**
Industrial **4%**
No external funding **9%**

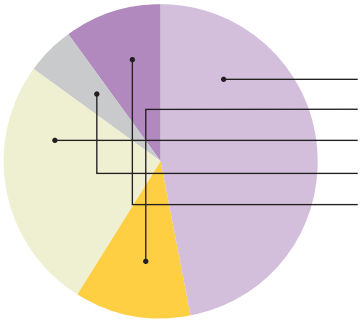

Allocated time

EPSRC **47%**
BBSRC **12%**
Other agencies **26%**
Industrial **5%**
No external funding **10%**

Projects with more than one funding source were counted only once. Other agencies that are funding facility users are: British Heart Foundation, Innovate UK, Leverhulme Trust, Newton International Fellowship, Royal Society, ERC, agencies from Greece, Iraq and Sweden as well as industry (Agilent, BP Chemicals, Bruker, GlaxoSmithKline and Johnson Matthey).

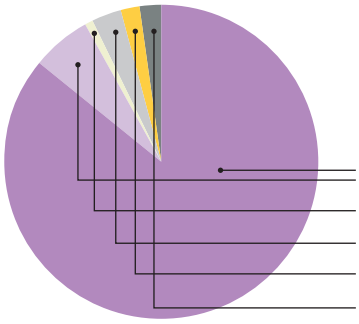

Spectrometer time

5 Jan 2015 – 31 Dec 2015 (the facility operates 24 hours a day, 7 days a week)

TAP allocated days **86%**
Facility manager research **6%**
Maintenance **1%**
Fast track **3%**
Industrial **2%**
Compensation **2%**

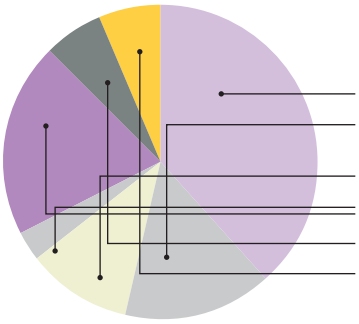

Facility users

5 Jan 2015 – 31 Dec 2015

PIs **25**
EPSRC PhD students* **10**
Other PhD students** **7**
Industrial PhD **2**
PDRAs*** **13**
Research staff **4**
Overseas collaborators **4**

*2 students partially funded by industry

**1 overseas (Iraq), 1 European Union (Marie Curie), 5 UK university funding

***1 BBSRC, 5 EPSRC, 2 Leverhulme Trust, 2 Industrial, 1 Royal Society, 1 European, 1 University

Results from User Questionnaire Jan 2015 – Dec 2015

Facility users are asked to complete feedback questionnaires which contain a series of questions and provide the opportunity for visitors to make comments and suggestions. The responses are graded from 1 (least satisfied) to 5 (most satisfied). The average scores are based on the responses from 19 PIs and 50 visitors for visits over the period January to December 2015.

Section 1 to be completed by the PI

Application for time

1 Ease of application process
2 Transparency of application process
3 Feedback on any unsuccessful time request

Scheduling of time awarded

4 Scheduling of your time by the facility

Overall impact

5 Quality of results obtained

Section 2 to be completed by the visitor

Accommodation

6 Ease of arranging accommodation
7 Quality of accommodation
8 Location of accommodation

At the 850 MHz Facility

9 Support from the Facility Manager upon arrival
10 Support from the Facility Manager throughout your visit
11 Quality of the NMR facilities
12 Quality of the sample preparation area and storage facilities
13 Ease of access to the facility out of hours
14 Your overall time at the facility

Post visit experience

15 Arrangements for accessing data
16 Arrangements for returning any samples
17 Reimbursement of expenses

Average scores from feedback questionnaires over period January to December 2015

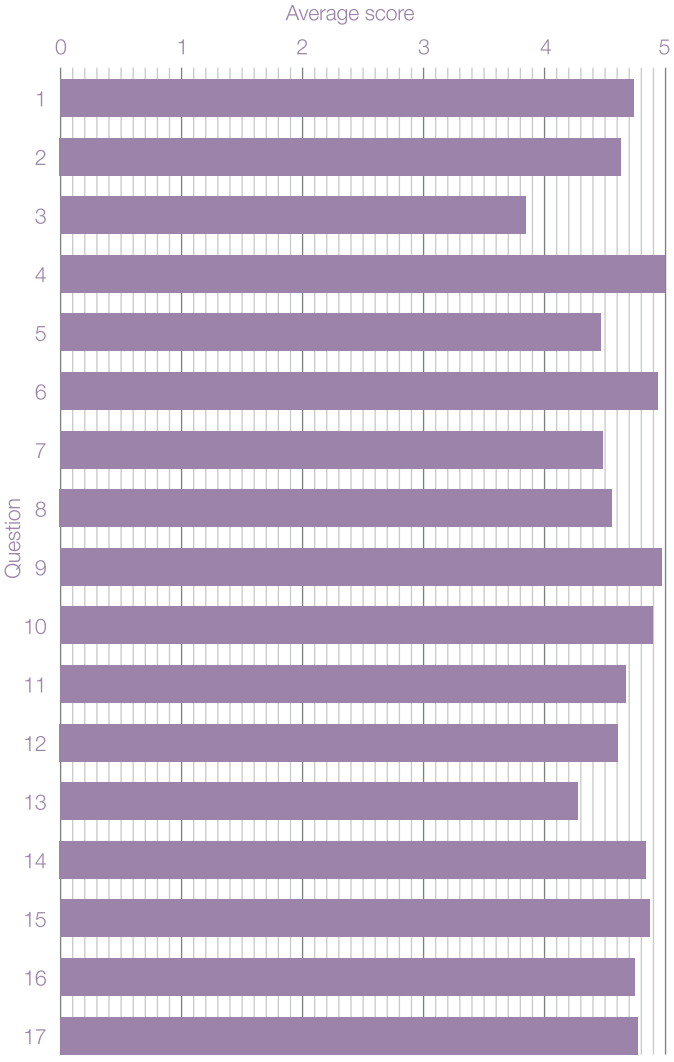

UK 850 MHz Solid-State NMR Facility 5th Annual Symposium

Thursday March 26th 2015
Millburn House
University of Warwick
Symposium Organiser:
Ray Dupree

List of talks

1 *A 3D Experiment that Provides Isotropic Homonuclear Correlation of Half-Integer Quadrupolar Nuclei*
Dinu Iuga (University of Warwick)

2 *Solid-State NMR Studies of the Local Environment of Alkaline Earth Metal Ions in Inorganic and Hybrid Biomaterials*
Danielle Laurencin (Institut Charles Gerhardt de Montpellier, France)

3 *Investigating FAM-N Conversion Pulses for MQMAS*
Henri Colaux (University of St Andrews)

4 *Investigating the Defect Chemistries in Fast Ion Conductors by Solid-State NMR Spectroscopy*
Frédéric Blanc (University of Liverpool)

5 *The UK 850 MHz Solid-State NMR Facility - Future Operation*
Steven Brown (University of Warwick)

6 *Explaining Bone Pathologies: a Multinuclear NMR Spectroscopy Approach Provides a New Model of Bone Mineral*
Melinda Duer (University of Cambridge)

7 *Understanding Self-Assembly Process at Molecular Level: Structure and Function of Guanosine Derivatives*
Manjunatha Reddy (University of Warwick)

8 *ADORable Zeolites and Magnetic MOFs*
Russell Morris (University of St Andrews)

9 *Indirect Detection of Nitrogen-14 in Biological Molecules by Solid-State NMR*
James Jarvis (University of Southampton)

10 *New In-situ NMR Strategies for Monitoring Crystallization Processes*
Kenneth Harris (Cardiff University)

Publications 2015

Intercalation of benzoxaborolate anions in layered double hydroxides, toward hybrid formulations for benzoxaborole drugs. S. Sene, S. Begu, C. Gervais, G. Renaudin, A. Mesbah, M. E. Smith, P. H. Mutin, A. van der Lee, J.-M. Nedelec, C. Bonhomme, D. Laurencin. *Chemistry of Materials*, 27, 1242-1254 (2015).

Coordination Polymers Based on Alkylboronate Ligands: Synthesis, Characterization, and Computational Modelling. D. Berthomieu, C. Gervais, G. Renaudin, M. Reinholdt, S. Sene, M. E. Smith, C. Bonhomme, D. Laurencin. *European Journal of Inorganic Chemistry*, 1182-1191 (2015).

Interplay of Noncovalent Interactions in Ribbon-like Guanosine Self-Assembly: an NMR Crystallography Study. G. N. M. Reddy, A. Marsh, J. T. Davis, S. Masiero, S. P. Brown *Crystal Growth and Design*, 15, 5945-5954 (2015).

Intermolecular Interactions and Protein Dynamics by Solid-State NMR Spectroscopy. J. M. Lamley, C. Öster, R. A. Stevens, J. R. Lewandowski. *Angewandte Chemie International Edition*, 54, 15374-15378 (2015).

Unraveling the complexity of protein backbone dynamics with combined ^{13}C and ^{15}N solid-state NMR relaxation measurements. J. M. Lamley, M. J. Lougher, H. J. Sass, M. Rogowski, S. Grzesiek, J. R. Lewandowski. *Physical Chemistry Chemical Physics*, 17, 21997-22008 (2015).

Combined experimental and computational NMR study of crystalline and amorphous zeolitic imidazolate frameworks. E. F. Baxter, T. D. Bennett, C. Mellot-Draznieks, C. Gervais, F. Blanc, A. K. Cheetham. *Physical Chemistry Chemical Physics*, 17, 25191-25196 (2015).

Measuring ^{19}F shift anisotropies and ^{1}H–^{19}F dipolar interactions with ultrafast MAS NMR. F. Martini, H. K. Miah, D. Iuga, M. Geppi, J. J. Titman. *Journal of Magnetic Resonance*, 259 102-107 (2015).

The contribution of solid-state NMR spectroscopy to understanding biomineralization: Atomic and molecular structure of bone. M. J. Duer. *Journal of Magnetic Resonance*, 253, 98-110 (2015).

Structure and properties of binder gels formed in the system $Mg(OH)_2$–SiO_2–H_2O for immobilisation of Magnox sludge. S. A. Walling, H. Kinoshita, S. A. Bernal, N. C. Collier, J. L. Provis. *Dalton Transactions*, 44, 8126-8137 (2015).

^{14}N overtone NMR under MAS: signal enhancement using symmetry-based sequences and novel simulation strategies. I. M. Haies, J. A. Jarvis, H. Bentley, I. Heinmaa, I. Kuprov, P. T. F. Williamson, M. Carravetta. *Physical Chemistry Chemical Physics*, 17, 6577-6587 (2015).

Characterisation of magnesium potassium phosphate cements blended with fly ash and ground granulated blast furnace slag. L. J. Gardner, S. A. Bernal, S. A. Walling, C. L. Corkhill, J. L. Provis, N. C. Hyatt. *Cement and Concrete Science*, 74, 78-87 (2015).

Unusual Intermolecular "Through-Space" J Couplings in P–Se Heterocycles. P. Sanz Camacho, K. S. Athukorala Arachchige, A. M. Z. Slawin, T. F. G. Green, J. R. Yates, D. M. Dawson, J. D. Woollins, S. E. Ashbrook. *Journal of the American Chemical Society*, 137, 6172-6175 (2015).

Synthesis and characterisation of an open-cage fullerene encapsulating hydrogen fluoride. A. Krachmalnicoff, R. Bounds, S. Mamone, M. H. Levitt, M. Carravetta, R. J. Whitby. *Chemical Communications*, 51, 4993-4996 (2015).

Comparisons with Amyloid-β Reveal an Aspartate Residue That Stabilizes Fibrils of the Aortic Amyloid Peptide Medin. H. A. Davies, J. Madine, D. A. Middleton. *Journal of Biological Chemistry*, 290, 7791-7803 (2015).

Probing the Molecular Architecture of Arabidopsis thaliana Secondary Cell Walls Using Two-and Three-Dimensional ^{13}C Solid State Nuclear Magnetic Resonance Spectroscopy. R. Dupree, T. J. Simmons, J. C. Mortimer, D. Patel, D. Iuga, S. P. Brown, P. Dupree. *Biochemistry*, 54, 2335-2345 (2015).

A NMR Crystallography Study of the Hemihydrate of 2′, 3′-O-Isopropylidineguanosine. G. N. M. Reddy, D. S. Cook, D. Iuga, R. I. Walton, A. Marsh, S. P. Brown. *Solid State Nuclear Magnetic Resonance*, 65, 41-48 (2015).

Computational Identification and Experimental Realisation of Lithium Vacancy Introduction into the Olivine $LiMgPO_4$ L. Enciso-Maldonado, M. S. Dyer, M. D. Jones, M. Li, J. L. Payne, M. J. Pitcher, M. K. Omir, J. B. Claridge, F. Blanc, M. J. Rosseinsky *Chemistry of Materials*, 27, 2074-2091 (2015).

Characterization of the Dynamics in the Protonic Conductor CsH_2PO_4 by ^{17}O Solid-State NMR Spectroscopy and First-Principles Calculations: Correlating Phosphate and Protonic Motion. G. Kim, J. M. Griffin, F. Blanc, S. M. Haile, C. P. Grey *Journal of the American Chemical Society*, 137, 3867-3876 (2015).

Monitoring the evolution of crystallization processes by in-situ solid-state NMR spectroscopy. K. D. M. Harris, C. E. Hughes, P. A. Williams. *Solid State Nuclear Magnetic Resonance*, 65, 107-113 (2015).

New In-Situ Solid-State NMR Techniques for Probing the Evolution of Crystallization Processes: Pre-Nucleation, Nucleation and Growth. C. E. Hughes, P. A. Williams, V. L. Keast, V. G. Charalampopoulos, G. R. Edwards-Gau, K. D. M. Harris. *Faraday Discussions*, 179, 115-140 (2015).

In addition, users reported 60 talks and 33 posters at conferences and seminars in 2015, where results obtained at the UK 850 MHz Solid-State NMR Facility were presented.

Theses 2015

Student	Department	University	Supervisor	Title	Date
PhD Theses					
Martin Peel	Chemistry	St Andrews	Sharon E. Ashbrook and Philip Lightfoot	*'A Crystallographic Study of Group 1 Niobate Perovskites'*	Jan 2015
Robert T. Kelly	Life Sciences	Warwick	Steven P. Brown and Oleg N. Antzutkin	*'Investigating the Structure of Amyloid Aggregates using Solid-State Nuclear* Magnetic Resonance'	Feb 2015
John P. Corley	Chemistry	Liverpool	Frédéric Blanc	*'Investigating the Conductivity Pathway of Na-doped $SrSio_3$ Using Solid-State NMR'*	Jun 2015

The UK 850 MHz Solid-State NMR Facility PhD Travel Fund

Supported by Bruker

The UK 850 MHz Solid-State NMR Facility PhD travel fund supported by Bruker provides funding for: (a) attendance at an internationally recognised, high-profile conference where a PhD student presents results he/she obtained at the 850 MHz Facility, or (b) a "start-up" visit to another lab to learn new methods to be implemented at the 850 MHz Facility. For further details see: **http://go.warwick.ac.uk/850mhz/travel_fund/**

2015 Awards

Ibraheem Haies (University of Southampton) awarded £1000 to attend the 56th Experimental Nuclear Magnetic Resonance Conference in Asilomar, Pacific Grove, California, USA (April 2015) and give a talk entitled *High Resolution Overtone ^{14}N NMR.*

James Jarvis (University of Southampton) awarded £1000 to attend the 56th Experimental Nuclear Magnetic Resonance Conference in Asilomar, Pacific Grove, California, USA (April 2015) and give a talk entitled *An Efficient Solid State NMR Method for Characterisation of ^{14}N Sites by Indirect Detection in Biological Samples.*

Giulia Bignami (University of St Andrews) awarded £900 to attend the 9th Alpine Conference on Solid-State NMR Chamonix Mont-Blanc, France (September 2015) and present a poster entitled *Solid-State NMR Characterisation of ^{17}O- and ^{29}Si-Enriched UTL-Derived Zeolites*

Paula Sanz Camacho (University of St Andrews) awarded £400 to attend the, 9th Alpine Conference on Solid-State NMR Chamonix Mont-Blanc, France (September 2015) and present a poster entitled *Investigating J couplings in crowded frameworks*

User comments

"By combining high-field measurements with in-house data, we were able to determine the number of crystallographically-distinct Cu species in a series of Cu(I) cyanide coordination polymers. This information has enabled us to determine their crystal structures (which could not be determined from powder diffraction measurements alone)."

Sharon E. Ashbrook, University of St Andrews

"The ^{14}N results we collected using the 850 MHz Facility firstly would not have been possible using our group's spectrometer due to probe configuration and secondly the higher field gave significant improvement in resolution highlighting additional resonances that may not have been observed at lower field strengths."

Richard J. Darton, Keele University

"We obtained superb ^{43}Ca MAS and DOR spectra that are shedding light on the complexity of defective mineral phases in bone. ^{43}Ca spectra of this resolution are simply not obtainable at lower fields."

Melinda J. Duer University of Cambridge

"The UK 850 MHz Solid-State NMR Facility provides unique opportunities to expand the application of solid-state NMR in new directions. For example, access to this facility has been pivotal in our recent development of in-situ solid-state NMR techniques for understanding the time-evolution of crystalline processes."

Kenneth D. M. Harris, Cardiff University

Service Level Agreement 2015 Performance

Query Log

Respond to query within 5 working days: 99.6% (317 queries)
(green >99%; amber between 90 and 99%; red <90%)

Credit Control Contact and Account Manager Contact

Respond to query within 5 working days: N/A (no queries)
(green >90%; amber between 80 and 90%; red <80%)

Percentage Downtime of Total Available Time within Period: 3.8%*

(green <10%; amber between 10 and 20%; red >20%)
*This includes maintenance days and compensation days

Number of University / Research Groups Involved:

1st TAP period: 19 PIs from 11 universities (10 Chemistry, 3 Physics, 2 Biochemistry, 1 Biological Sciences, 1 Cell and Molecular Biophysics, 1 Earth Sciences, 1 Physical and Geographical Sciences)
2nd TAP period: 18 PIs from 9 universities (13 Chemistry, 3 Physics, 1 Biochemistry, 1 School of Medical Sciences)

Number of Customer Complaints and Response Time: 0 complaints

3 working days for first response. 10 working days to resolve issue: N/A
(green >95%; amber between 90 and 95%; red <90%)

User Satisfaction Scores (average)*:

4.68 (for visitors, after each visit, 50 responses) and 4.54 (for PIs, annually, 19 responses)
(green >4; amber between 3 and 4; red <3)
*see page 8 of report for detailed breakdown of questionnaire responses

Time Allocation Panel (sum over 2 rounds):

Number of applications made: 57
Number of applications awarded time (including partial award of time): 53
Number of access days requested: 431
Number of access days awarded: 292

Percentage of Access Requests Responded to within Stated Window: 100%

Respond within 10 working days of the TAP meeting
(green >95%; amber between 90 and 95%; red <90%)

Dissemination activity: 1 (annual symposium, see page 9)

Minimum one per year

Number of publications: 20

(9 have an author from the Facility Executive; 5 have an author from the host organisation; 9 are for all other users, i.e., have neither an author from Facility Executive nor from the host organisation)
(green 15+; amber between 10 and 14; red <10)

Number of Research Outputs (including talks and posters): 93

(green 50+; amber between 30 and 50; red <30)

Binding of Curcumin to Amyloid-β Oligomers

Oleg N. Antzutkin,[1,2] Józef R. Lewandowski,[3] Dinu Iuga,[1] Nikita V. Shtyrlin,[4] Roman S. Pavelyev,[4] and Andrei V. Filippov[2]

[1]*Department of Physics, University of Warwick*

[2]*Chemistry of Interfaces, Luleå University of Technology, Luleå, Sweden*

[3]*Department of Chemistry, University of Warwick*

[4]*Scientific and Educational Centre of Pharmaceutics, Kazan Federal University, Russian Federation*

Overview

One of the well-known antioxidants and inhibitors of amyloidosis is a natural compound curcumin (see Figure 1 left) present in large quantities in *Turmeric* roots, traditional Indian spices. It has been reported that curcumin and its analogues are prone to bind to Alzheimer's amyloid-β plaques and fibrils.[1-3] Previous solid-state NMR studies have already revealed that curcumin strongly and specifically interacts with $A\beta_{(1-42)}$ fibrils: chemical shifts of residues of predominantly hydrophobic regions of $A\beta_{(1-42)}$ (Val12, Leu17-Ala21)[2] or (Val12, D23, L34)[3] in fibrils are altered by the methoxy- and hydroxyl groups of curcumin. Interestingly, though a number of groups have reported on binding of curcumin to Aβ fibrils[2,3] and binding of curcumin analogues to Alzheimer's amyloid plaques,[1] no site-specific NMR studies on binding of curcumin to the most neurotoxic species of Aβ, oligomers and protofibrils, were yet performed, probably, because of the transient nature and structural diversity of oligomers and a high level of polymorphism of protofibrils and amyloid fibrils, usually all coexisting in the same NMR sample.

A decade ago, β-sheet rich stable oligomers and protofibrils of model Alzheimer's $A\beta_{(1-42)}$cc and $A\beta_{(1-40)}$cc peptides were stabilised by the specific double mutation (A21C and A30C) followed by intramolecular cysteine-cysteine cross-linking.[4] These variants of Aβcc are "arrested" at the oligomer/protofibril state, i.e. they cannot form amyloid fibrils.[4,5] This is because of the 0.5 nm steric restriction (the Cys21-Cys30 linker) in the Val12 – Val40 bend region formed by intermolecular parallel-β sheets in $A\beta_{(1-40)}$ fibrils[6] adopting a *ca.* 1 nm inter-β-sheet space filled with amino acid side-chains. Aβcc and wild-type $A\beta_{(1-42)}$ oligomers have the same size and morphology (from TEM and AFM), similar binding properties to conformation specific antibodies and the ANS dye, similar CD and FT-IR spectra, etc. More importantly, $A\beta_{(1-42)}$cc oligomers exhibit *ca.* 100-fold higher apoptotic caspase-3/7 activity for SH-SY5Y human neuroblastoma cell lines, compared with amyloid fibrils of the wild-type $A\beta_{(1-42)}$.[5] Therefore, Aβcc oligomers are an ideal system for future drug development to prevent Alzheimer's disease, either as antigens for future vaccines, or for testing of substances, which are able to inhibit Aβcc oligomers' nerve cell toxicity and are also able to penetrate the blood-brain-barrier, such as curcumin and its analogues.[1]

Solid-State NMR on ^{13}C-Curcumin Bound to $A\beta_{(1-42)}$cc Oligomers

We recently solved the supramolecular structure of stable $A\beta_{(1-42)}$cc oligomers using a range of multi-dimensional solid-state NMR methods applied to a range of dry, hydrated and 'sedimented-into-rotors' samples of synthetic selectively ^{13}C/^{15}N labelled and recombinant uniformly ^{13}C/^{15}N-enriched $A\beta_{(1-42)}$cc oligomers (see Figure 1 right).[7] As a continuation of this project we address one of the most plausible neurotoxicity hypothesis of Aβ peptides, namely, incorporation of small Aβ oligomers into phospholipid membranes and formation of ion-channels/pores: (i) whether and how curcumin and/or its complexes bind to Aβ oligomers, in particular to a more neurotoxic $A\beta_{(1-42)}$ variant, and (ii) whether and how curcumin and its complexes block Aβ channels/pores in phospholipid membranes. In order to answer on Question (i) we use ^{1}H-detected ultra-fast MAS 2D and 3D ^{1}H-^{13}C correlation NMR spectroscopy on sub-mg amounts of complexes of selectively ^{13}C-labelled curcumin with $A\beta_{(1-42)}$cc oligomers. The 850 MHz Facility with a range of probes for ultra-fast MAS (0.8, 1.0 and 1.3 mm rotor diameters) has proven very useful for this type of experiments, because of the higher sensitivity and improved resolution in both ^{1}H and ^{13}C dimensions. We were able to directly prove that curcumin is binding to $A\beta_{(1-42)}$cc oligomers. Moreover, resonance lines of different keto-enolic forms of ^{13}C labelled curcumin are not overlapping with resonance lines of carbonyl carbons of Aβ making it convenient to study (nonspecific) binding for ^{13}C-curcumin to $A\beta_{(1-42)}$cc oligomers even for the natural abundance ^{13}C in Aβ (see Figure 2). The work on specific site binding using a combination of ^{1}H-detection with ultra-high MAS NMR on samples of selectively labelled ^{13}C-curcumin and ^{13}C/^{15}N labelled $A\beta_{(1-42)}$cc oligomers is currently in progress.

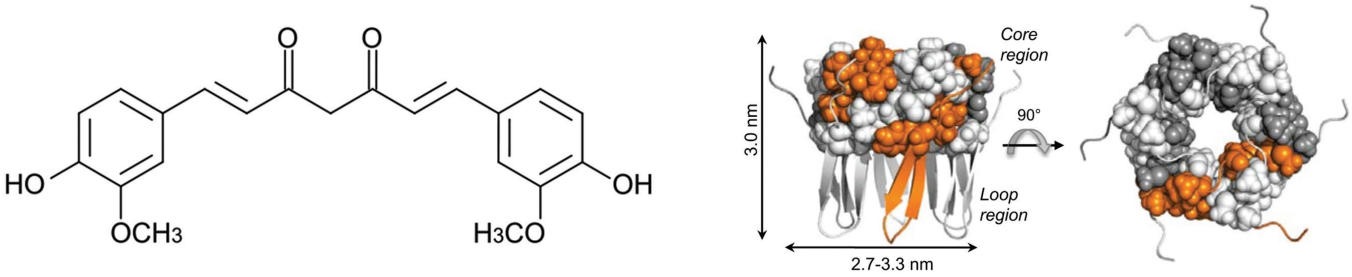

Figure 1. (left) Molecular structure of curcumin present in Turmeric roots; (right) Solid-state NMR structure of hexameric Aβ$_{(1-42)}$cc oligomers (adapted from ref.[7]) showing dimensions of the hexameric barrel with a central pore characteristic for ion-channel-like structures. Side chains of the hydrophobic core are shown as spheres. The two images are rotated by 90° relative to each other.[7]

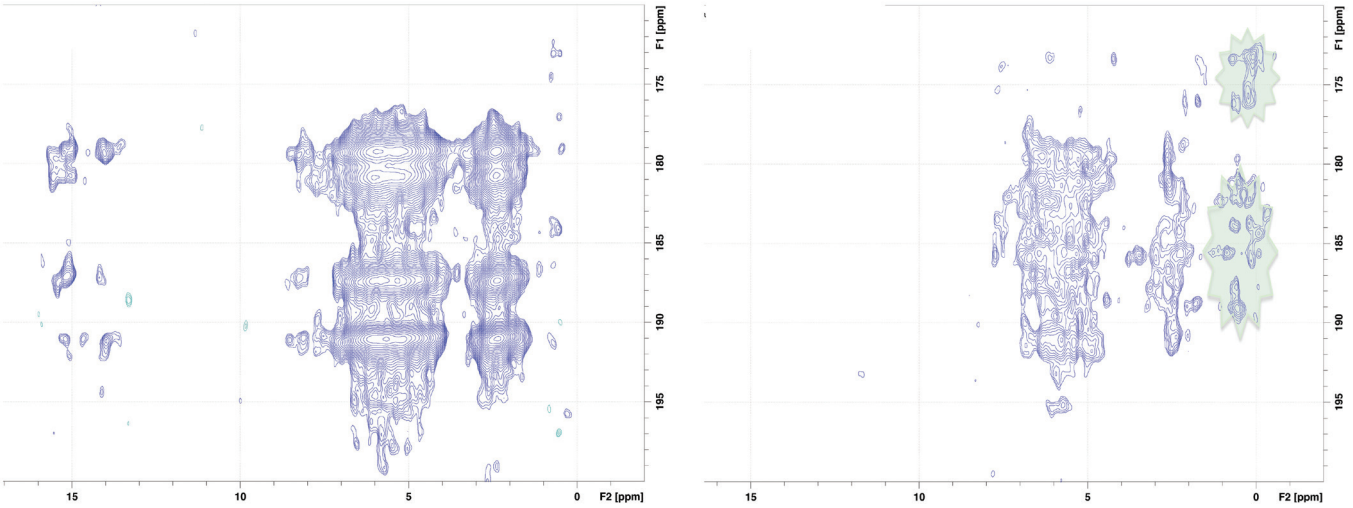

Figure 2. ^{1}H-detected ^{1}H-^{13}C NMR spectra (carbonyl region in ^{13}C) of a sample of ^{13}CO-labelled curcumin prepared in the same buffer solutions and then lyophilised following preparation protocols of Aβ$_{(1-42)}$cc oligomers (left) and a sample of oligomers prepared from Aβ$_{(1-42)}$cc (natural abundance ^{13}C) with ^{13}CO-labelled curcumin (3 to 1 excess of curcumin) (right). NMR spectra were obtained at 20.0 T and 60 kHz MAS using 1.3 mm rotors with RFDR mixing. The green shadowed areas are depicting ^{13}CO NMR signals of Aβ$_{(1-42)}$cc (n.a.) and cross peaks between curcumin and Aβ$_{(1-42)}$cc that suggests binding of curcumin to Aβ$_{(1-42)}$cc oligomers (F_1: ^{13}C-dimension, F_2: ^{1}H dimension).

References

1. Zhang, X.; Tian, Y.; Li, Z.; Tian, X.; Sun, H.; Liu, H.; Moore, A.; Ran, C. *J. Am. Chem. Soc.* **2013**, *135*, 16397.
2. Masuda, Y.; Fukuchi, M.; Yatagawa, T.; Tada, M.; Takeda, K.; Irie, K.; Akagi, K., Monobe, Y.; Imazawa, T.; Takegoshi, K. *Bioorg. Med. Chem.* **2011**, *19*, 5967.
3. Mithu, V. S.; Sarkar, B.; Bhowmik, D.; Das, A. K.; Chandrakesan, M.; Maiti, S.; Madhu, P. K. *J. Biol. Chem.* **2014**,*16*, 11122.
4. Hoyer, W.; Grönwall, C.; Jonsson, A.; Ståhl, S.; Härd, T. *Proc. Natl. Acad. Sci. U.S.A.* **2008**,*105*, 5099.
5. Sandberg, A.; Luheshi, L. M.; Sollvander, S.; de Barros, T. P.; Macao, B.; Knowles, T. P. J.; Biverstål, H.; Lendel, C.; Ekholm-Petterson, F.; Dubnovitsky, A.; Lannfelt, L.; Dobson, C. M.; Härd, T. *Proc. Natl. Acad. Sci. U.S.A.* **2010**, *107*, 15595.
6. Antzutkin, O. N.; Balbach J. J.; Leapman, R. D.; Rizzo, N. W.; Reed, J.; Tycko, R. *Proc. Natl. Acad. Sci. U.S.A.* **2000**, *97*, 13045.
7. Lendel, C.; Bjerring, M.; Dubnovitsky, A.; Kelly, R. T.; Filippov, A.; Antzutkin, O. N.; Nielsen, N. C.; Härd, T. *Angew. Chem. Int. Ed.* **2014**, *53*, 12756.

High-Field $^{63/65}$Cu NMR Study of Cu(I) Coordination Polymers

Daniel M. Dawson,[1] Francesca Grifasi,[2] Michele R. Chierotti[2] and Sharon E. Ashbrook[1]

[1]*School of Chemistry, EaStCHEM and Centre of Magnetic Resonance, University of St Andrews*

[2]*Department of Chemistry, University of Turin, Italy*

Overview

Luminescent coordination polymers (CPs) are an area of active interest, as the chemisorption of small molecules to a CP can alter its luminescence,[1] providing potential applications in molecular sensing. While Cu(I) CPs have not been widely explored relative to other metals, CPs based on CuCN have attracted particular attention. CuCN contains one-dimensional chains of two-coordinate metal centres with bridging cyano ligands.[2] Pure CuCN is weakly luminescent but coordination of nucleophilic ligands shifts the luminescence from the near UV to the visible region, with the intensity increasing by several orders of magnitude. In some cases, small differences in the ligands cause large differences in the emission colours of the CPs. We have synthesised luminescent CPs mechanochemically by grinding CuCN directly with thiourea (tu) and derivatives such as N-methylthiourea (mtu), N-phenylthiourea (ptu), N,N'-diphenylthiourea (dptu) and 2,4-difluorophenylthiourea (fptu). The different steric bulks of these ligands allow tuning of both the luminescence and porosity of the resulting CPs. All of our CPs show a broad excitation feature in the 250–350 nm range, similar to the parent CuCN. Their luminescence is enhanced compared with that of the starting material and all (except CuCN(tu)) exhibit good emission quantum yields of 3–20%. The lifetime of the emissive excited state falls in the μs range (*ca.* three orders of magnitude greater than for CuCN) for all of the CPs.[3]

The main drawback of mechanochemical synthesis is that the products often do not form single crystals of suitable quality for structure determination. While we have obtained structures from single-crystal XRD for CuCN(tu), CuCN(ptu), CuCN(dptu) and CuCN(fptu), the structures of the other compounds must be obtained from powder XRD. Structural solution from powder XRD is possible, but challenging in the absence of prior structural constraints. The process can be greatly facilitated by including information such as the stoichiometry and the number of crystallographically-distinct metal and ligand species present. Solid-state NMR spectroscopy should be capable of determining both the number and coordination modes of the CN ligands, as well as the number and point symmetry of the Cu species. ^{13}C NMR spectra have already revealed the presence of bridging CN ligands, with no terminal CN detected and, here, we aimed to solve the final piece of the puzzle by probing the local environment of the Cu atoms.

Cu has two isotopes ^{63}Cu (I = 3/2, nat. ab. = 69.15%, ν_0 = 225 MHz at 20.0 T) and ^{65}Cu (I = 3/2, nat. ab. = 30.85%, ν_0 = 241 MHz at 20.0 T), both of which can be studied by NMR spectroscopy. The slightly higher ν_0 and lower quadrupole moment (Q_{65Cu}/Q_{63Cu} = 0.93) of ^{65}Cu mean that this nuclide will provide higher resolution but lower sensitivity than ^{63}Cu. However, as the sensitivity of both isotopes is good, there are two probes of every crystallographic Cu site: a fact that can be exploited to determine more accurately the electric field gradient parameters. Here, we present the results of our initial $^{63/65}$Cu NMR spectroscopic characterisation of some of the CuCN-based CPs.

Results

The quadrupolar coupling constants, C_Q, present at the Cu centres in our CPs vary dramatically, from ~0 in $Cu_2I_2(dabco)_2$, **1**, (dabco = 1,4-diazabicyclo[2.2.2]octane), through 13.9 MHz in Cu(SCN)(dabco) form I, **2**, to ~82 MHz for Cu(CN)(mtu) form II, **3.** This makes selecting the appropriate acquisition conditions challenging, as demonstrated by the spectra in Figure 1. The ^{63}Cu NMR spectrum of **1** was recorded at 9.4 T with 10 kHz MAS, with the sharp line (~1 kHz) indicative of relatively high symmetry at the Cu site (*cf.* 480 Hz for CuCl); the ^{65}Cu NMR spectrum of **2** could be recorded with sufficiently rapid (60 kHz) MAS at 20.0 T, while the ^{63}Cu central transition of **3** is 5 MHz wide at 20.0 T and was recorded with a static sample, using frequency-stepped CPMG. An additional challenge when recording these spectra is the signal from the metallic Cu in the coil (2300 ppm) and, for very broad ^{63}Cu resonances, the overlap with the ^{23}Na (*ca.* –2100 ppm relative to CuCl) and ^{27}Al (*ca*. –17000 ppm relative to CuCl) shift ranges. The very large range of C_Q is indicative of a range of coordination geometries from nearly tetrahedral in **1**, where the Cu is in a CuN_2I_2 coordination environment (shown in Figure 1a) to linear for **3** (shown schematically in Figure 1c), where C_Q is close to the ~70-80 MHz determined by Kroeker *et al*. for pure CuCN, in a nuclear quadrupolar resonance (NQR) study.[4]

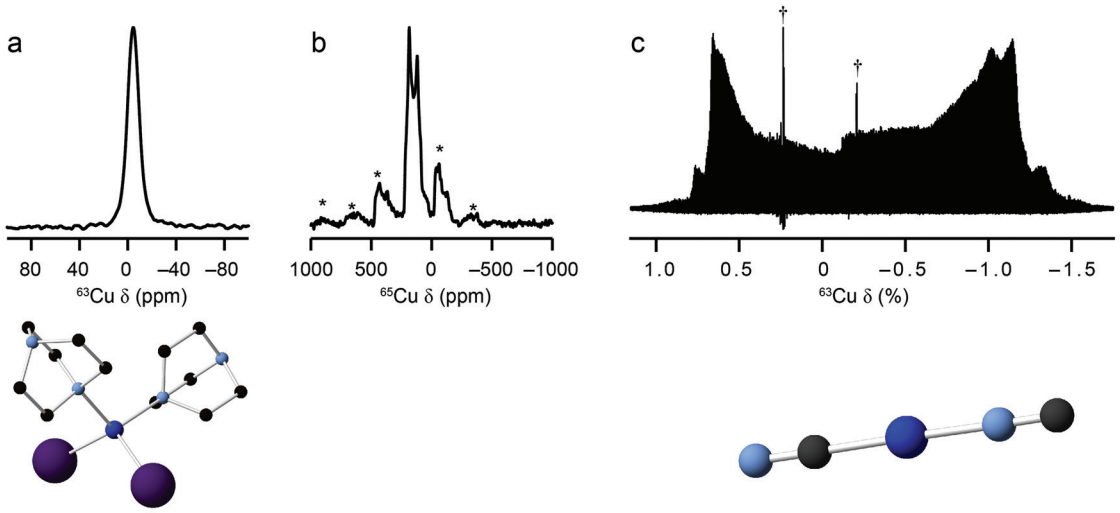

*Figure 1. (a) ^{63}Cu (9.4 T, 10 kHz MAS) NMR spectrum of **1** and the local coordination environment of Cu in this CP, (b) ^{65}Cu (20.0 T, 60 kHz MAS) NMR spectrum of **2**, * indicates spinning sidebands and (c) ^{63}Cu (20.0 T, static frequency-stepped CPMG) NMR spectrum of **3** and a possible linear coordination environment for Cu in this material.* N.B. *the scale for (c) is in %, where 1% = 10000 ppm. † indicates signals from metallic Cu in the coil (0.23%) and an unidentified Na-containing impurity (–0.21%).*

Figure 2 demonstrates the power of recording NMR spectra of both ^{63}Cu and ^{65}Cu in determining the Cu NMR parameters. The wideline $^{63/65}$Cu NMR spectra of Cu(CN)(dptu), **4**, are shown and, while both spectra are dominated by the signal from the coil (owing to small sample volume), the singularities can clearly be distinguished. Analysis, using the QUEST simulation software, indicates that two Cu species are present, with the approximate C_Q and η_Q values shown (neglecting any contributions from the chemical shift anisotropy, which will be determined using lower-field experiments). As we have also previously demonstrated for $^{69/71}$Ga,[5] the ability to probe the same crystallographic sites with two NMR-active nuclei in the same sample is very valuable for more accurately determining their NMR parameters.

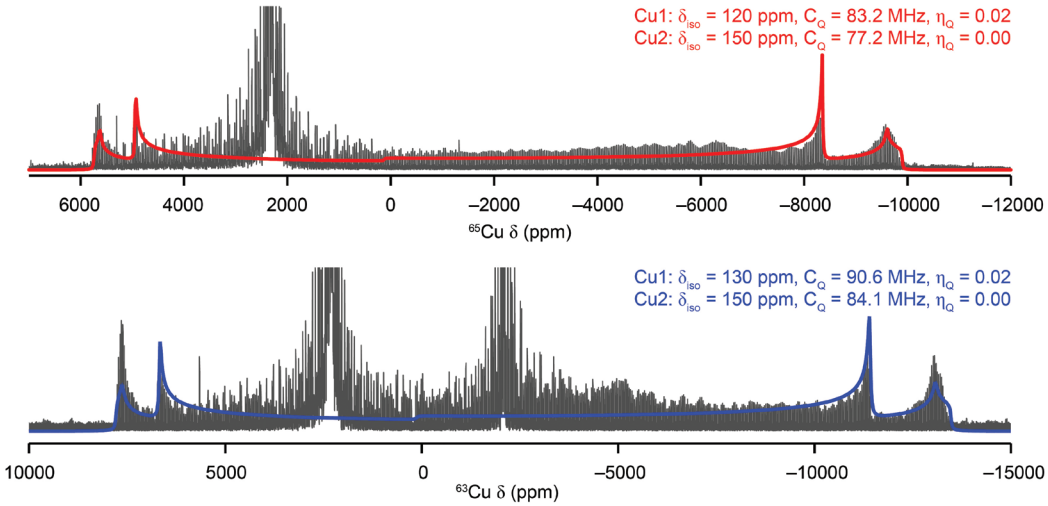

*Figure 2. Static (20.0 T) ^{65}Cu (top) and ^{63}Cu (bottom) WURST-QCPMG NMR spectra of **4** (grey lines) and the corresponding simulated spectra (red and blue lines), using the parameters indicated. Note that the intense signals from metallic Cu (2300 ppm in both spectra) and an unknown Na-containing impurity (–2100 ppm in the ^{63}Cu NMR spectrum) have been truncated vertically.*

References

1. Ropp, R. C. *Luminescence and the Solid State*, 2nd ed.; Elsevier: Amsterdam, **2004.**
2. Bayse, C. A.; Brewster, T. P.; Pike, R. D. *Inorg. Chem.* **2009**, *48*, 174.
3. Miller, K. M.; McCullough, S. M.; Lepekhina, E. A.; Thibau, I. J.; Pike, R. D.; Li,X.; Killarney, J. P.; Patterson, H. H. *Inorg. Chem.* **2011**, *50*, 7239.
4. Kroeker, S.; Wasylishen, R. E.; Hanna, J. V. *J. Am. Chem. Soc.* **1999**, *121*, 1582.
5. Amri, M.; Ashbrook, S. E.; Dawson, D. M.; Griffin, J. M.; Walton, R. I.; Wimperis, S. *J. Phys. Chem. C.* **2012**, *116*, 15048.

High-Field Multinuclear NMR Study of High-Pressure Glasses

Nasima Kanwal,[1] Eleanor R. Mare,[2] Daniel M. Dawson,[1] Andrew J. Berry[2] and Sharon E. Ashbrook[1]

[1]*School of Chemistry, EaStCHEM and Centre of Magnetic Resonance, University of St Andrews*

[2]*Research School of Earth Sciences, Australian National University, Canberra, Australia*

Overview

Magma has been involved in many important geological processes throughout the Earth's history: shaping landforms, transporting and concentrating metals, and enabling the Earth to segregate a metallic core and a silica-rich crust. Many of these processes occur deep in the Earth under high-pressure conditions,[1] and so characterising the structure and properties of magma at high pressure is necessary to understand these processes. Tetrahedrally-coordinated cations in natural silicate magmas convert gradually to have higher coordination with increasing pressure.[2] These coordination changes have been well established for many of the major elements in natural melts,[3] however the coordination behaviour of other major elements, such as Mg, and trace elements, such as Ga, in these melts has never been studied. This is important because trace element partitioning is widely used in the studies of geochemical processes, including the formation of Earth's core.[4] In this work we have attempted to investigate the coordination behaviour of major and trace elements in gallium-doped calcium magnesium aluminosilicate (CMAS) glasses melted under different pressure conditions through ^{25}Mg, ^{27}Al, ^{29}Si and ^{71}Ga MAS NMR along with X-ray absorption near edge spectroscopy (XANES).

^{71}Ga (I = 3/2) and ^{25}Mg (I = 5/2) are quadrupolar nuclei with natural abundance of ~40% and ~10%, respectively. Although these nuclei can be useful probes for investigating the local environment, in each case spectral acquisition can be challenging, owing either to the very broad lines associated with large quadrupolar coupling constants (^{71}Ga) or to a low natural abundance and low Larmor frequency (^{25}Mg). However, due to the inverse dependence of the second-order quadrupolar interaction with the magnetic field strength, higher magnetic fields offer considerable advantages. Further sensitivity improvements can be achieved by using approaches to improve the population difference of the central transition, *e.g.*, double frequency sweeps (DFS) or hyperbolic secant (HS) pulses or the use of Carr-Purcell-Meiboom-Gill (CPMG) echo trains in acquisition.

MAS NMR of High-Pressure Glasses

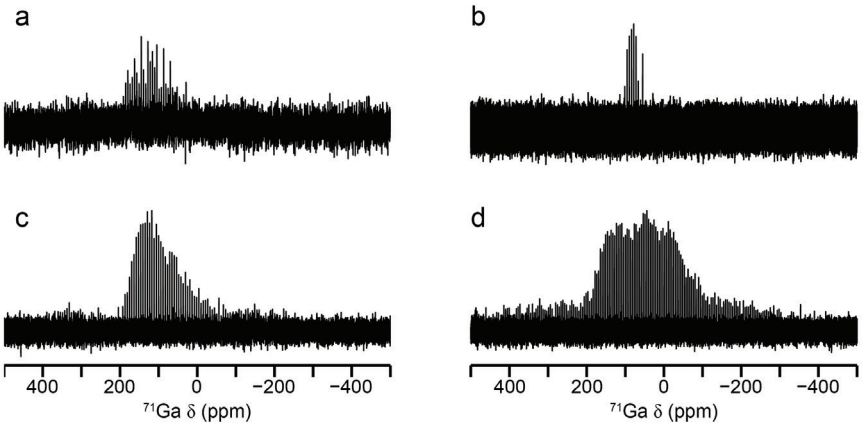

Figure 1. ^{71}Ga (20.0 T, 60-70 kHz MAS) spectra of CMAS glasses prepared using (a) 1 GPa, 1 mol% Ga_2O_3, (b) 5 GPa 2.5 mol% Ga_2O_3, (c) 0 GPa 9 mol% Ga_2O_3 and (d) 5 GPa 9 mol% Ga_2O_3.

Figure 1 shows ^{71}Ga spectra of different CMAS glass samples acquired at 20.0 T. Figures 1a and b concern samples with low Ga_2O_3 content (1 or 2.5 mol%) melted at 1 and 5 GPa, respectively. The broad line with overlapping resonances in the low-pressure sample confirms the presence of 4-, 5- and 6-coordinate Ga species, whereas the narrow line observed in the sample prepared at 5 GPa shows only 4-coordinate Ga is present. For the samples with higher Ga_2O_3 content (9 mol%) melted at 0 and 5 GPa, in Figures 1c and d, respectively, 4-, 5- and 6- coordinate Ga is present in both samples. It can be seen that the Ga coordination number

in samples prepared at higher pressure increases with the Ga content. The sample melted at 5 GPa with the lower Ga content (1 mol%) shows a decrease in the average coordination number compared to the sample melted at lower pressure, whereas the reverse is true for the sample with the higher Ga content. This correlates with the change in coordination of Al (a major component of the glass), as shown in Figure 2. Al adopts a four-fold coordinated environment in samples prepared at low pressure (Figures 2a and c), with 4-, 5- and 6-coordinate Al observed in the samples prepared at higher pressure (Figures 2b and d). A higher percentage of 4- and 5-coordinate species is seen in the high-pressure sample with the higher Ga content.

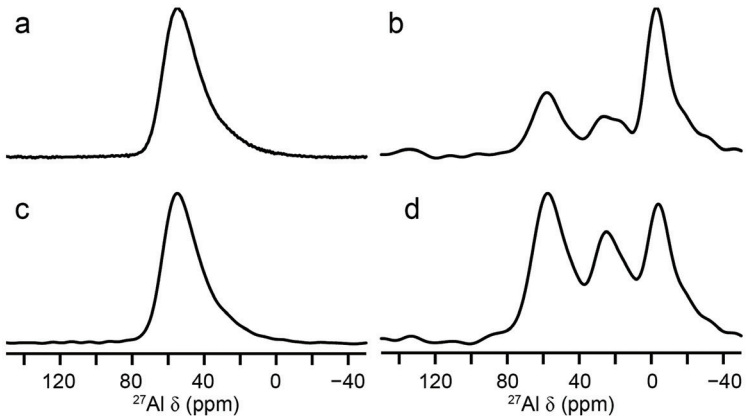

Figure 2. ^{27}Al (14.1 T, 20 kHz MAS) spectra of CMAS glasses prepared using (a) 0 GPa, 1 mol% Ga_2O_3, (b) 5 GPa 1 mol% Ga_2O_3, (c) 0 GPa 9 mol% Ga_2O_3 and (d) 5 GPa 9 mol% Ga_2O_3.

Figure 3a shows ^{25}Mg CPMG MAS spectra of the CMAS glasses acquired at 20.0 T. The lineshape for the different samples is very similar, suggesting that the coordination environment of Mg does not change significantly with the change in pressure. Figure 3b shows analytical fits of the ^{25}Mg CPMG MAS spectra of 2.5 GPa sample acquired at 20.0 and 9.4 T. The chemical shift from the fitted spectra (45 ppm) possibly indicates a tetrahedral environment for Mg, with moderate C_Q.

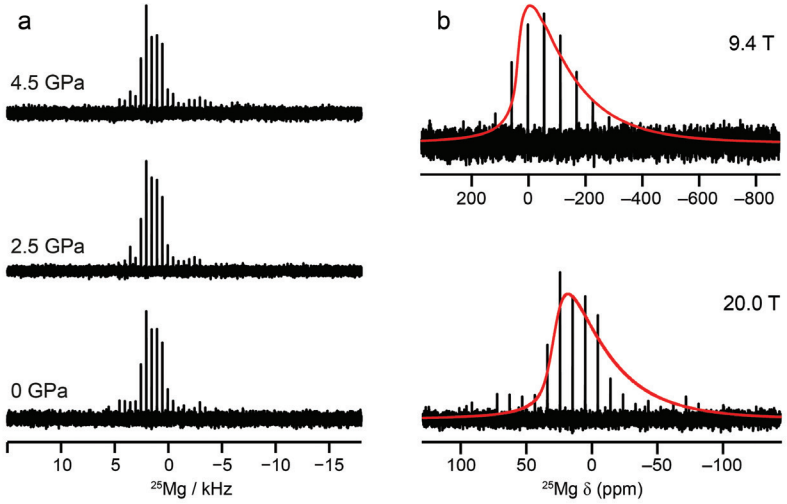

Figure 3. (a) ^{25}Mg CPMG MAS NMR spectra of CMAS glasses with 1 mol% Ga_2O_3 (20.0 T, 14 kHz MAS), with (b) showing the fit (red line) of the spectrum of the sample prepared at 2.5 GPa.

This work has shown that solid-state NMR spectroscopy is a very sensitive probe for the coordination environment of both trace and major elements in geochemically-relevant glasses. The changes observed for the major elements are influenced both by the proportion of the trace element present, and its preferred coordination environment.

References

1. Zhang, J.; Utsumi, W.; Liebermann, R. C. *Phys. Chem. Miner*. **1996**, *23*, 1.
2. Waff, H. S. *Geophys. Res. Lett.* **1975**, *2*, 193.
3. Allwardt, J. R. *Am. Mineral.* **2005**, *90*, 1218.
4. Righter, K. *Ann. Rev. Earth Planet. Sci*. **2003,** *31*, 135.

Structural Investigation of a Double Perovskite with Li on both A- and B- Sites Using ^{6}Li and ^{17}O NMR

Kenneth K. Inglis,[1] Michael J. Pitcher,[1] Matthew S. Dyer,[1] Matthew J. Rosseinsky[1] and Frédéric Blanc[1,2]

[1]*Department of Chemistry, University of Liverpool*

[2]*Stephenson Institute for Renewable Energy, University of Liverpool*

Overview

Investigation of Li defect chemistry using solid-state NMR alongside diffraction data and computer aided calculations is becoming more important in identifying new Li ion conductors for use in all solid-state Li batteries.[1-3] A material of composition $La_3Li_3W_2O_{12}$ was recently synthesised and was found using X-ray diffraction to adopt the distorted double perovskite structure (space group $P2_1/n$) with WO_6 and LiO_6 octahedra ordered in a rock salt arrangement on the B-site, and La and Li on the A-site with a 3:1 ratio. The location of the Li atoms, however, was not easily refined due to the low scattering index of Li. A computational model using DFT calculations, based on the diffraction data, identified Li atoms on both A- and B-sites of the crystal structure (Figure 1a) with different Li–O coordination, representing a type of structure which has not been reported in literature. The A-site Li is distorted away from the centre of the A-cage and relaxes to a four-fold coordination with oxygen, closer to one of the faces of the tetrahedra (Figure 1b).

Structural investigation using both ^{6}Li and ^{17}O MAS NMR for this sample proved to be important. We show here that ^{6}Li MAS NMR identifies the two distinct Li sites in the double perovskite. Through the use of ^{17}O MAS and 3Q MAS NMR, we also reveal the large structural distortion of $La_3Li_3W_2O_{12}$ which we observe in the calculated model, with good agreement to ^{17}O shifts calculated by the GIPAW approach[4,5] for the low energy configurations calculated by DFT.

^{6}Li and ^{17}O NMR

Figure 1c presents a ^{6}Li MAS NMR spectrum of ^{6}Li-enriched $La_3Li_3W_2O_{12}$ which exhibits a second peak as a shoulder of the main peak. Based on the known relationship between ^{6}Li shifts and Li–O coordination numbers,[6–8] the peaks at 0 and –0.4 ppm are assigned to LiO_5 and LiO_6 lithium environments. Integral ratios of the spectral deconvolution yields a 1:2 ratio for these sites, and are in agreement with the A:B-site Li ratios as predicted in the calculated model.

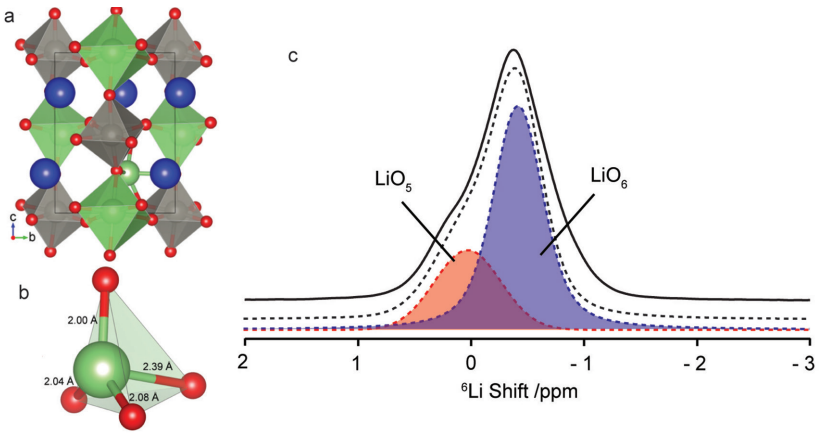

Figure 1. (a) DFT-calculated model of $La_3Li_3W_2O_{12}$ with A-site Li in its most stable position. Oxygen polyhedra are shown around B-site cations W and Li. Lanthanum, lithium, tungsten and oxygen are represented by blue, green, grey and red spheres, respectively. (b) A-site Li in its most stable position, forming a four-fold coordination with one Li–O bond length much longer than the others. (c) ^{6}Li MAS (10 kHz) NMR (20 T) spectrum of ^{6}Li-enriched $La_3Li_3W_2O_{12}$ with spectral deconvolution. The black dashed line corresponds to the overall simulation of the two different ^{6}Li resonances at 0 ppm (red dashed line) and –0.4 ppm (blue dashed line), corresponding to LiO_5 and LiO_6 local environments, respectively.

A ^{17}O Hahn echo NMR spectrum of ^{17}O-enriched $La_3Li_3W_2O_{12}$ obtained at 20 T (Figure 2a, red) shows a range of broad resonances spanning approximately 200 ppm with possibly three intense peaks at ~350, ~400 and ~450 ppm. The spectrum of the same material recorded at 9.4 T is very similar (Figure 2a, blue) and also covers around ~200 ppm; this suggests that the ^{17}O NMR line shape is dominated by a distribution of shifts as anticipated in a distorted oxide material. The GIPAW method[4,5] was used to calculate the ^{17}O shifts of the various oxygen environments – $OLaLi_3$, OLa_2Li_2, OLa_3Li and OLa_4. Results are given as histograms in Figure 2a and are distributed over the 300 – 480 ppm range, agreeing well with the experimental results. A weak correlation is seen between the ^{17}O shifts and the number of La and Li atoms on the A-site around the O atoms, with higher shifts being obtained for the larger number of Li^+ ions surrounding a single O^{2-} ion, while the large spread of ^{17}O shifts – especially seen with the OLa_3Li moiety (cyan in Figure 2a) – is caused by the actual position of Li^+ in the A-cage. A ^{17}O 3Q MAS NMR spectrum obtained at 9.4 T (Figure 2b) only shows signal along the +1 diagonal. This also indicates a large distortion in the crystal structure and is in agreement with the ^{17}O shifts calculated for the DFT structural models.

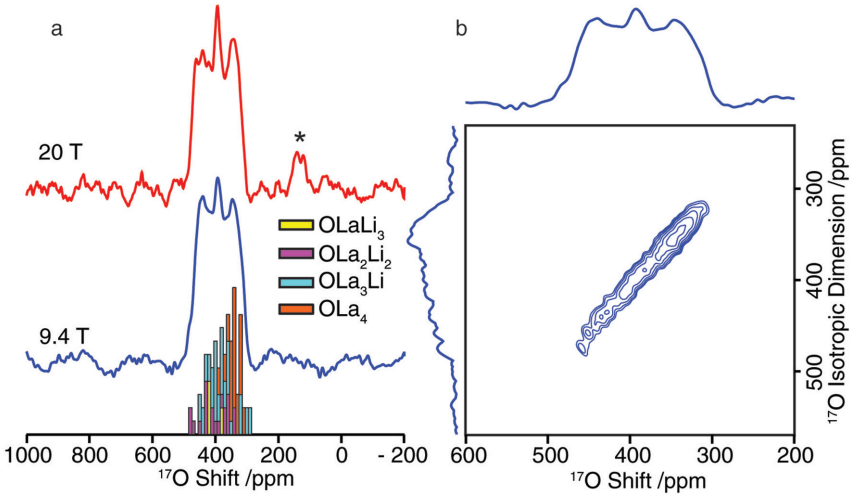

Figure 2. (a) ^{17}O Hahn echo NMR (blue: 9.4 T, 13 kHz MAS; red: 20 T, 22 kHz MAS) spectra of ~10% ^{17}O-enriched $La_3Li_3W_2O_{12}$. The histogram represents ^{17}O shifts calculated by the GIPAW approach[4,5] with the distinct bars being distinguished based on the different A-site La:Li ratios surrounding a single O^{2-} ion – $OLaLi_3$ (yellow), OLa_2Li_2 (purple), OLa_3Li (cyan) and OLa_4 (orange). (b) A ^{17}O 2D z-filtered 3Q MAS spectrum of ^{17}O-enriched $La_3Li_3W_2O_{12}$ recorded at 9.4 T at a MAS frequency of ν_r = 13 kHz. Top: A ^{17}O Hahn echo NMR spectrum of ^{17}O-enriched $La_3Li_3W_2O_{12}$. Asterisks (*) denote spinning sidebands.

References

1. Liu, T.; Leskes, M.; Yu, W.; Moore, A. J.; Zhou, L.; Bayley, P. M.; Kim, G.; Grey, C. P. *Science* **2015**, *350*, 530.
2. Deng, Y.; Eames, C.; Chotard, J.-N.; Lalère, F.; Seznec, V.; Emge, S.; Pecher, O.; Grey, C. P.; Masquelier, C.; Islam, M. S. *J. Am. Chem. Soc.* **2015**, *137*, 9136.
3. Buschmann, H.; Dölle, J.; Berendts, S.; Kuhn, A.; Bottke, P.; Wilkening, M.; Heitjans, P.; Senyshyn, A.; Ehrenberg, H.; Lotnyk, A.; Duppel, V.; Kienle, L.; Janek, J. *Phys. Chem. Chem. Phys.* **2011**, *13*, 19378.
4. Pickard, C. J.; Mauri, F. *Phys. Rev. B* **2001**, *63*, 245101.
5. Yates, J. R.; Pickard, C. J.; Mauri, F. *Phys. Rev. B* **2007**, *76*, 024401.
6. MacKenzie, K. J. D.; Smith, M. E. *Multinuclear Solid-State Nuclear Magnetic Resonance of Inorganic Materials*; Elsevier: Oxford, 2002; Vol. 6.
7. Xu, Z.; Stebbins, J. F. *Solid State Nucl. Magn. Reson.* **1995**, *5*, 103.
8. Xu, Z.; Stebbins, J. F. *Science* **1995**, *270*, 1332.

Structure and Sodium Ion Dynamics in Sodium Strontium Silicate Investigated by Multinuclear Solid-State NMR

Kenneth K. Inglis,[1] John P. Corley,[1] Pierre Florian,[2] Jordi Cabana,[3] Ryan D. Bayliss[3] and Frédéric Blanc[1,4]

[1]*Department of Chemistry, University of Liverpool*

[2]*Conditions Extrême et Matériaux: Haute Température and Irradiation, Orléans, France*

[3]*Department of Chemistry, University of Illinois at Chicago, USA*

[4]*Stephenson Institute for Renewable Energy, University of Liverpool*

Overview

After the initial report by Singh and Goodenough that shows very high oxygen conductivity in Na-doped strontium silicate $SrSiO_3$[1] (i.e. $Sr_{0.55}Na_{0.45}SiO_{2.775}$), the material was at the centre of high debate in terms of its structure, chemical composition, ionic conductivity and the nature of the charge carriers. In an effort to replicate the original study, Bayliss *et al*[2] proposed that there is no Na-doping and that the material is not single phase. Rather, it was suggested that this is a mixture consisting of $SrSiO_3$ and an amorphous sodium disilicate glass (suggested as $Na_2O{\cdot}2SiO_2$), with the Na-containing glass being responsible for the high conductivity observed,[1] and this was confirmed in subsequent studies.[3-7] The overall conductivity of the material was still up for discussion with the associated activation energy for charge carrier mobility ranging by a factor of 3 in different studies.[1,4,6] This was postulated to arise from differences in the thermal history and devitrification processes of $Sr_{0.55}Na_{0.45}SiO_{2.775}$ and crystallisation of $Na_2O{\cdot}2SiO_2$ into one of the polymorphs of $Na_2Si_2O_5$.[8]

Here we present a structural investigation of $Sr_{0.55}Na_{0.45}SiO_{2.775}$ that is part of an extended structure and dynamics study of this phase.[7] Using ^{23}Na MAS NMR, we demonstrate the absence of Na-doping in $SrSiO_3$ and re-identify $Na_2O{\cdot}2SiO_2$ as the single Na-containing amorphous material. ^{17}O MAS NMR data collected on ^{17}O-enriched devitrified $Sr_{0.55}Na_{0.45}SiO_{2.775}$ show the presence of both α-$Na_2Si_2O_5$ and α-$SrSiO_3$, and the absence of any other phases, confirming the two phase nature of this material.

Phase Identification Using ^{23}Na and ^{17}O MAS NMR Spectroscopy

Figure 1a presents a ^{23}Na MAS NMR spectrum obtained for $Sr_{0.55}Na_{0.45}SiO_{2.775}$. A single broad peak spanning 10s of ppm is observed, indicating the presence of significant disorder and a range of local Na sites in the sample. Figure 1b displays a ^{23}Na MAS NMR spectrum for $Sr_{0.55}Na_{0.45}SiO_{2.775}$ devitrified at 800 °C in air for 4 hours, and shows a typical second-order quadrupolar broadened line shape corresponding to α-$Na_2Si_2O_5$, in agreement with the identification of this phase by XRD.[7] Importantly, the lineshape (dashed

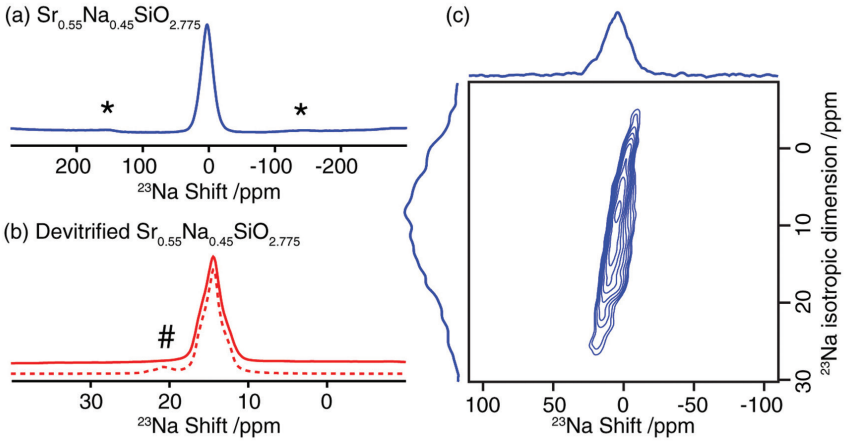

Figure 1. ^{23}Na MAS (33 kHz) NMR spectra (20 T) of (a) $Sr_{0.55}Na_{0.45}SiO_{2.775}$ and (b) devitrified $Sr_{0.55}Na_{0.45}SiO_{2.775}$. Asterisks (*) indicate spinning sidebands while # denotes the outer satellite transition. The dashed line in (b) corresponds to a line shape simulation using the known NMR parameters for α-$Na_2Si_2O_5$.[9] (c) A ^{23}Na 3Q MAS (33 kHz) NMR spectrum (20 T) of $Sr_{0.55}Na_{0.45}SiO_{2.775}$. The nutation frequency was ~15 kHz for the selective pulse and 100 kHz for the excitation and reconversion pulses.

line in Figure 1b) simulated using the known parameters fits the experimental data very well.[9] These results reinforce the absence of Na doping in $SrSiO_3$, and confirms the presence of a single Na-containing glass phase $Na_2O{\cdot}2SiO_2$ present in $Sr_{0.55}Na_{0.45}SiO_{2.775}$ as proposed in the literature.[2-4] A ^{23}Na 3QMAS NMR spectrum of $Sr_{0.55}Na_{0.45}SiO_{2.775}$ (Figure 1c) shows a single resonance with a large distribution of shifts. This observation verifies the large disorder present, typically observed in glasses.

Figure 2 presents a ^{17}O MAS NMR spectrum of ^{17}O-enriched devitrified $Sr_{0.55}Na_{0.45}SiO_{2.775}$ (prepared by gas-solid exchange reaction under 60% ^{17}O enriched O_2 atmosphere at 750 ^{o}C for 4 hours) recorded at 20 T. Broad signals ranging between ~100 ppm and 0 ppm are observed, revealing multiple resonances. The shifts anticipated for the two bridging oxygens O1 and O2 at a higher ppm value, and one non-bridging oxygen O3 of α-$Na_2Si_2O_5$ at a lower ppm value are observed (Figure 2, black). A weak signal is revealed at about 105 ppm and corresponds very well with the position of the non-bridging oxygens O1 and O2 in α-$SrSiO_3$ (Figure 2, green). The NMR signal for bridging oxygen O3 in α-$SrSiO_3$ overlaps with that for α-$Na_2Si_2O_5$.[9]

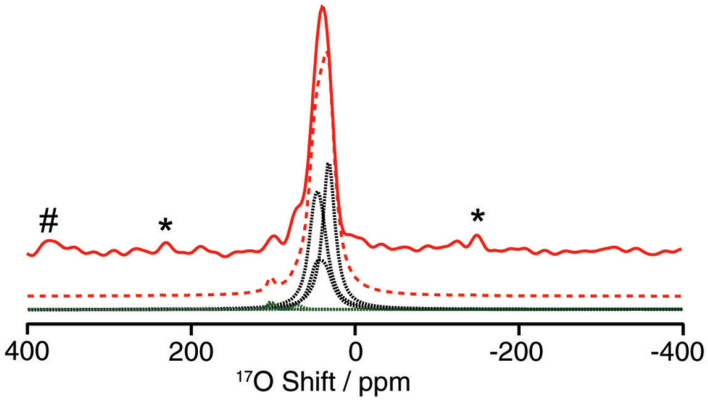

Figure 2. A ^{17}O Hahn echo NMR spectrum (20 T, 22 kHz MAS) of ^{17}O enriched devitrified $Sr_{0.55}Na_{0.45}SiO_{2.775}$. Black and green lines represent line shape simulations for α-$Na_2Si_2O_5$ and α-$SrSiO_3$ respectively using their known quadrupolar parameters.[9] The red dashed line represents the overall simulated line shape. Asterisks (*) indicates spinning sidebands while # denotes the ^{17}O signal from the ZrO_2 rotor.

References

1. Singh, P.; Goodenough, J. B. *J. Am. Chem. Soc.* **2013**, *135*, 10149.
2. Bayliss, R. D.; Cook, S. N.; Fearn, S.; Kilner, J. A.; Greaves, C.; Skinner, S. J. *Energy Environ. Sci.* **2014**, *7*, 2999.
3. Bayliss, R. D.; Cook, S. N.; Scanlon, D. O.; Fearn, S.; Cabana, J.; Greaves, C.; Kilner, J. A.; Skinner, S. J. *J. Mater. Chem. A* **2014**, *2*, 17919.
4. Tealdi, C.; Malavasi, L.; Uda, I.; Ferrara, C.; Berbenni, V.; Mustarelli, P. *Chem. Commun.* **2014**, *50*, 14732.
5. Evans, I. R.; Evans, J. S. O.; Davies, H. G.; Haworth, A. R.; Tate, M. L. *Chem. Mater.* **2014**, *26*, 5187.
6. Peet, J. R.; Widdifield, C. M.; Apperley, D. C.; Hodgkinson, P.; Johnson, M. R.; Evans, I. R. *Chem. Commun.* **2015**, *51*, 17163.
7. Inglis, K. K.; Corley, J. P.; Florian, P.; Cabana, J.; Bayliss, R. D.; Blanc, F. *Chem. Mater.* **2016**, *28*, 3850.
8. Williamson, J.; Glasser, F. P. *Phys. Chem. Glasses* **1966**, *7*, 127.
9. MacKenzie, K. J. D.; Smith, M. E. *Multinuclear Solid-State Nuclear Magnetic Resonance of Inorganic Materials*; Elsevier: Oxford, 2002; Vol. 6.

Understanding Self-Assembly at the Molecular Level: Structure and Function of Guanosine (G) Derivatives

G. N. Manjunatha Reddy,[1] Gretchen M. Peters,[2] Jeffrey T. Davis,[2] Andrew Marsh[3] and Steven P. Brown[1]

[1]*Department of Physics, University of Warwick*

[2]*Department of Chemistry and Biochemistry, University of Maryland, USA*

[3]*Department of Chemistry, University of Warwick*

Overview

Molecular self-assembly can be exploited to engineer biomimetic and functional materials in solution, on surfaces and in the solid state, for example, using DNA/RNA bases.[1, 2] High-field solid state NMR (20 T, up to 75 kHz MAS) has been employed to characterize the process leading to self-assembly of guanosine (G)-based derivatives. Results for two specific examples are presented here: (1) unravelling the role of noncovalent interactions driving ribbon-like self-assembly in the solid-state [3,4] (2) study of the incorporation process of small molecule drugs into G-quartet borate hydrogels.[5]

The Role of Non-Covalent Interactions in G-Ribbons

Ribbon-like structures are formed in the absence of cations when Hoogsteen faces of individual G monomers are interconnected by means of N-H···N and N-H···O hydrogen bonds (see Figure 1).[1, 2] G-ribbons are of high interest for generating functional materials such as liquid crystals, thin films and molecular electronic devices; however, not all ribbon-like assemblies exhibit such functionalities. Here we employ solid-state NMR in conjugation with DFT calculations to understand the factors that influence the formation of G-ribbons. For G, there are two molecules in the asymmetric unit cell, namely A and B, resulting in the modulation of ribbon-like assemblies of the form of A-A-A and B-B-B with distinct magnitudes and directionalities of N1-H1···N7 and N1-H2b···O6 hydrogen bonds. Such minor differences in hydrogen bonding geometries have dramatic effect on the NH and NH2 proton chemical shifts as evidenced by both experimental ^{1}H solid state NMR (see Figure 1: ^{1}H double-quantum (DQ) and ^{14}N-^{1}H HMQC spectra recorded at 850 MHz with 75 kHz MAS recorded using a JEOL 1 mm probe) and GIPAW (gauge-including projector augmented wave) DFT calculated chemical shits for the full crystal and isolated molecules.[3] More importantly, hydroxyl groups of sugar moieties are sensitive to moisture content leading to the formation of morphologically different hydrates over time. Studies performed on three different G derivatives have demonstrated that, in addition to the NH···N and N–H···O hydrogen bonds which are interconnecting guanosine units, several other non-covalent interactions such as O–H···N, O–H···O and CH–π contacts contribute to stabilizing the overall three-dimensional structures in a cooperative manner.[3, 4]

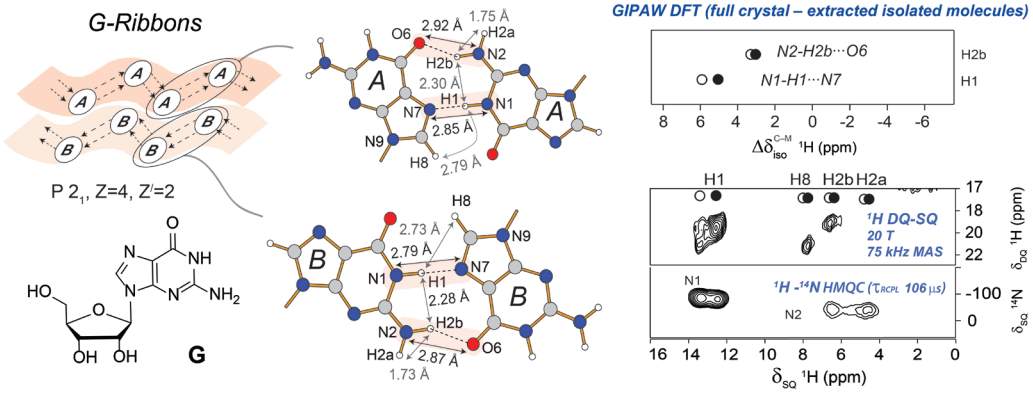

*Figure 1. For **G**, a cartoon representation (left) of the modulation of ribbon-like structures for two molecules in the asymmetric cell, namely A and B. Middle: A schematic representation of the DFT geometry optimized structure of **G**.2H$_2$O illustrating the N–H···N and N–H···O intermolecular hydrogen-bonding interactions together with the intermolecular proximities. Right: Experimental ^{1}H DQ and ^{14}N-^{1}H HMQC two-dimensional solid-state MAS NMR spectra recorded at 20.0 T and 75 kHz MAS are presented together with GIPAW DFT NMR shielding calculations for the full crystal and isolated molecules (filled and hollow circles correspond to the A and B molecules, respectively).[3]*

Probing the Absorption Process of Small Molecules into G4.M$^+$ Borate Gels

G-quartets (planar tetramer arrangement of G monomers stabilized by both hydrogen bonds and cation dipole interactions) have attracted supramolecular chemists to build highly ordered structures such as hydrogels.[1, 2] Recently, we have studied the formation of functional hydrogels made by mixing G 1 with 0.5 equivalent of alkali metal borate salts.[5] Gelation occurred through the formation of extended networks of G-quartets entangled by borate crosslinks. ^{11}B MAS NMR is a powerful probe for directly identifying borate monoester 2 and diester 3, and hence sol and gel components (see Figure 2). G4.M$^+$ borate hydrogels can uptake small molecules drugs such as Methylene Blue (MB, 4). While incorporating at lower concentrations (less than 20 mM), MB was predominantly retained in the gel phase, whereas at higher loading rates (typically greater than 25 mM of MB), a gel to sol transition occurs causing the disentanglement of G-quartets as evidenced by ^{1}H and ^{11}B MAS NMR experiments and vial inversion tests.[5]

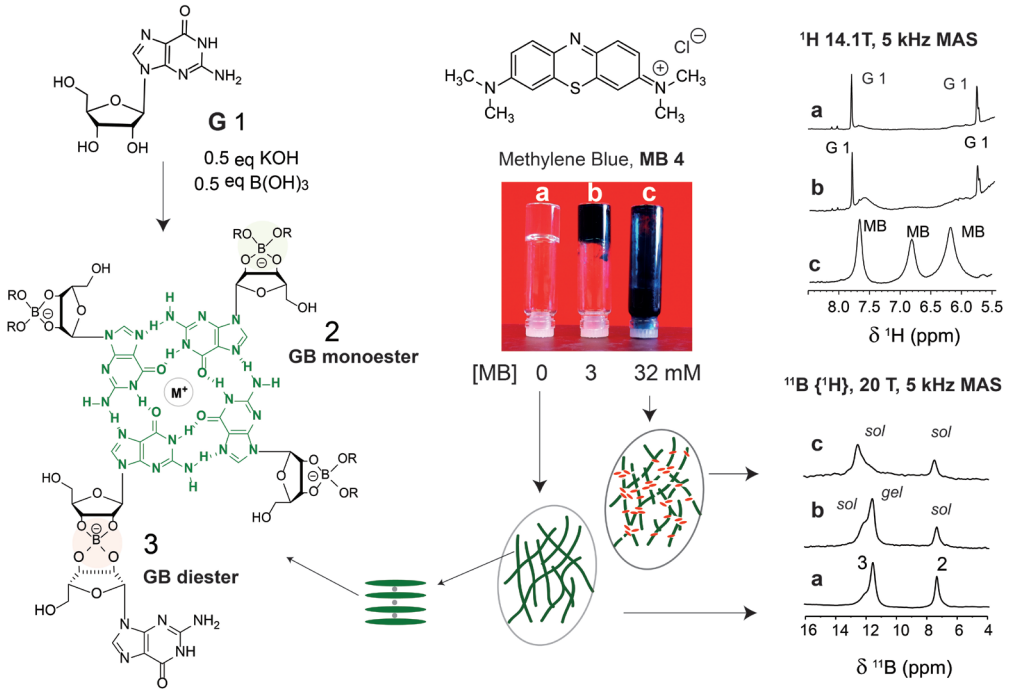

Figure 2. Gelation between G and alkali metal borate salts (left) followed by the photographs of 72 mM G4·M$^+$ borate hydrogels taken before and after the incorporation of methylene blue (MB) (a: 0 mM, b: 3 mM and c: 32 mM). ^{1}H and ^{11}B MAS NMR (20 T, 5 kHz MAS) spectra (left) of G•K$^+$ borate gels before (a) and after (b, c) the incorporation of MB.[5]

References

1. Davis J. T., *Angew. Chem.* **2004**, *43*, 668.
2. Davis J. T.; Spada G. P. *Chem. Soc. Rev.*, **2007**, 36, 296.
3. Reddy G. N. M.; Marsh A.; Davis J. T.; Masiero S.; Brown S. P. *Cryst. Growth Des.* **2015**, 15, 5945.
4. Reddy G. N. M.; Cook D. S.; Iuga D.; Walton R. I.; Marsh A.; Brown, S. P. *Solid State Nucl. Magn. Reson.* **2015**, *65*, 41.
5. Peters G. M.; Scala L. P.; Plank T. N.; Hyman B. J.; Reddy G. N. M.; Marsh A.; Brown, S. P.; Davis J. T. *J. Am. Chem. Soc.* **2014**, *136*, 12596.

Probing Structure and Dynamics in Orotic Acid Monohydrate and Organolithium Compounds

Ann-Christin Poeppler, Dinu Iuga and Steven P. Brown

Department of Physics, University of Warwick

Overview

Work on two different systems was carried out at the 850 MHz Facility. One project evolved around pharmaceutically active hydrate structures for which orotic acid monohydrate was analysed as presented herein. The second project involves air- and moisture sensitive organolithium compounds, which could be successfully studied at fast MAS frequencies using inert gas handling and sample cooling.

Mobility in Orotic Acid Monohydrate

Orotic acid monohydrate[1] was initially studied due to its role as a starting material for the formation of several hydrate forming salts. As shown in Figure 1, while the NH and CH ^{1}H resonances narrow as expected upon increasing MAS frequency, a broadening and change in peak position to a lower ppm value is observed for the carboxylic acid and the water resonances, indicating mobility due to the increase in temperature due to frictional heating. To address this, the ^{1}H(DQ)-^{1}H(SQ) correlation spectrum shown in Figure 2 was recorded using cooling. Good agreement between the experimental cross peaks and those expected for a GIPAW calculation (yellow crosses) are observed. Interestingly, crystal structure prediction results presented by Braun and co-workers found a structure, which only differs from the X-ray structure in the orientation of one of the water protons,[2] whereby the overall packing was predicted to be less dense and rearrangements were postulated to be possible. Our results indicating mobility are consistent with this postulation.

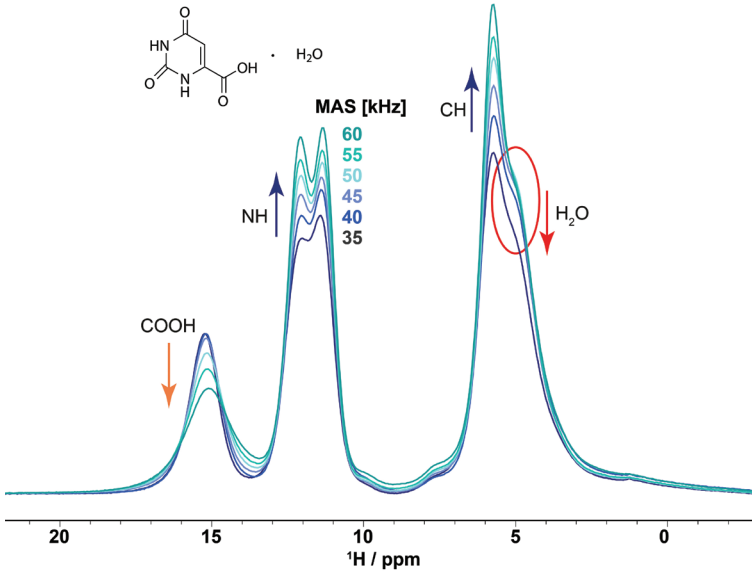

Figure 1. ^{1}H (850 MHz) NMR spectra of orotic acid monohydrate recorded at different MAS frequencies. The NH and CH resonances narrow with increasing spinning frequency (and increasing temperature), while the COOH and H_2O resonances broaden and shift to lower ppm values.

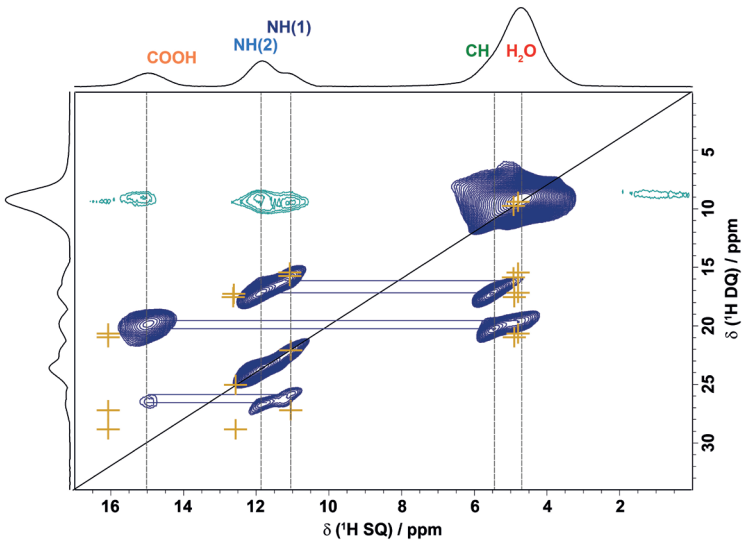

Figure 2. A ^{1}H (850 MHz) DQ MAS (60 kHz) spectrum with skyline projections of orotic acid monohydrate recorded using one rotor period of BABA recoupling and cooling at 273 K to counteract frictional heating. Yellow crosses indicate GIPAW calculated DQ peak positions.

NMR Crystallography of an Organolithium Compound

Organolithium compounds are an important class of reagents employed for the synthesis of drug candidates or in polymerization reactions, with this being in spite of their air- and moisture sensitivity. Most existing NMR studies of this class of compounds were carried out before current proton detected experiments and NMR crystallographic approaches were widely available.[3] To understand the underlying inter- and intramolecular interactions, experiments were performed at the 850 MHz Facility. Specifically, a ^{1}H DQ MAS spectrum is shown in Figure 3 alongside a one-pulse ^{1}H MAS NMR spectrum (red) and a stick spectrum representing GIPAW (CASTEP) calculated chemical shifts (yellow bars) – note that due to the large number of atoms in the unit cell (792 atoms), this calculation was performed at the UK National Supercomputing Service ARCHER.

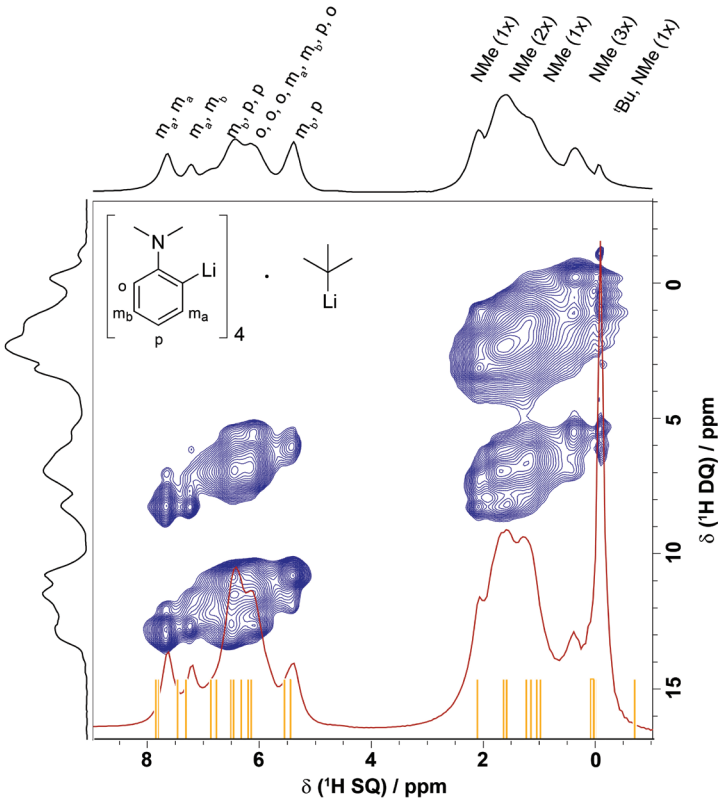

Figure 3: A ^{1}H (850 MHz) DQ MAS (60 kHz) spectrum of an organolithium cocrystal whereby the asymmetric unit contains a tetramer of o-lithiated dimethylaniline and one quarter of a tBuLi tetramer, which shows additional disorder in the crystal structure due to rotation of the $C(CH)_3$ groups. The spectrum was recorded using one rotor period of BABA recoupling with cooling at 273 K. A one pulse ^{1}H NMR spectrum (red) as well as a stick spectrum representing GIPAW (CASTEP) calculated chemical shifts (yellow) are overlaid.

References

1. Portalone, G. *Acta Cryst. E* **2008**, *64*, o656.
2. Braun, D. E.; Nartowski, K. P.; Khimyak, Y. Z.; Morris, K. R.; Byrn, S. R.; Griesser, U. J. *Mol. Pharm.* **2016**, *13*, 1012.
3. Johnels, D.; Günther, H. *Solid State NMR Spectroscopy in Organolithium Chemistry in Patai's Chemistry of Functional Groups, Wiley* **2004**.

Solid-State NMR on HF Encapsulated Inside a Fullerene Cage

Richard Bounds, Salvatore Mamone, Shamim Alom, Richard J. Whitby, Malcolm H. Levitt and Marina Carravetta

School of Chemistry, University of Southampton

Overview

A new and interesting member of the endohedral fullerene family was prepared at the University of Southampton and has HF as a guest molecule inside a fullerene. In this project, the 850 MHz Facility has been used to study the ^{1}H and ^{19}F environments and the strength of the HF intramolecular interaction. We performed variable spinning measurements on this system to characterise the anisotropic parameters. Our first study was the characterisation of the open caged fullerene denoted HF@1 for simplicity,[1] after successfully closing the cage, we then characterised the closed HF@C_{60}. The key experimental results are shown below, and they are further discussed and compared with other characterization methods in a recently accepted publication.[2]

^{13}C, ^{1}H, ^{19}F Spectra of Closed Fullerene: HF@C_{60}

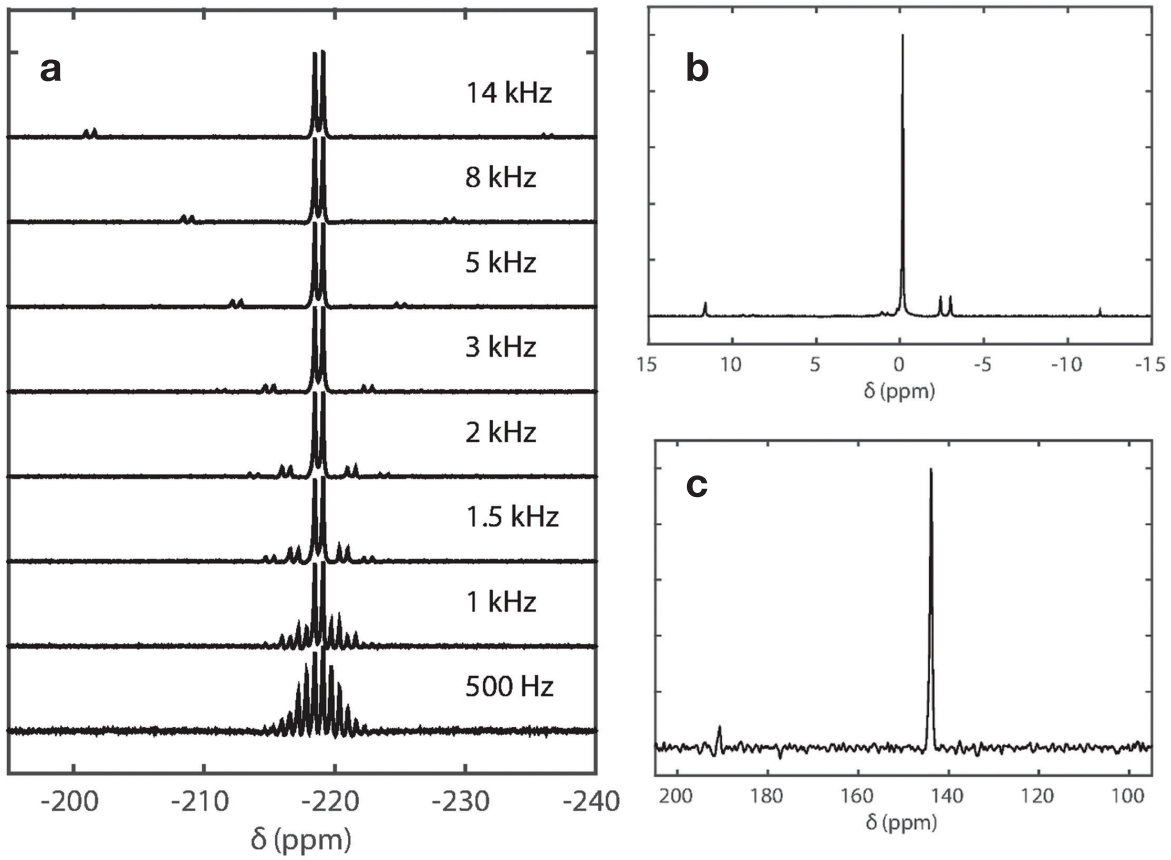

Figure 1. NMR spectra of 10 mg of HF@C_{60} recorded at 20.0 T. (a) ^{19}F spectra with variable spinning frequency. A HF J doublet is visible and corresponds to ~500 Hz. Spectra are the result of 256 coadded transients collected using a spin echo and the spectral width is 500 kHz. The ^{19}F chemical shift scale is referenced to β-Polyvinylidene fluoride (PVDF) with a chemical shift of –91 ppm.[3] (b) A ^{1}H spectrum of HF@C_{60} with a HF doublet visible centered around –3 ppm. Spectra are the result of 256 coadded transients collected using a single pulse with a MAS frequency of 10 kHz and a spectral width of 50 kHz. The ^{1}H chemical shift scale is referenced to adamantane at 1.8 ppm.[3] (c) A ^{13}C spectrum of HF@C_{60}; the spectrum is the result of 1024 coadded transients collected using a single pulse with a MAS frequency of 10 kHz. The ^{13}C chemical shift scale is referenced with respect to the downfield peak of adamantane at 38.5 ppm.[3] The observed chemical shift is consistent with C_{60}.[4]

Figure 1 provides the characterization of the sample via ^{19}F, ^{1}H and ^{13}C NMR. The ^{19}F spectra were recorded at a number of spinning frequenices in order to evaluate the NMR parameters. The splitting between the peaks is the result of the ^{1}H -^{19}F J coupling. This was removed in Figure 2 by means of ^{1}H decoupling.

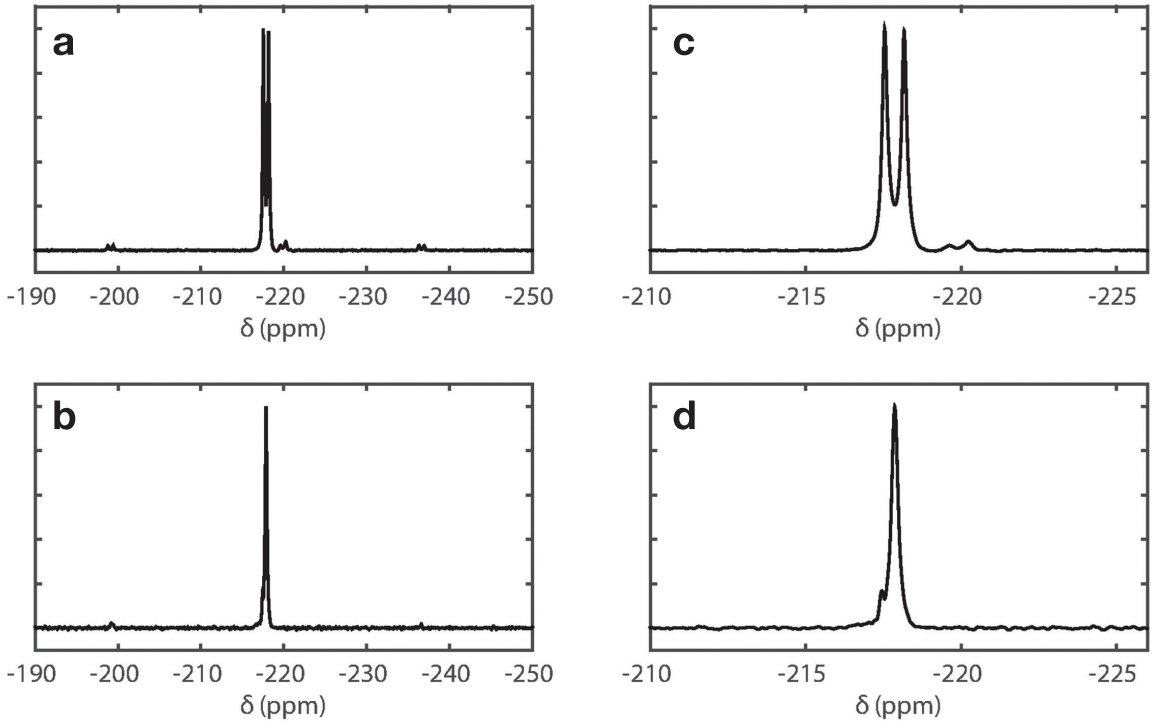

Figure 2. Solid-state ^{19}F spectra of HF@C_{60}. Spectra were recorded at 20.0 T using a MAS frequency of 10 kHz. (c) and (d) are expansions of (a) and (b), respectively. The spectra were recorded under identical conditions apart from the presence of ^{1}H decoupling for spectrum (b) and (d). The spectra shown are the result of 256 transients with a recycle delay of 2 seconds, a single pulse was used with a rf nutation frequency of 38 kHz. ^{19}F spectra were indirectly referenced to the CH_2 ^{13}C signal in adamantane.[3] The processing of the spectra was performed using the matNMR package for Matlab.[5]

References

1. Krachmalnicoff, A.; Bounds, R.; Mamone, S.; Levitt, M. H.; Carravetta, M.; Whitby, R. J. *Chem. Commun.* **2015**, *51*, 4993.
2. Krachmalnicoff, A.; Bounds, R.; Mamone, S; Alom, S.; Concistre, M;. Meier, B.; Horsewill, A. J.; Shugai, A.; Nagel, U.; Room, T.; Carravetta, M.; Levitt, M. H.; Whitby, R. J. *Nature Chem.*, in press.
3. Morcombe, C. R.; Zilm, K. W. *J. Magn. Reson.* **2003**, *162*, 479.
4. Pennington, C.; Stenger, V. *Rev. Mod. Phys.* **1996**, *60*, 855.
5. van Beek, J. D. *J. Magn. Reson.* **2007**, *187*, 19.

Application of ^{14}N MAS NMR Spectroscopy for the Study of the Ordering of Structure Directing Agents in Pure Silica Zeolites

Shelley L. Brace and Richard J. Darton

School of Physical & Geographical Sciences, Keele University

Overview

Zeolites are microporous inorganic framework materials, constructed of SiO_4 and AlO_4^- tetrahedra, which have well-defined internal channels and cavities that are of variable size and are shape selective towards organic molecules and metal ions. They have wide-ranging and extremely useful applications in many of today's industrial processes and are now produced in large quantities each year for use as catalysts, ion-exchangers, and for gas separation and absorption. Given the widespread use of zeolites and related materials, very little is known about their mechanisms of formation or how these can be influenced to give new or improved materials. Of particular interest is the exact role of the structure directing agent (SDA), which is usually a tetraalkylammonium salt. It has recently been demonstrated that ^{14}N spectral parameters of selected SDAs can be used as a probe of the local ordering within zeolites.[1-3] Here we show further applications of this method to the local ordering of SDAs within MFI zeolites using the UK 850 MHz Solid-State NMR facility.

^{14}N Spectra

Figure 1 shows a comparison of ^{14}N MAS spectra for tetrapropylammonium F, MFI and ethyltripropylammonium F, MFI materials and accompanying simulated spectra using quadrupolar coupling parameters of C_Q = 54 kHz and η_Q = 0.32 and C_Q = 57 kHz and η_Q = 0.43, respectively. Both materials show the expected asymmetrical ^{14}N environment of the tetralkylammonium ions, with this being slightly more pronounced in the ethyltriproylammonium sample that is believed to be due to the preferred orientation of this SDA within the MFI channel intersections. In addition to the singular asymmetric ^{14}N environment for the ethyltripropylammonium sample, an additional resonance centered on –16 ppm shows the presence of a spherically symmetrical ^{14}N environment, due to the presence of some residual NH_4^+ ions, which were present as ammonium fluoride in the syntheses.

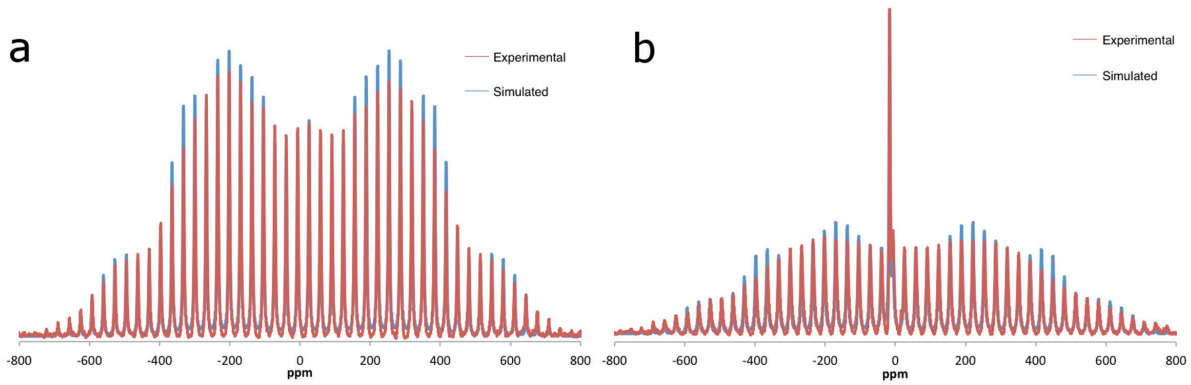

Figure 1. ^{14}N direct-polarisation (20.0 T, 3 kHz MAS, 5 hours experimental time) spectra (red trace) and simulated fittings (blue trace) for (a) tetrapropylammonium F, MFI and (b) ethyltripropylammonium F, MFI.

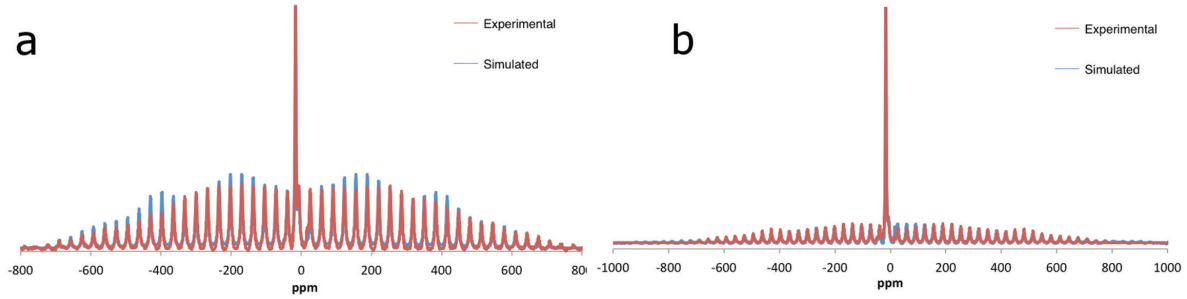

Figure 2. ^{14}N direct-polarisation (20.0 T, 3 kHz MAS, 5 hours experimental time) spectra (red trace) and simulated fittings (blue trace) for (a) methyltripropylammonium F,MFI and (b) pentyltributylammonium F,MFI.

Changing the alkyl arm lengths even more from the standard tetrapropylammonium leads to an increase in the quadrupolar parameters, as illustrated in Figure 2. Decreasing one arm, from ethyl to methyl, leads to a significant change in the asymmetry parameter for methyltripropylammoium-F,MFI (C_Q = 57 kHz and η_Q = 0.47). However, using a much larger SDA such as pentyltributylammonium leads to an increase in both of the quadrupolar parameters, giving values of C_Q = 61 kHz and η_Q = 0.57. These differences in quadrupolar parameters reflect the preferred orientation of different arms within the MFI channel systems (straight and sinusoidal) that may be linked to the strength of interaction between the positively charged N^+ and the negatively charged $[SiO_{4/2}F]^-$ units, that reside at specific locations at the MFI channel intersections.[4] Further work to investigate this is currently in progress.

References

1. Fyfe, C. A.; Darton R. J.; Schneider C.; Scheffler F. *J. Phys Chem. C* **2008**, *112*, 80.
2. Dibb, E.; Giminez, A.; Mineva, T.; Alonso, B. *Dalton Trans.* **2015**, *44*, 16680.
3. Dibb, E.; Mineva, T.; Gaveau, P.; Alonso, B. *Phys. Chem. Chem. Phys.* **2013**, *15*, 18349.
4. Brace, S. L.; Wormald, P.; Darton, R. J. *Phys. Chem. Chem. Phys.* **2015**, *17*, 11950.

^{43}Ca MAS NMR of Octacalcium Phosphate (OCP) Derived Hybrid Phases

Danielle Laurencin,[1] Christian Bonhomme,[2] Dinu Iuga,[3] Yang Li,[4] Melinda J. Duer[4]

[1]*ICG, Université de Montpellier, France*

[2]*Université Pierre et Marie Curie, Sorbonne Universités, Paris, France*

[3]*Department of Physics, University of Warwick*

[4]*Department of Chemistry, University of Cambridge*

Overview

Work published recently by Duer's research group[1] has led to a paradigm shift in the structural model for bone mineral. At its heart is the appreciation that bone mineral platelets do not have an independent existence, and that it is the "stacks" of mineral platelets that are the basic particles that make up the mineral phase in bone. Thus, we now view bone mineral as partially ordered stacks of very thin ordered mineral zones with more disordered regions between, and the octacalcium phosphate phase (OCP, $Ca_8H_2(PO_4)_6.5H_2O$) can be used as a good model of the surface/interface regions.

There are three groups of organic acids that are potentially relevant for forming pathological phases in bone mineral: (1) those resulting from altered equilibria in the citric acid cycle; (2) those resulting from non-enzymatic chemical reactions such as glycation; (3) organic acids arising from impaired cell metabolism, *e.g.* lactic acid from cells operating under anaerobic conditions. In this project, we have characterized hybrid double salts of octacalcium phosphate with a range of these possible pathological organic acids, *i.e.* succinic, lactic, citric and/or formic acids by ^{43}Ca MAS (natural abundance samples), 3Q MAS and DOR (labeled samples).

^{43}Ca MAS, DOR and 3Q MAS of ^{43}Ca-Enriched OCP-Succinate

The hybrid OCP-succinate phase labelled in ^{43}Ca (and ^{13}C) was successfully synthesized for optimal sensitivity. ^{43}Ca is a very low natural abundance (0.14%) low-γ quadrupolar nucleus. It follows that demanding experiments such as double rotation (DOR) and 3Q MAS applied to this particular nucleus require extensive labelling. Figure 1 presents ^{43}Ca MAS and DOR spectra of labelled OCP-succinate. Though ^{43}Ca sites are usually characterized by small quadrupolar coupling constants,[2] MAS does not lead to complete averaging of second-order quadrupolar effects. Under DOR conditions, a net increase in resolution was observed leading to the observation of isotropic (shifted) lines. An excellent signal to noise ratio was obtained in both cases in short experimental times.

In order to compare ^{43}Ca spectral resolution between high resolution experiments dedicated to quadrupolar nuclei, a ^{43}Ca 3Q MAS experiment was implemented as well, a rarely-used experiment for difficult nuclei like ^{43}Ca.[3] The corresponding 2D spectrum is presented in Figure 2 (with the corresponding DOR spectrum for comparison).

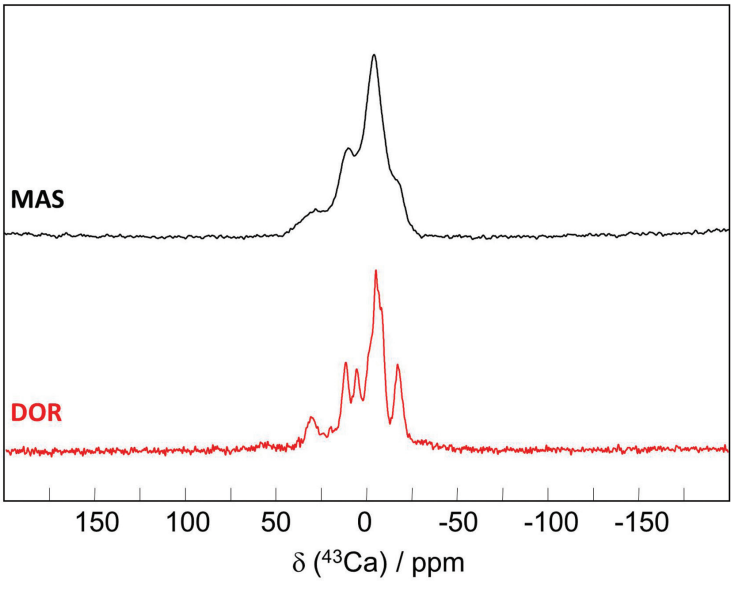

Figure 1. ^{43}Ca MAS and DOR spectra of doubly-labelled OCP-succinate recorded at 20 T. MAS spectrum: 3.2 mm HX low γ probe, 12.5 kHz, experimental time ~8 min. DOR spectrum: outer and inner rotation frequencies of 1.48 kHz and 6.95 kHz, experimental time ~2.5 hours.

Clearly, the DOR experiment gives the better resolution and is now being used to study possible models for pathological mineral phases. Full interpretation of the spectra is challenging as the structure of (pure) OCP is characterized by 8 non-equivalent crystallographic calcium sites. DOR data at a different magnetic field strength (600 MHz) and computational models for OCP-succinate (and pure OCP) at the DFT level in order to compute all ^{43}Ca NMR parameters by using GIPAW are all essential for this and this is currently in progress. Such a combined experimental/computational approach should lead to the full interpretation of ^{43}Ca NMR data and plausible structural models for the OCP-succinate phase.

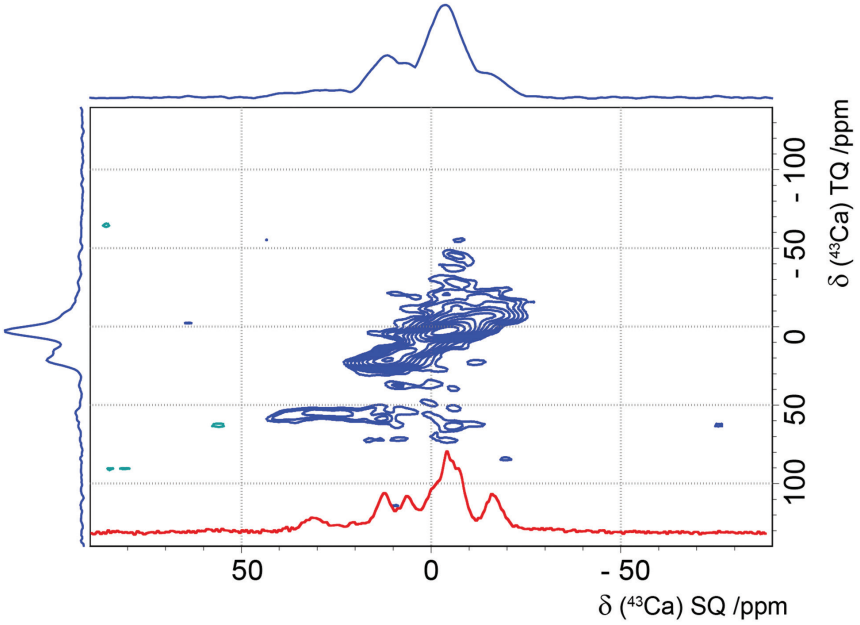

Figure 2. A ^{43}Ca 3Q MAS spectrum of OCP-succinate recorded at 20 T. MAS and 3Q MAS projections are presented in blue, while the DOR spectrum reproduced from Figure 1 is presented in red.

^{43}Ca MAS of Natural Abundance Samples

Figure 3 shows ^{43}Ca spectra obtained at 20 T for several hybrid OCP phases at *natural abundance*. In this case, the combined use of high magnetic field and a large volume rotor (7 mm) favours the collection of spectra with high signal to noise. All experiments were performed at a MAS frequency of 5 kHz, without any ^{1}H decoupling. The experimental time remained reasonable thanks to the implementation of the multi-DFS scheme which here gave an enhancement factor ~7.[3,4] Differences were observed between the spectra demonstrating that ^{43}Ca NMR is sensitive enough to the structural modifications of OCP in the presence of organic moieties. These will be correlated with differences in the mechanical and thermodynamic properties of each phase.

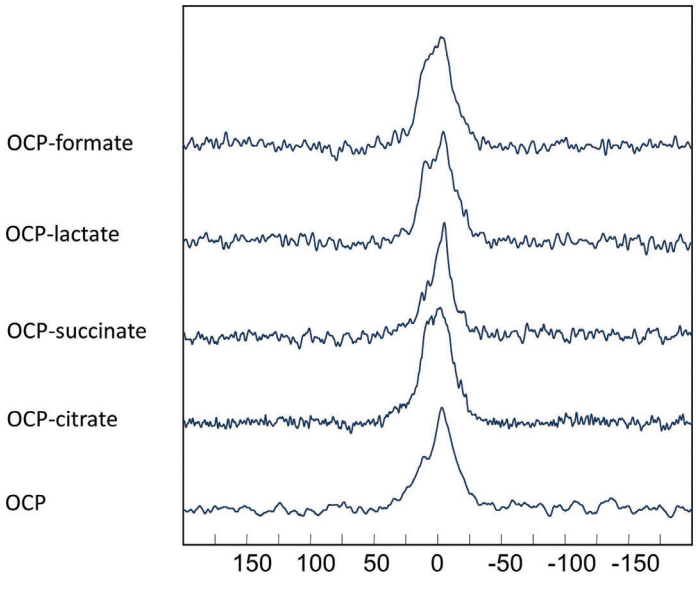

Figure 3. ^{43}Ca natural abundance MAS spectra of pure OCP and hybrid derided phases at 20 T. MAS spectra: 7 mm X low γ probe, 5 kHz MAS, experimental time ~9 hours.

References

1. Davies, E.; Müller, K. H.; Ching Wong, W.; Pickard, C. J.; Reid, D. G.; Skepper, J. N.; Duer, M. J. *Proc. Nat. Acad. Sci. U.S.A.* **2014**, *111*, E1354.
2. Laurencin, D.; Smith, M. E. *Prog. Nucl. Magn. Res. Spectr*. **2013**, *68*, 1.
3. Brinkman, A.; Kentgens, A. P. *J. Phys. Chem. B* **2006**, 110, 16089.
4. Burgess, K. M. N.; Perras, F. A.; Moudrakovski, I. L.; Xu, Y.; Bryce, D. *Can. J. Chem.* **2015,** 93, 799.

^{13}C MAS NMR Studies of Plant Stems

Thomas J. Simmons,[1] Jennifer C. Mortimer,[1] Oigres Daniel Bernardinelli,[1,2,3] Eduardo Azevedo,[3] Steven P. Brown,[2] Ray Dupree,[2] and Paul Dupree[1]

[1]*Department of Biochemistry, University of Cambridge*

[2]*Department of Physics, University of Warwick*

[3]*Department of Physics, University of Sao Carlos, Brazil*

Overview

A major technological challenge in using plant biomass for renewable energy is to release the sugars from the main polysaccharides – cellulose and xylan – effectively and cheaply. Pilot biofuel production processes involve the use of harsh energy-intensive biomass pretreatments, and also require the addition of high quantities of enzymes to break down the biomass. Progress in improving these steps is restrained by the limited understanding of the molecular basis of plant cell wall 'recalcitrance' – the difficulty in deconstructing lignocellulose into fermentable sugars. Despite being crucial to this recalcitrance, the molecular architecture (the rotational conformation and molecular arrangement) of the different polymers in the cell walls of woody materials is poorly understood. To enable detailed studies of cell wall molecular architecture, we have analysed never dried, mature stems of the model plant *Arabidopsis*, grown in air enriched with $^{13}CO_2$ as the carbon source achieving ~97% ^{13}C incorporation. The stems were inserted into MAS rotors with minimal physical pre-treatment and no chemical treatments to allow 1D and 2D ^{13}C NMR experiments. We have begun to use mutant *Arabidopsis* plants to continue work on assignments in the spectra. Specifically, the use of cellulose-deficient plant mutants has allowed us to begin to understand signals arising from different domains of the microfibrils, and to study new cellulose-deficient mutants.

Results

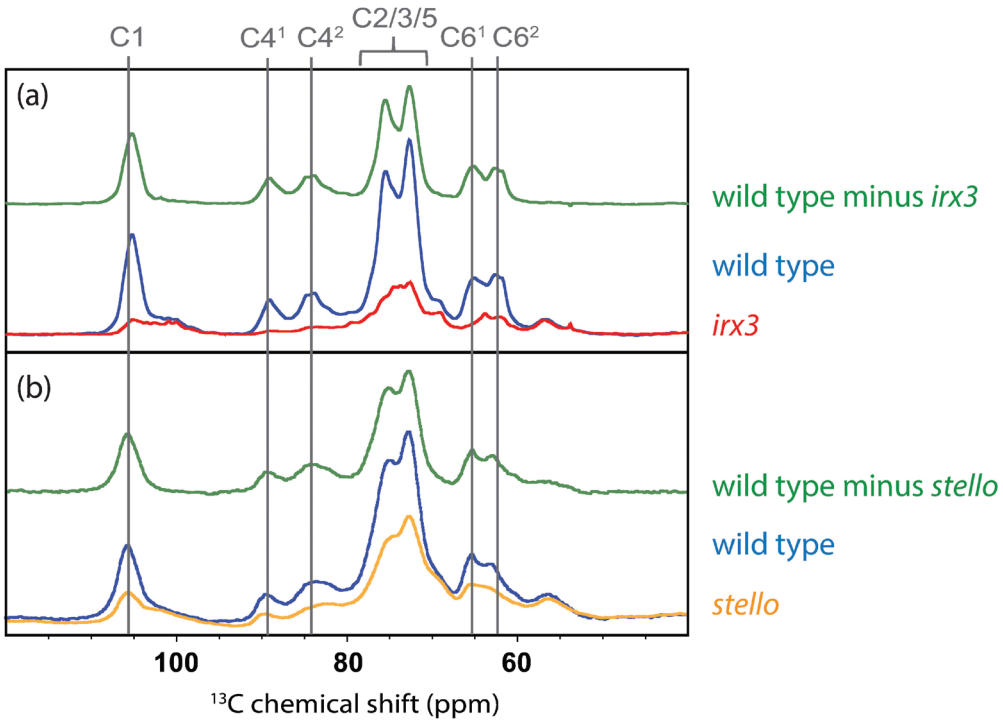

Figure 1. 1D ^{1}H (850 MHz)-^{13}C CP MAS (12.5 kHz, 4 mm rotor) spectra of ^{13}C-labelled mature Arabidopsis stems. (a) The irx3 *cellulose-deficient mutant shows loss specifically in peaks of cellulose. (b) The stello mutant shows loss of cellulose peaks, suggesting it is a novel cellulose-deficient mutant. In each case, both spectra were normalised to the protein region before subtraction of the mutant from the wild type spectrum.*

To investigate the cell wall composition in native never-dried material, we analysed never-dried stems of home-grown ^{13}C-labelled wild type Arabidopsis stems. 1D cross polarisation CP MAS spectra of ^{13}C-labelled mature *Arabidopsis* stems detected the relatively immobile components, such as cellulose and polymers bound to the cellulose fibrils. The *irx3* mutant is defective in cellulose in secondary cell walls,[1] and therefore we grew labelled plants and studied the 1D CP MAS spectra to determine any missing signals arising from cellulose (Figure 1). Subtraction of the spectrum of the mutant from the spectrum of wild type shows that indeed, this *irx3* mutant lacks the peaks corresponding to cellulose. Next, a previously uncharacterised mutant discovered in our laboratory, *stello*, was similarly studied as we suspected it has cell wall alterations. Subtraction of the *stello* spectrum from the WT again displayed specifically a loss of cellulose. We therefore showed that this *stello* mutant is the first to reveal that cellulose synthesis relies on plant Golgi-localised glycosyltransferase enzymes.[2]

To study in more detail changes to cellulose signals in *irx3*, we studied wild type and *irx3* with CP refocused ^{13}C INADEQUATE experiments, which emphasises the less mobile species. Regions of the refocused INADEQUATE spectra showing C2-C3, C3-C4, C4-C5 and C5-C6 cross peaks are shown in Figure 2. In the wild type sample, peaks corresponding to surface/amorphous cellulose and to crystalline cellulose can be seen. Many peaks could be resolved including subtly different environments within these assigned cellulose species, demonstrating the benefits of looking at never dried material at the 850 MHz Facility.[3] In the *irx3* sample, the peaks corresponding to crystalline cellulose were scarcely detectable, confirming the reduction of cellulose in the mutant. Interestingly, many additional peaks were visible, suggesting a change in composition, conformation, or mobility of the remaining cell wall polymers. The assignment of these peaks is ongoing. These spectra will be invaluable for further understanding the importance of cellulose for plant cell wall architecture.

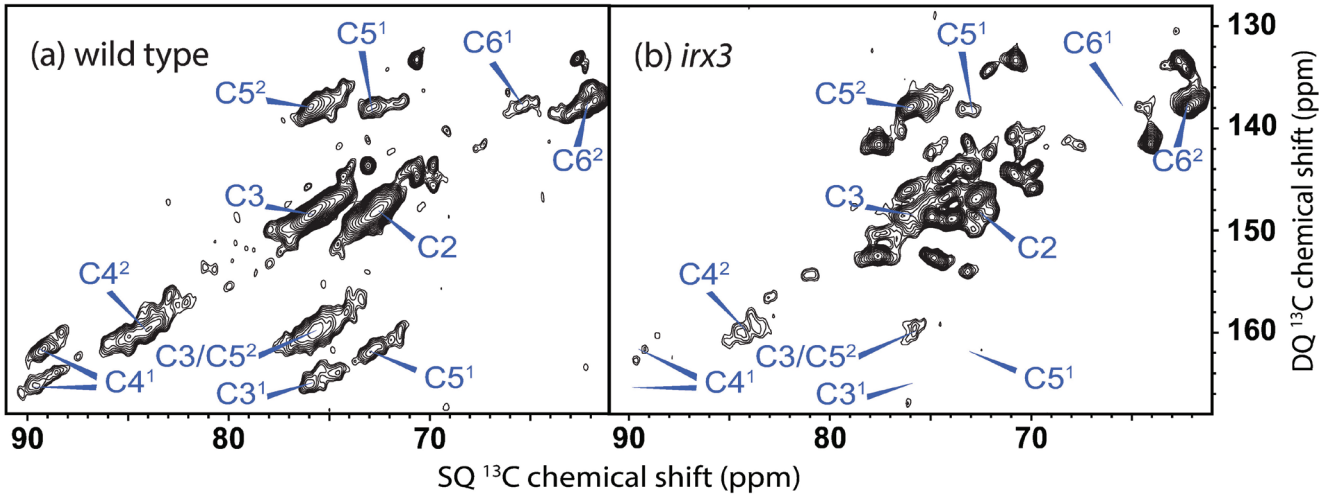

Figure 2. ^{1}H (850 MHz)-^{13}C CP MAS (15 kHz, 3.2 mm rotor) ^{13}C refocused INADEQUATE spectra of never-dried Arabidopsis stems. (a) wild type (b) the irx3 *cellulose-deficient mutant. ^{13}C chemical shifts assigned to the major cellulose peaks are indicated*.

References

1. Ha, M. A.; MacKinnon, I. M.; Sturcová, A.; Apperley, D. C.; McCann, M. C.; Turner, S. R.; Jarvis, M. C. *Phytochemistry* **2002,** *61*, 7.

2. Zhang, Y.; Nikolovski, N.; Sorieul, M.; Vellosillo, T.; McFarlane, H. E.; Dupree, R.; Kesten, C.; Schneider, R.; Driemeier, C.; Lathe, R.; Lampugnani, E.; Yu, X.; Ivakov, A.; Doblin, M. S.; Mortimer, J. C.; Brown, S. P.; Persson, S.; Dupree P. *Nat. Commun.* **2016,** *7*, 11656.

3. Dupree, R.; Simmons, T. J.; Mortimer, J. C.; Patel, D.; Iuga, D.; Brown, S. P.; Dupree, P. *Biochemistry* **2015,** *54*, 2335.

Natural Abundance ^{43}Ca MAS NMR Study of the Ca Environments in the Apatite End Members of Hydroxyapatite, Fluorapatite and Chlorapatite

James F. MacDonald,[1] Jo Duncan,[2] David Quigley,[1] John V. Hanna,[1] Iain R. Gibson[2]

[1]*Department of Physics, University of Warwick*

[2]*Department of Chemistry, University of Aberdeen*

Overview

Natural abundance ^{43}Ca measurements on crystalline solids utilising high magnetic fields and signal enhancing techniques such as Rotor Assisted Population Transfer (RAPT) allow for a satisfactory signal-to-noise in a relatively short time, thus avoiding the need for expensive ^{43}Ca labelling.[1] We show here through the use of the 850 MHz Facility utilising the 7 mm low gamma probe that ^{43}Ca RAPT experiments on native and substituted calcium phosphate apatite end members are achievable, and when these data are used in combination with GIPAW DFT calculations it is possible to resolve some of the outstanding questions regarding the proper identification of crystalline phase present.[2]

^{43}Ca RAPT NMR Data

The data for three very similar calcium phosphate apatitic materials in the form of hydroxyapatite (HAp), fluroapatite (FAp) and chlorapatite (ClAp) are shown in Figures 1 - 3, respectively. The only major difference between these systems are the nature of the substituting OH^-, F^- or Cl^- anion that resides in the channels structure.[3] Depending on the resultant monoclinic or hexagonal crystal structure symmetry describing each system, two or five distinct Ca environments are expected maintaining a 3:2 ratio, with one/three Ca environments forming triangles around the monovalent anion and the other one/two Ca species forming columns with the PO_4 tetrahedra.

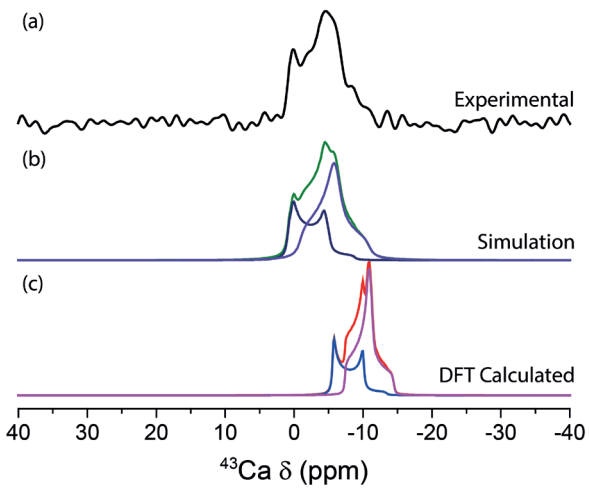

Figure 1. A ^{43}Ca natural abundance MAS spectrum of FAp recorded at 20.0 T and 5 kHz MAS using a RAPT experiment with a rf offset of 150 kHz, a recycle delay of 5 s and an acquisition time of 24 hours. A lineshape simulation and DFT calculated spectrum are also shown.

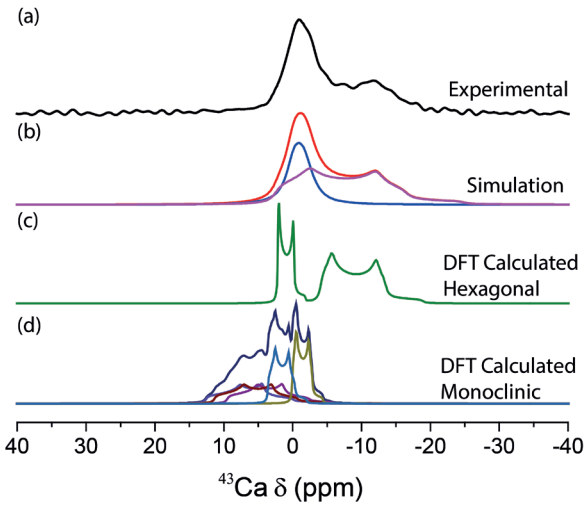

Figure 2. A ^{43}Ca natural abundance MAS spectrum of ClAp recorded at 20.0 T and 5 kHz MAS using the RAPT experiment with a rf offset of 150 kHz, a recycle delay of 2.5 s and an acquisition time of 24 hours. A lineshape simulation and DFT calculated spectra are also shown.

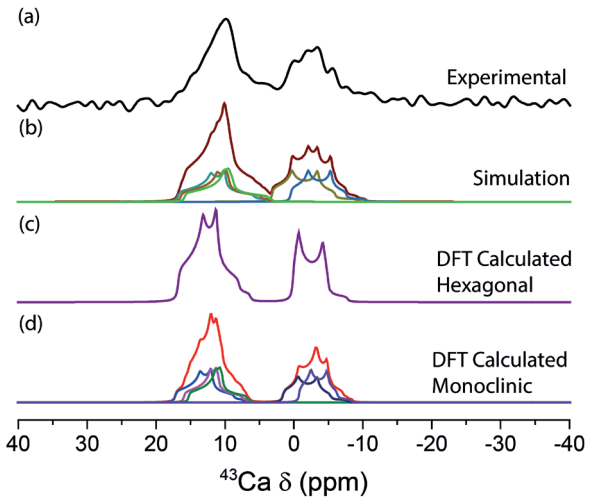

Figure 3. A ^{43}Ca natural abundance MAS spectrum of HAp recorded at 20.0 T and 5 kHz MAS using the RAPT experiment with a rf offset of 150 kHz, a recycle delay of 2.5 s and an acquisition time of 24 hours. A lineshape simulation and DFT calculated spectra are also shown.

Figure 1 presents experimental ^{43}Ca RAPT NMR data for the FAp sample alongside calculated DFT data based on its hexagonal crystal structure. The deconvolution/simulation of the experimental ^{43}Ca data of Figure 1a is shown in Figure 1b; these data can be characterised by two second order quadrupolar resonances with isotropic shifts of δ_{iso} = 2.2 and –0.9 ppm with quadrupole tensor C_Q/η_Q values of 2.41 MHz/ 0.04 and 2.13 MHz/ 0.96, respectively. The resonance intensities maintain the 3/2 ratio of the two different Ca sites in the structure. The calculated spectrum using CASTEP DFT output is presented in Figure 1c, and it is observed that there is reasonable agreement between the calculated and experimental ^{43}Ca data. However, as in previously observed ^{43}Ca DOR NMR studies using isotopic enrichment which are also compared to DFT calculated δ_{iso}, C_Q and η_Q values, the calculated C_Q values for ^{43}Ca are found to be under-represented by ~18%.[4]

Figure 2 presents experimental ^{43}Ca RAPT NMR data and corresponding DFT calculated data for the hexagonal and monoclinic ClAp structures. Figures 2a and 2b show the measured RAPT data and associated deconvolution of the data, respectively. In comparison, Figures 2c and 2d show the calculated DFT data obtained from the hexagonal (Figure 2c) and monoclinic (Figure 2d) forms, clearly showing that the experimental data is in good agreement with the hexagonal crystal form. The simulation in Figure 2b depicts two resonances (again preserving a 3:2 ratio of the Ca positions), characterised by isotropic shifts of δ_{iso} 4.5 and 0.7 ppm, and quadrupole tensor C_Q/η_Q values of 3.85 MHz/ 0.3 and 1.48 MHz/ 0.0, respectively. Although agreement for the hexagonal DFT spectrum is visually much better than that of the corresponding monoclinic form, some inconsistencies still remain. The predicted isotropic chemical shifts (δ_{iso}) are inverted for the Ca positions in question, and the predicted and measured values for C_Q do not follow the same pattern as with previously observed ^{43}Ca NMR calculations where the calculated data is consistently under-represented by ~18%.[4] However, inconsistencies are also observed in the corresponding ^{31}P MAS NMR data and the associated DFT calculations for ClAp (not shown), suggesting that there may be errors with the available structure (cif) file, or that the ClAp sample may be non-stoichiometric pertaining to its Cl content.

In contrast, Figure 3 presents ^{43}Ca RAPT data measured for HAp along with corresponding DFT calculated data for the associated hexagonal and monoclinic structures. A comparison of Figures 3a and 3b demonstrates that five Ca positions are described by the simulation of the experimental data and that a 3:2 ratio is maintained between the two distinct types of Ca position, thus suggesting the occurrence of a monoclinic HAp system (in contrast to the previously described FAp and ClAp systems). As observed from the calculated spectra for the hexagonal and monoclinic structures of Figures 3c and 3d, there is very little difference between the expected isotropic chemical shifts (δ_{iso}) and the quadrupole parameters (C_Q/η_Q) from these different crystal forms, and that only the multiplicity of the Ca positions is able to discriminate this basic characteristic feature. This observation illustrates why the true structural nature of HAp can often be uncertain, especially when some degree of disorder is present. The monoclinic form of this sample is also confirmed from ^{31}P MAS NMR and X-ray diffraction data (not shown). The deconvolution of the ^{43}Ca RAPT data (see Figure 3a) into the five constituent resonances (see Figure 3b) yields isotropic chemical shifts δ_{iso} of 17.0, 16.5, 15.9, 3.8 and 1.1 ppm and quadrupole tensor C_Q/η_Q values of 2.48 MHz/ 0.7, 2.44 MHz/ 0.8, 2.40 MHz/ 0.9, 2.56 MHz/ 0.4 and 2.40 MHz/ 0.4, which are in excellent agreement with the DFT calculated NMR parameters characterising this system.

References

1. Bryce, D. *Dalton Trans.* **2010**, *39*, 8577.
2. Haverty, D.; Tofail, S. A. M.; Stanton, K. T.; McMonagle, J. B. *Phys. Rev.* **2005**, *B71*, 094103.
3. Young, R. A.; Elliot, J. C. *Arch. Oral Biol.* **1966**, *11*, 699.
4. MacDonald J. F. PhD Thesis, University of Warwick **2012**, p. 140.

In-Situ NMR Studies of Solvent-Free Co-Crystal Formation

Colan E. Hughes, P. Andrew Williams and Kenneth D. M. Harris

School of Chemistry, Cardiff University

Overview

Recently, the first examples of polymorphism in co-crystals formed between α,ω-dihydroxyalkanes and urea were reported, with the new polymorphs prepared by mechanochemical milling.[1] During milling, high pressure and temperature combine to create conditions under which novel chemistry can occur. However, it is difficult to measure the instantaneous heating and pressurization which occurs when the milling ball strikes the sample. With the aim of disentangling these effects, we have exploited the pressure generated by magic-angle spinning (MAS) together with controlled heating to try to identify the conditions necessary for formation of new polymorphs in this family of co-crystals.

Results

In-situ solid-state ^{13}C NMR experiments (20 T) were carried out on physical mixtures (2:1 molar ratio) of: (i) ^{13}C-urea and 1,6-dihydroxyhexane (**6**), and (ii) ^{13}C-urea and 1,8-dihydroxyoctane (**8**). For **6**/urea at 20 °C, MAS at 12 kHz led to a significant amount of co-crystal formation within minutes. For **8**/urea, no co-crystal formation was observed under these conditions. In other experiments, each sample was heated above the melting point of the dihydroxyalkane; on cooling to 20 °C, co-crystal formation was observed together with pure solid urea (peak at 162.6 ppm). From the region of the spectrum characteristic of urea in co-crystal phases (164 - 165 ppm), a single peak is observed for **6**/urea (Figure 1) whereas two overlapped peaks are observed for **8**/urea (Figure 2).

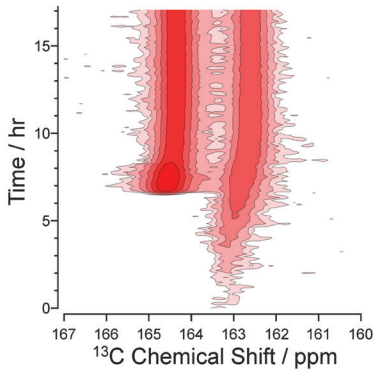

*Figure 1. In-situ ^{13}C CP MAS NMR spectra of cooling urea and **6** from the melt.*

Discussion

For α, ω-dihydroxyalkane/urea co-crystals, the chemical shift of ^{13}C-urea is largely governed by whether the structure contains parallel (P) or anti-parallel (A-P) urea ribbons, as assigned previously.[2] For the co-crystals of **6**/urea formed both at 20 °C under MAS and by cooling the melt, the ^{13}C-urea chemical shift is consistent with the presence of A-P urea ribbons, probably representing the A-P/O polymorph that is known to be obtained for **6**/urea by milling.[1] For the co-crystals of **8**/urea produced by cooling the melt, one of the two ^{13}C-urea peaks matches the polymorph (P/A) produced by solution crystallization while the other peak is consistent with the presence of A-P urea ribbons; this second peak is likely to represent the A-P/O polymorph, which is known to be obtained for **8**/urea by milling.[1]

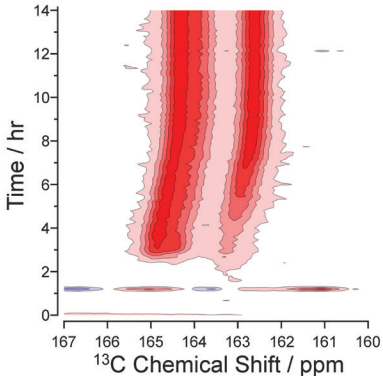

*Figure 2. In-situ ^{13}C CP MAS NMR spectra of cooling urea and **8** from the melt.*

Concluding Remarks

For **6**/urea, co-crystal formation can be induced simply by subjecting a physical mixture of the components to MAS. For **8**/urea, multiple co-crystal phases are produced by crystallization from the molten phase. These results yield new insights on the conditions for co-crystal formation in these systems. The formation of the **6**/urea co-crystal at 20 °C in our experiments represents a rare example of a mechanochemical transformation induced simply by subjecting a physical mixture of the solid components to MAS.

References

1. Zhou, Y.; Guo, F.; Hughes, C. E.; Browne, D. L.; Peskett, T. R.; Harris, K. D. M. *Cryst. Growth Des.* **2015**, *15*, 2901.
2. Martí-Rujas, J.; Kariuki, B. M.; Hughes, C. E.; Morte-Ródenas, A.; Guo, F.; Glavcheva-Laleva, Z.; Taştemür, K. L.; Ooi, L.-L.; Yeo, L.; Harris, K. D. M. *New J. Chem.* **2011**, *35*, 1515.

Studying the Effects of MAS on the Miscibility of Liquids

Colan E. Hughes, Alexander J. Bukvic and Kenneth D. M. Harris

School of Chemistry, Cardiff University

Overview

In our various *in-situ* NMR studies of crystallization processes from solution,[1,2] we have found evidence, in one specific set of experiments, that magic-angle spinning (MAS) may have an effect on the miscibility of a binary liquid mixture relative to the miscibility under static conditions. Specifically, in experiments involving co-crystallization of urea and long-chain alkanes from methanol, we have observed that phase separation of the pure alkane occurs when the system is subjected to MAS, under conditions of temperature and concentration that would be expected to give a homogeneous solution. To investigate this phenomenon in more detail, we have carried out systematic studies of the effects of MAS on the miscibility of binary liquid mixtures.

Results

We focus on the miscibility of a mixture of undecane (6.6 wt%) and methanol. At 50 °C and with MAS at 12 kHz, the ^{13}C direct-excitation NMR spectrum (Figure 1, black) has five peaks, indicating a homogeneous undecane/methanol solution phase (the ^{13}C resonances for the three central CH_2 groups of undecane are unresolved). On decreasing temperature to 40 °C or below, a new set of peaks appears at higher ppm, indicating the appearance of a second phase which we ascribe to either pure undecane or an undecane-rich phase, as seen at 20 °C in Figure 1 (green).

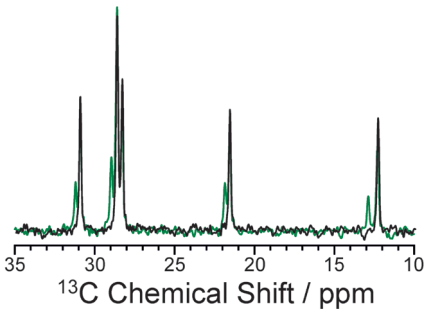

Figure 1. ^{13}C MAS NMR spectra (20 T) of undecane in methanol at 20 °C (green) and 50 °C (black) with MAS at 12 kHz.

Holding the sample at 40 °C and decreasing the MAS frequency from 12 kHz has no observable effect until the MAS frequency reaches 1 kHz (Figure 2). With MAS at 1 kHz, the additional peaks disappear, indicating that the mixture becomes miscible only at this very slow frequency.

Discussion

Our results demonstrate that, except at sufficiently high temperature, the solution of undecane in methanol tends to undergo phase separation when subjected to MAS. At 40 °C, a homogeneous solution is formed only when the MAS frequency is 1 kHz or lower. For a MAS frequency of 1 kHz, the maximum centripetal pressure experienced by the solution is estimated to be *ca*. 2.5 × 10^4 Pa. For a MAS frequency of 2 kHz (at which phase separation is observed), the maximum centripetal pressure is *ca*. 10^5 Pa. Thus, at 40 °C, phase separation is induced by an *increase* in pressure of part of the solution by only *ca*. 0.25 - 1.00 atm.

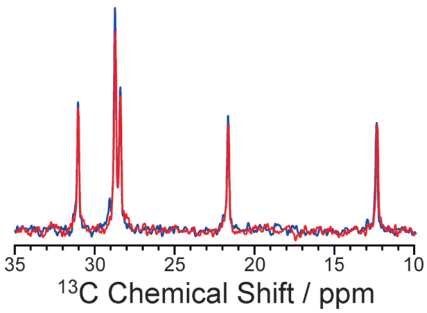

Figure 2. ^{13}C MAS NMR spectra (20 T) of undecane in methanol at 40 °C with MAS at 12 kHz (blue) and 1 kHz (red).

Concluding Remarks

Even low MAS frequencies have an effect on the miscibility of undecane/methanol solutions. Beyond the consequences for our studies of crystallization of alkane/urea inclusion compounds from methanol, we may conclude that, for some systems, miscibility of solvent mixtures and hence solubility in such mixed solvents may be affected critically by MAS. Further studies are required to understand why the miscibility of long-chain alkanes in methanol is particularly susceptible to the pressure changes induced by MAS.

References

1. Hughes, C. E.; Williams, P. A.; Harris K. D. M. *Angew. Chem. Int. Ed.* **2014**, *53*, 8939.
2. Harris, K. D. M.; Hughes, C. E.; Williams, P. A. *Solid State Nucl. Magn. Reson.* **2015**, *65*, 107.

In-situ NMR Study of Crystallization of Menthol from the Melt

Colan E. Hughes, P. Andrew Williams and Kenneth D. M. Harris

School of Chemistry, Cardiff University

Overview

While most of our previous *in-situ* NMR studies[1] have focused on crystallization from solution, we are now extending such studies to crystallization from the molten state. We chose to study menthol as polymorphism has been reported for both L-menthol and DL-menthol in previous work[2] in which crystallization from the melt was studied indirectly using differential scanning calorimetry (DSC).

Results

In-situ NMR studies of crystallization were carried out with both slow cooling and fast cooling (so-called quenching). In slow cooling (0.25 °C/min) of DL-menthol, a previously unreported glass transition was observed after *ca*. 25 mins, leading to the appearance of broad peaks in ^{13}C CP MAS NMR spectra (Figure 1) due to the amorphous phase and disappearance of the signal in ^{13}C direct-excitation NMR spectra. At *ca*. 45 mins, the amorphous solid was observed to crystallize as the α polymorph. In the slow cooling of L-menthol (Figure 2), a glass transition was not observed. Instead, after *ca*. 25 mins, the melt crystallized directly to form the α polymorph.

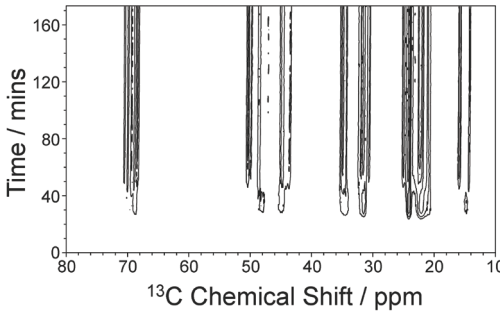

Figure 1. In-situ ^{1}H→^{13}C CP MAS (12 kHz) NMR spectra (20 T) of DL-menthol recorded on slow cooling of the melt.

Experiments with fast cooling (to different temperatures between 5 and 15 °C) were carried out on both DL- and L-menthol. In all cases, the only solid product was the α polymorph of DL- or L-menthol, with no evidence for the transient formation of any other solid forms. The same observations were made in further experiments in which the MAS frequency was reduced as low as 2 kHz.

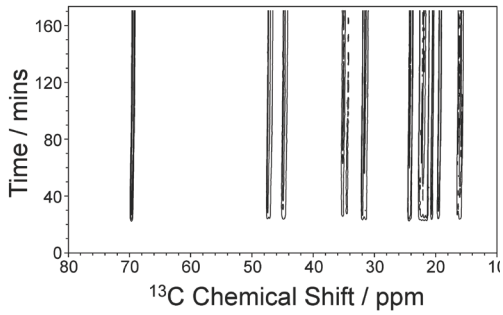

Figure 2. In-situ ^{1}H→^{13}C CP MAS (12 kHz) NMR spectra (20 T) of L-menthol recorded on slow cooling of the melt.

Discussion

Under the conditions of the fast cooling experiments, we anticipated, on the basis of the previous DSC study,[2] that the β polymorphs of DL- and L-menthol might be observed. The absence of any evidence for these polymorphs could suggest one of three possibilities: (i) the cooling rate may have been too slow, (ii) the pressure due to MAS may have prevented the formation of the β polymorphs, and/or (iii) in the case of DL-menthol, the formation of the amorphous phase (not reported in the previous DSC work) may have inhibited crystallization *via* the β polymorph.

Concluding Remarks

There is currently considerable interest in the role played by amorphous phases in crystallization processes, as such phases may act as intermediates in two-step crystallization mechanisms, contrasting with the single-step mechanism of classical nucleation theory. The results reported here demonstrate that *in-situ* NMR can readily detect amorphous phases (in contrast to diffraction techniques), pointing the way towards further experiments on crystallization from solution aimed at detecting amorphous intermediates.

References

1. Harris, K. D. M.; Hughes, C. E.; Williams, P. A. *Solid State Nucl. Magn. Reson.* **2015**, *65*, 107.
2. Corvis, Y.; Négrier, P.; Massip, S.; Leger, J.-M.; Espeau, P. *CrystEngComm* **2012**, *14*, 7055.

Application of CLASSIC NMR to Study Cement Hydration

Colan E. Hughes,[1] Laura J. Gardner,[2] Samuel A. Walling,[2] Dale Prentice,[2] Lucas S. Girotto,[3] Ana Paula Kirchheim,[3] Susan A. Bernal,[2] John L. Provis[2] and Kenneth D. M. Harris[1]

[1]*School of Chemistry, Cardiff University*

[2]*Department of Materials Science and Engineering, University of Sheffield*

[3]*NORIE, Universidade Federal do Rio Grande do Sul, Brazil*

Overview

The setting of cement occurs through a complex series of hydration reactions. Given that commercial cements typically contain several active components, elucidating the full chemical pathway is an enormous challenge. To address this problem, our CLASSIC NMR technique[1,2] has been applied for *in-situ* studies of both liquid- and solid-state NMR spectra during hydration reactions involving various components of cement. Focusing on aluminate containing cements, we have exploited ^{27}Al NMR to reveal the species present during the first stages of cement hydration.

Results and Discussion

Initially, hydration of calcium aluminate ($CaAl_2O_4$), a component used in some "quick-setting" cements, was carried out at 20 °C. Figure 1 shows ^{27}Al NMR spectra of the product phase as a function of reaction time. The reaction is initially slow but accelerates after *ca*. 16 hrs. Hydration at 60 °C revealed a much faster initial reaction rate, leading to a different product from that formed at 20 °C. This observation is consistent with literature reports that calcium aluminate decahydrate ($CaAl_2O_4{\cdot}10H_2O$) is produced at low temperature and hydrogarnet ($Ca_3Al_2O_6{\cdot}6H_2O$) is produced at higher temperature.

We have also studied a number of components relating to white Portland cement. Figure 2 shows ^{27}Al NMR spectra recorded during hydration of cubic tricalcium aluminate (top) and sodium-doped orthorhombic tricalcium aluminate (bottom), each mixed with gypsum and water. At early age (within the first four hours of hydration), there are clear differences in the behaviour of the two tricalcium aluminate polymorphs. In particular, the sodium-doped orthorhombic phase dissolves more rapidly and yields an initial transient phase before stabilizing, which is not observed for the cubic tricalcium aluminate.

Concluding Remarks

The ability to use *in-situ* NMR to probe the chemical processes that take place during cement hydration, presented here with a focus on the aluminate phases responsible for many of the early-age setting characteristics of cements, provides a new level of power and insight in the analysis of these materials and the mechanisms by which they gain strength during hydration.

References

1. Hughes, C. E.; Williams, P. A.; Harris K. D. M. *Angew. Chemie Int. Ed.* **2014**, *53*, 8939.
2. Harris, K. D. M.; Hughes, C. E.; Williams, P. A. *Solid State Nucl. Magn. Reson.* **2015**, *65*, 107.

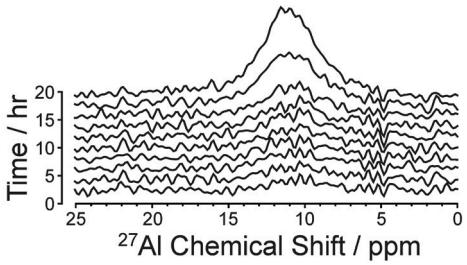

Figure 1. In-situ ^{27}Al direct-excitation MAS (10 kHz) NMR spectra (20 T) of the hydration product of calcium aluminate at 20 °C.

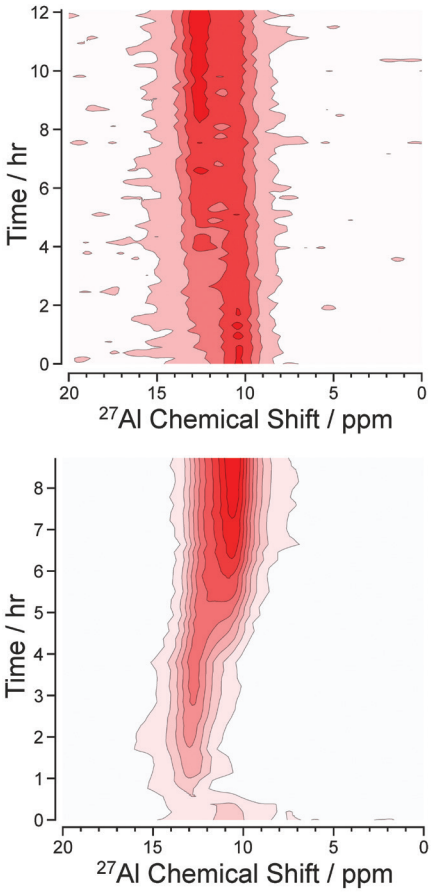

Figure 2. In-situ ^{27}Al direct-excitation MAS (10 kHz) NMR spectra (20 T) of tricalcium aluminate (top) and sodium-doped tricalcium aluminate (bottom) hydrating in the presence of gypsum.

^{1}H Solvent Paramagnetic Relaxation Enhancements as a Tool for Probing Interaction Interfaces in Large Complexes

Jonathan M. Lamley,[1] Carl Öster,[1] Simone Kosol,[1] Dinu Iuga,[2] Ago Samoson,[3] and Józef R. Lewandowski[1]

[1]*Department of Chemistry, University of Warwick*

[2]*Department of Physics, University of Warwick*

[3]*Technical University of Tallinn, Estonia*

Overview

Formation of protein-protein complexes is commonly exploited in the regulation of biological processes. Consequently, the knowledge of protein-protein interactions is central to understanding molecular level details of these processes. Thanks to truly impressive methodological progress over the last five years, solid-state NMR has become a real alternative high-resolution approach to obtain atomic resolution information on protein-protein complexes.[1,2] Such applications are possible because, in the solid state and unlike in the solution state, due to the lack of overall tumbling, the NMR line widths are independent of the size of the system.

There are different approaches one can take to characterise protein-protein interfaces. In solution NMR, an increasingly popular method to determine protein-protein interaction sites is to use solvent Paramagnetic Relaxation Enhancements (PREs).[3] In this approach, the increase in ^{1}H relaxation rates is monitored as a function of concentration of paramagnetic dopants.[4] For the solvent accessible residues, the relaxation rates increase quickly as a function of concentration due to enhanced paramagnetic relaxation. For the residues involved in the protein-protein interface and thus with low solvent accessibility the measured relaxation rates increase only moderately or not at all under the same conditions.

^{1}H is an ideal nucleus for measuring solvent PREs due to very strong paramagnetic effects and thus the long-range nature of the probe (on the order of 20 Å).[4] However, in the solid state similar implementations are not possible under most conditions because of the very strong ^{1}H-^{1}H diffusion, which leads to averaging of the relaxation rates from different sites and loss of site-specific information. However, it has been reported that at 100 kHz spinning ^{1}H-^{1}H spin diffusion is supressed sufficiently that site-specific variation in the rates is observed.[5] The suppression of ^{1}H-^{1}H spin diffusion also can be enhanced by diluting the proton network by deuteration.[6]

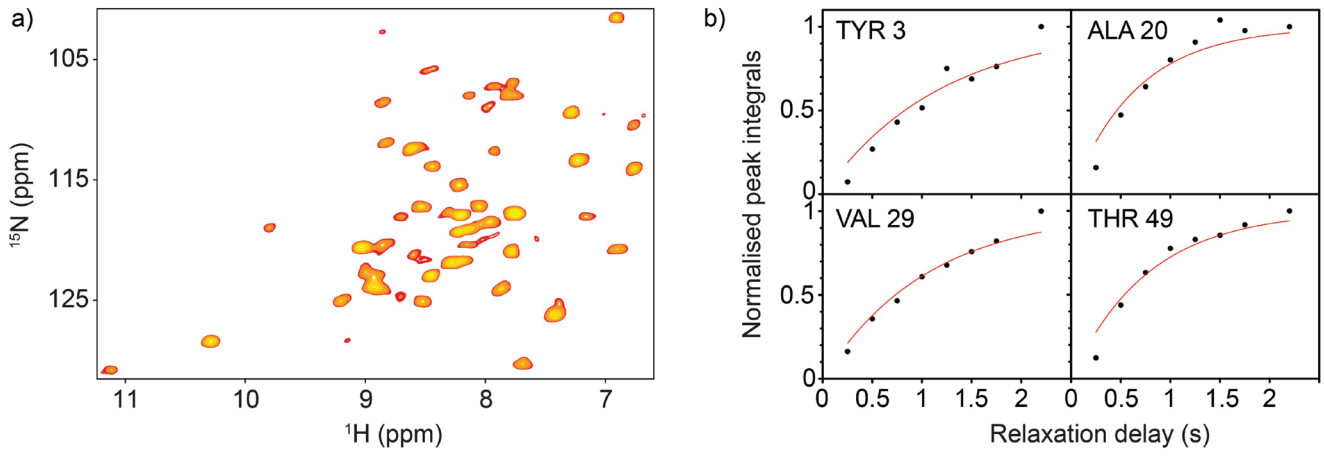

Figure 1. (a) A 2D ^{15}N-^{1}H correlation spectrum of 100% H_2O [U-^{2}H,^{13}C,^{15}N]GB1 in a complex with human immunoglobulin. (b) Example saturation recovery curves from measurement of ^{1}H spin-lattice relaxation on the complex. Experiments were performed at ν_r = 100 kHz and ν_0(^{1}H) = 850 MHz using a Samoson 0.81 mm MAS probe.

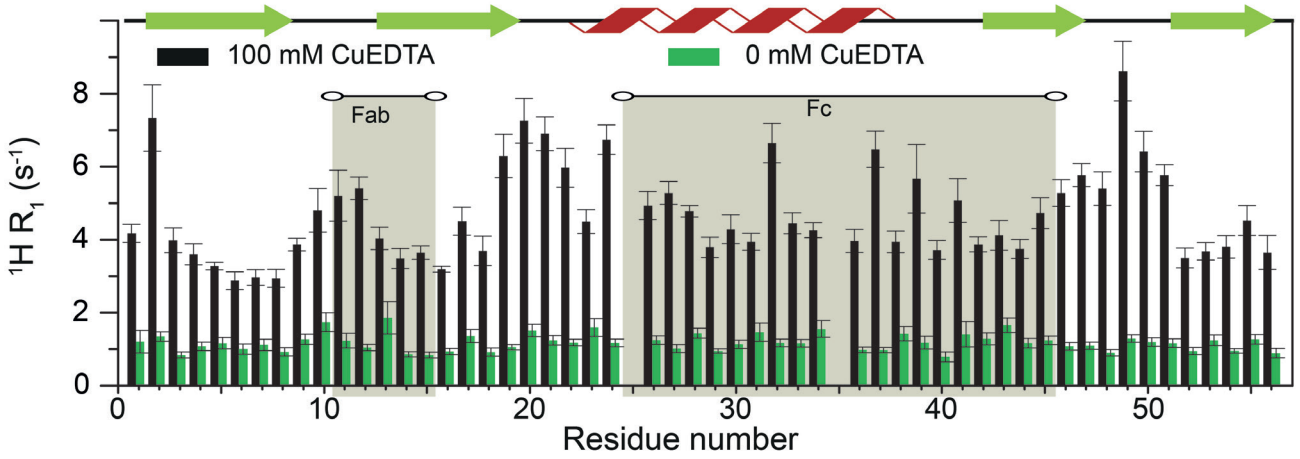

Figure 2. Comparison of ^{1}H R_1 relaxation measurements on 100% H_2O [U-^{2}H,^{13}C,^{15}N] GB1:IgG complex in the presence and absence of 100 mM CuEDTA. Experiments were performed at ν_r = 100 kHz and $\nu_0(^1H)$ = 850 MHz using a Samoson 0.81 mm MAS probe.

In this project, we demonstrate that solvent PREs based on measurements of ^{1}H spin-lattice relaxation at 100 kHz spinning can be used to characterise protein-protein interface in a > 300 kDa precipitated complex of GB1 with full length immunoglobulin G (IgG).[1]

^{1}H Solvent PREs

Figure 1a shows an example of a 2D ^{1}H-^{15}N correlation spectrum obtained on the 100% H_2O [U-^{2}H,^{13}C,^{15}N]GB1:IgG complex. Figure 1b shows example saturation recovery curves illustrating the quality of the ^{1}H R_1 relaxation measurements.

Figure 2 shows a comparison of ^{1}H R_1 rates measured in the complex in the presence and absence of 100 mM CuEDTA. In the presence of the paramagnetic dopant we observe an increase of the rates for all residues as expected from the long range of the ^{1}H solvent PREs. However, the increase is not uniform and the solvent accessible parts of GB1 are characterised by significantly enhanced rates. The large variations in the rates from residue to residue indicate that ^{1}H-^{1}H spin diffusion is well-supressed. The pattern of the solvent PREs confirm the extensive binding interface in the complex with only loops 2 and 4 being solvent accessible.

References

1. Lamley, J. M.; Iuga, D.; Öster, C.; Sass, H.-J.; Rogowski, M.; Oss, A.; Past, J.; Reinhold, A.; Grzesiek, S.; Samoson, A.; Lewandowski, J. R. *J. Am. Chem. Soc.* **2014**, *136*, 16800.
2. Barbet-Massin, E.; Huang, C.-T.; Daebel, V.; Hsu, S.-T. D.; Reif, B. *Angew. Chem. Int. Ed.* **2015**, *54*, 4367.
3. Madl, T.; Bermel, W.; Zangger, K. *Angew. Chem. Int. Ed. Engl.* **2009**, *48*, 8259.
4. Hocking, H. G.; Zangger, K.; Madl, T. *ChemPhysChem* **2013**, *14*, 3082.
5. Ye, Y. Q.; Malon, M.; Martineau, C.; Taulelle, F.; Nishiyama, Y. *J. Magn. Reson.* **2014**, *239*, 75.
6. Del Amo, J. M. L.; Agarwal, V.; Sarkar, R.; Porter, J.; Asami, S.; Rübbelke, M.; Fink, U.; Xue, Y.; Lange, O. F.; Reif, B. *J. Biomol. NMR* **2014**, *59*, 241.

Exploiting ^{17}O Enrichment to Understand ADORable Zeolites

Giulia P. M. Bignami, Daniel M. Dawson, Sharon E. Ashbrook and Russell E. Morris

School of Chemistry, EaStCHEM and Centre of Magnetic Resonance, University of St Andrews

Overview

The great utility and importance of zeolites in industry drives considerable work to develop new structural architectures with novel adsorption and catalytic properties. Hydrothermal synthesis and related solution-mediated techniques have dominated the field for many years. Recently, however, manipulation of zeolites into hierarchical porous structures and ultra-thin layers has also risen to great prominence as a method of introducing new features into zeolites.[1-3] The journal Science rated this type of research as one of the ten most important areas of current science.[4] In preliminary work, we have developed unprecedented routes to new zeolitic materials, which we are calling the assembly-disassembly-organisation-reassembly (ADOR) method.[5,6] Following this synthetic method, solids with targeted structures can be obtained by selectively disassembling a pre-prepared parent zeolite and then reassembling the products into a new topology, as shown in Figure 1. However, the hydrolytic mechanisms underlying the ADOR method are not entirely understood, requiring further investigation of the chemical and structural changes resulting from hydrolysis.

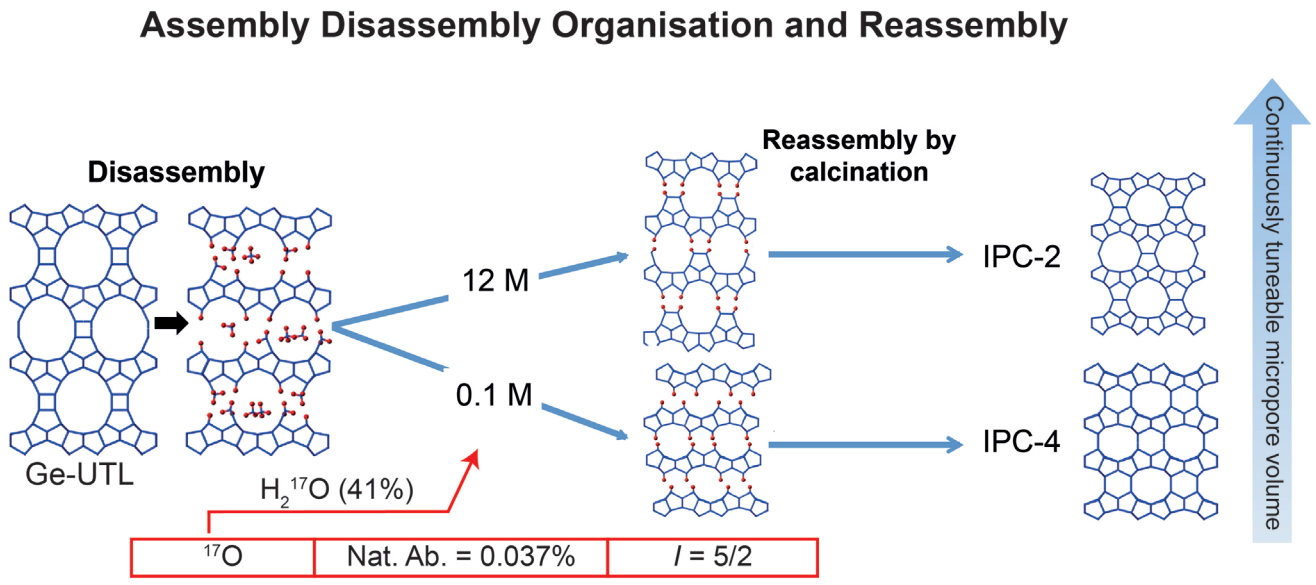

Figure 1. Schematic representation of the ADOR process with the ^{17}O enrichment pathway highlighted. The initial disassembly of the materials is independent of the hydrolysis conditions but, upon heating at 95 °C, the acid concentration makes a significant difference and the final material formed is dependent on two competing reactions, silica re-organisation and de-intercalation, yielding the two new zeolites, IPC-2 and IPC-4, respectively. Consequently, by controlling the acidity in the disassembly step, different outcomes can be targeted and the porosity of the final material can be tuned over a wide range.

^{17}O NMR spectroscopy can be usefully applied to the study of this type of material, aiming, in particular, to gain a detailed knowledge of the kinetic mechanism and structural outcomes deriving from the interaction of the zeolitic framework with water. ^{17}O is not commonly used for the NMR characterisation of zeolites because of its very low natural abundance (0.037%), moderate gyromagnetic ratio and quadrupolar nature (I = 5/2). For these reasons, to allow a complete and high-resolution spectroscopic investigation of the zeolitic structures, small-scale synthetic processes for isotopic enrichment have been optimised and successfully implemented in the ADOR method. Specifically, a Ge-UTL has been used as the parent zeolite and then disassembled in a low-volume hydrolysis using 6 M HCl, freshly prepared from 1.2 ml of 12 M HCl and 1.2 ml of 41% ^{17}O-enriched $H_2{}^{17}O$.

^{17}O NMR

Figure 2a shows a ^{17}O MAS spectrum acquired at 20.0 T using ^{1}H decoupling of an ^{17}O-enriched sample of Ge-UTL hydrolysed for 16 h at 95 °C using the experimental conditions described previously. The sharp signal at –5.5 ppm can be assigned to water, while the signals from the two main oxygen environments[6] present in layered zeolites, bulk Si-O-Si and interlayer Si-OH, remain unresolved. These signals can be resolved using high-field MQMAS experiments (with ^{1}H decoupling), as shown in Figure 2a. The low-intensity signal at δ_2 = 18 ppm aligns with the signal present in a ^{1}H-^{17}O CP spectrum (not shown), attributed to Si-OH. However, ^{1}H-^{17}O CP experiments, while feasible, result in very long acquisition times, due to very fast signal decay during the spin-lock. To overcome this, the multiple-contact CP (MCCP) pulse sequence[7] was used. A substantial saving in acquisition time is obtained as a result of the repeated short CP blocks used in the MCCP sequence circumventing the very fast ^{17}O $T_{1\rho}$ relaxation that affects standard CP experiments. The MCCP and MQMAS pulse sequences were then combined to achieve a pre-selection of the OH environment prior to the triple-quantum experiment. A preliminary MCCP-MQMAS experiment, shown in Figure 2b (along with a MCCP MAS NMR spectrum), shows, albeit with a low signal-to-noise ratio, the near complete removal of the signal from the Si-O-Si bulk environment and the signal from the preselected Si-OH aligned in the indirect dimension to the previously resolved signal in Figure 2a. Future work will involve further investigation of the MCCP pulse sequence on quadrupolar samples, exploiting the sensitivity enhancement resulting from the successfully ^{17}O-enriched hydrolysed sample, to achieve a better understanding of the hydrolytic kinetic mechanism of the ADOR method.

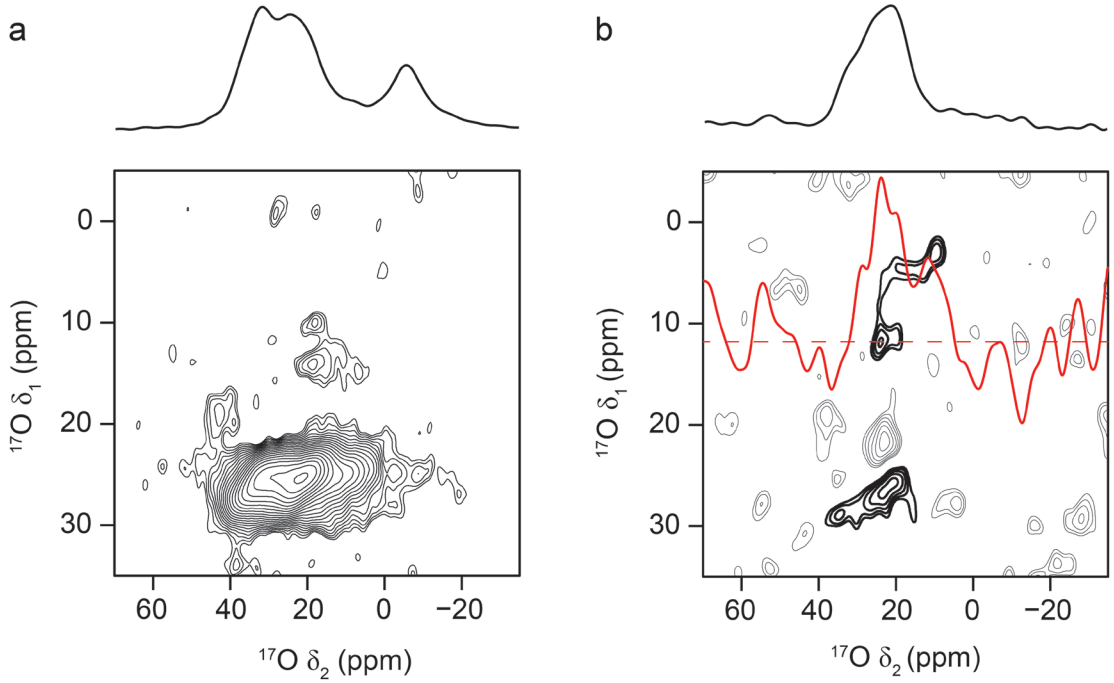

Figure 2. NMR spectra of ^{17}O-enriched hydrolysed Ge-UTL. (a) z-filtered ^{1}H-decoupled (CW) ^{17}O 3Q MAS (20.0 T, 20 kHz MAS, 22 hours), shown with a ^{1}H-decoupled ^{17}O MAS spectrum. (b) z-filtered ^{1}H-decoupled (CW) ^{17}O MCCP-3QMAS spectrum (20.0 T, 20 kHz MAS, 60 hours), shown with a ^{1}H-^{17}O MCCP MAS spectrum. The red line shows a cross-section taken at δ_1 = 11.8 ppm.

References

1. Na, K.; Jo, C.; Kim, J.; Cho, K.; Jung, J.; Seo, Y.; Messinger, R. J.; Chmelka, B. F.; Ryoo, R. *Science* **2011**, *333*, 328.
2. Ng, E.-P.; Chateigner, D.; Bein, T.; Valtchev, V.; Mintova, S. *Science* **2012**, *335*, 70.
3. Zhang, X.; Liu, D.; Xu, D.; Asahina, S.; Cychosz, K. A.; Agrawal, K. V.; Wahedi, Y. A.; Bhan, A.; Hashimi, S. A.; Terasaki, O.; Thommes, M.; Tsapatsis, M. *Science* **2012**, *336*, 1684.
4. *Science* **2011**, *334*, 1629.
5. Roth, W. J.; Nachtigall, P.; Morris, R. E.; Wheatley, P. S.; Seymour, V. R.; Ashbrook, S. E.; Chlubná, P.; Grajciar, L.; Položij, M.; Zukal, A.; Shvets, O.; Čejka, J. *Nature Chemistry* **2013**, *5*, 628.
6. Wheatley, P. S.; Chlubná-Eliášová, P.; Greer, H.; Zhou, W.; Seymour, V. R.; Dawson, D. M.; Ashbrook, S. E.; Pinar, A. B.; McCusker, L. B.; Opanasenko, M.; Čejka, J.; Morris, R. E. *Angew. Chem. Int. Ed.* **2014**, *53,* 13210.
7. Johnson, R. L.; Schmidt-Rohr, K. *J. Magn. Reson.* **2014**, *239*, 44.

Solid-state NMR Investigation of Proteins Bound to F-Actin

Nicola Pace,[1] Steven P. Brown[2] and Mark Pfuhl[1]

[1]*Randall Division, King's College London*

[2]*Department of Physics, University of Warwick*

Overview

Actin is a key protein without which even the most simple processes in a eukaryotic cell would be impossible. Its strong tendency to polymerise and the inability to crystallise the polymeric F-actin have made structural studies very difficult. The best approach to date is the fitting of high-resolution structures of monomeric G-actin, kept in this state by severing proteins bound to it, into F-actin envelopes obtained from electron microscopy or fibre X-ray diffraction.[1,2] The latter two methods operate at very low resolution which precludes the identification of detailed features directly. Furthermore, the observation of proteins bound to F-actin is severely limited to larger proteins which are easy to spot in difference density maps and proteins which are already folded, so that there is a structure that can be docked into any extra density. This means none of the important actin binding proteins that are unfolded in the free state such as calponin and nebulin can be studied.[3]

Surprisingly, despite its great importance, so far F-actin has not been characterised extensively using solid-state NMR.[4,5] Our aim is to use solid-state NMR to obtain detailed structural and functional information for proteins bound to F-actin. We initially start by studying small, F-actin binding proteins in complex with F-actin to evaluate the types of experiments that might be useful and the kind of information that could be obtained. For practical reasons (size, expression, affinity), we have chosen the villin head piece domain (VHD) of ABLIM2 bound to F-actin. Assignment and structure in solution have been obtained and the complex are being characterised extensively by a range of solid-state NMR experiments.

Results

To improve our chances of comprehensively mapping the actin binding surface of VHD, we want to look at amide proton chemical shifts, which together with nitrogen chemical shifts, are the staple of interaction mapping in solution-state NMR. Initial 2D spectra showed slightly broader lines than expected so that we measured ^{1}H and ^{15}N relaxation times to establish if the excessive linewidths were caused by slow internal dynamics or by sample heterogeneity.

Measurement of T_1 and T_2 times of ^{1}H and ^{15}N (approx. ^{1}H T_1 = 2.8 ms, T_2 = 2.72 ms; ^{15}N T_1 = 114 ms, T_2 = 5.9 ms) suggested that dynamics were not responsible for the observed line widths. Using this approach will be useful in the optimisation of sample preparation which is clearly the key for getting high quality ^{1}H detected spectra at higher field strengths.

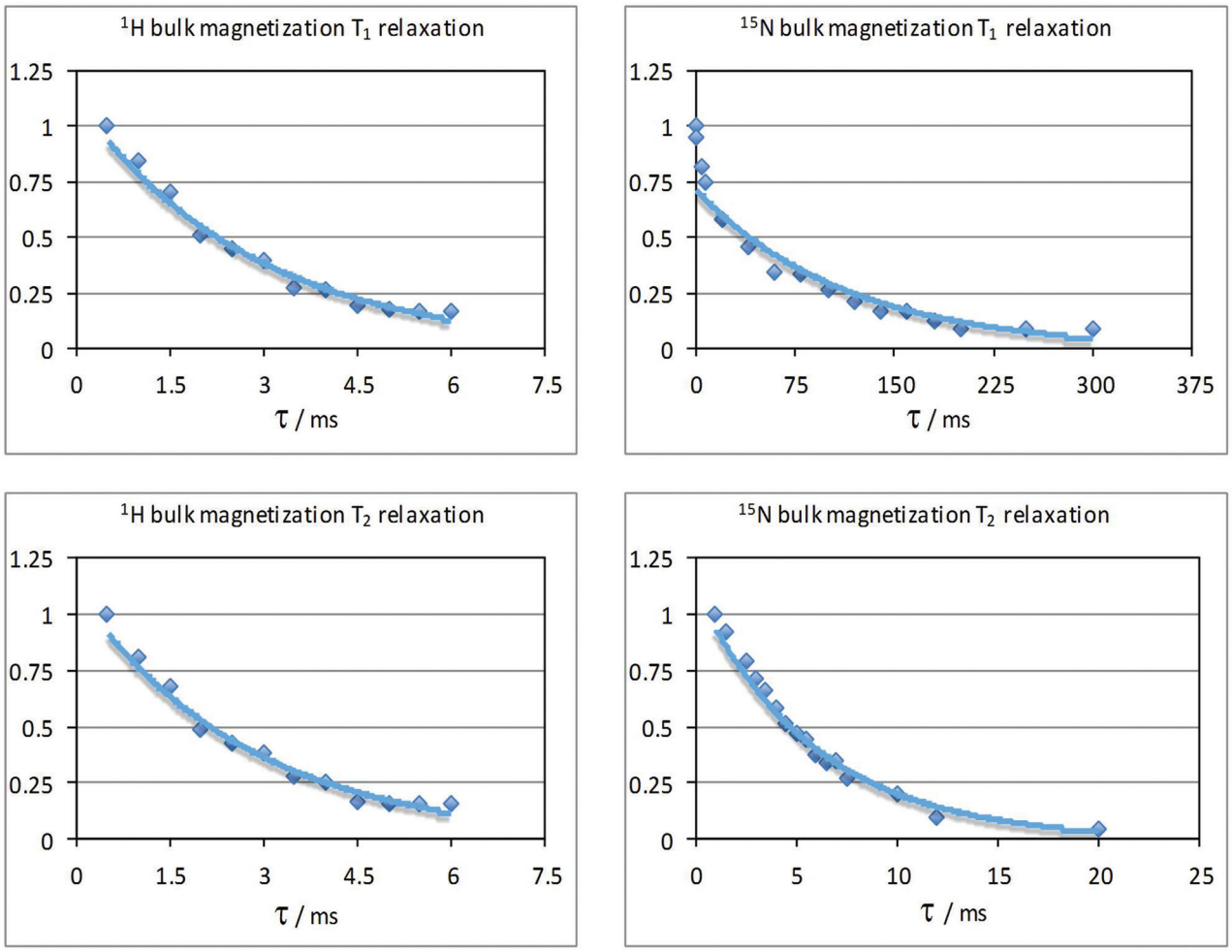

Figure 1: T_1 and T_2 bulk relaxation curves for ^{1}H and ^{15}N of ^{2}H/ ^{15}N/ ^{13}C labelled Villin Headpiece Domain (VHD) of ABLIM2 bound to F-actin at 20 T and 278 K using a MAS frequency of 50 kHz.

References

1. Holmes, K. C. *J. Struct. Biol.* **2010**, *170*, 184.
2. Oda, T.; Iwasa, M.; Aihara, T.; Maeda, Y.; Narita, A. *Nature* **2009**, *457*, 441.
3. Pfuhl, M.; Winder, S. J.; Pastore, A. *EMBO J.* **1994**, *13*, 1782.
4. Phillips, L.; Separovic, F.; Cornell, B. A.; Barden, J. A.; dos Remedios, C. G. *Eur. Biophys. J.* **1991**, *19*, 147.
5. Ahmed, M. A.; Bamm, V. V.; Shi, L.; Steiner-Mosonyi, M.; Dawson, J. F.; Brown, L.; Harauz, G.; Ladizhansky, V. *Biophys. J.* **2009**, *96*, 180.

BRAIN CP Made Simple for Less Common Nuclei (^{87}Sr, ^{137}Ba) and ^{23}Na MAS NMR as a Probe for Temperature Effects in Oxalates

Danielle Laurencin,[1] Christel Gervais,[2] Christian Bonhomme,[2] César Leroy,[2] John V. Hanna[3] and Mark E. Smith[3,4]

[1]*Institut Charles Gerhardt de Montpellier, France*

[2]*LCMCP University Paris 06, France*

[3]*Department of Physics, University of Warwick*

[4]*Vice-Chancellor's Office and Department of Chemistry, Lancaster University*

Overview

The application of ever higher magnetic fields to the study of quadrupolar nuclei in solids is opening the way to an increasing number of advanced sequences, such as BRAIN CP.[1] Development of the BRAIN CP experiment is being undertaken for unusual *half-integer* spin nuclei such as ^{87}Sr (I = 9/2) and ^{137}Ba (I = 3/2). To the best of our knowledge, BRAIN CP has never been implemented for quadrupolar nuclei (apart from ^{14}N, integer I = 1 spin). ^{23}Na MAS NMR was used to investigate some potentially important bidendate ligand compounds such as oxalates. Such ligands play a crucial role in pathological calcifications. Hydrated sodium hydrogenoxalate ($NaHC_2O_4.H_2O$) was studied by variable temperature experiments (varying the rotation frequency of the 3.2 mm rotor from 5 to 20 kHz). It is clearly demonstrated that subtle variations in δ_{iso}(^{23}Na) (< 0.4 ppm) could be observed with an increase of the sample temperature. Such variations were shown to be reversible and are of potentially key importance for further validation of "temperature effects" in GIPAW calculations, as implemented very recently by Nemausat *et al.*[2]

^{87}Sr BRAIN CP NMR of Labelled Strontium Malonate

CP transfer from the ^{1}H spin bath to quadrupolar nuclei remains a complex problem from both theoretical and experimental points of view. The problem of excitation during the CP transfer is partially circumvented by implementing the BRAIN approach recently developed by Harris *et al*.[1] Here, we applied the BRAIN sequence for the first time to a "strong" quadrupolar nucleus (^{87}Sr). In particular, the following experimental points were carefully optimised (starting from labeled strontium malonate): WURST excitation during the contact time (definition of the shape, duration of the contact pulse, shape on the ^{1}H channel, nutation frequencies for both channels), WURST shape during the acquisition of the echoes and {^{1}H} decoupling. Figure 1 shows a comparison between direct acquisition (DFS, WURST, QCPMG) and BRAIN CP VOCS acquisition. The result is very encouraging though the most deshielded part of the spectrum was underestimated under BRAIN conditions (even by adding more offsets on the left part of the spectrum). Work is currently in progress in order to extend the ^{87}Sr and ^{137}Ba BRAIN CP approach to non-labelled samples and preliminary tests on how to use the CP transfer more specifically for spectral editing have been performed.

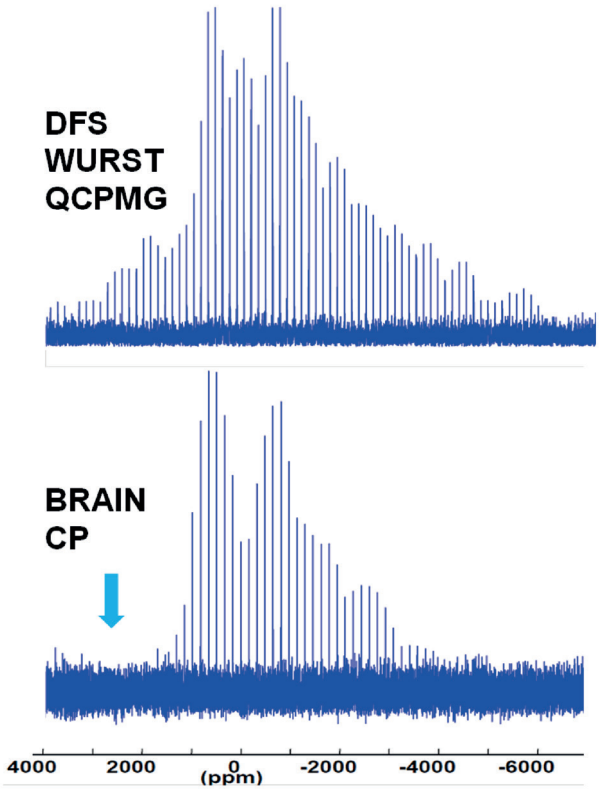

Figure 1. ^{87}Sr (20.0 T) static spectra of labelled strontium malonate. Top: DFS WURST QCPMG (1 offset, ~ 20 minutes). Bottom: BRAIN CP (from ^{1}H) VOCS (6 offsets, ~ 1h per offset). Arrow shows the under estimation of the intensity under BRAIN conditions.

^{23}Na MAS NMR of Hydrated Sodium Hydrogenoxalate

Hydrated oxalate derivates (mainly calcium) are of fundamental importance for the description of pathological calcifications such as kidney stones. They correspond to the main inorganic phases found in such natural biominerals. Large crystals of monohydrated sodium oxalate, $NaHC_2O_4.H_2O$, were synthesised by implementing the slow diffusion of solutions of sodium cations and oxalate anions in an agar-agar medium. The inset on the left part of Figure 2 presents the whole ^{23}Na MAS NMR spectrum recorded at moderate rotation frequency, ν_{rot} (here 5 kHz). The spectrum corresponds to the superposition of a unique central transition (CT) (in agreement with crystallographic data) and its spinning sidebands, as well as spinning sidebands of the satellite transitions (ST). The following set of parameters could be extracted by simulating the spectrum: $\delta_{iso}(^{23}Na)$ = 2.40 ppm, $C_Q(^{23}Na)$ = 1.86 MHz, $\eta_Q(^{23}Na)$ = 0.33. Very interestingly, the progressive increase of ν_{rot} (from 5 to 20 kHz) led to a slight *reversible* change of shielding of the NMR resonance (estimated as –0.35 ppm). Such a small variation of $\delta_{iso}(^{23}Na)$ is clearly a challenge in terms of *ab initio* calculations of NMR parameters[2] using the DFT approach under periodic boundary conditions (GIPAW). However, $C_Q(^{23}Na)$ calculations could be of particular interest to further validate such an approach. In order to reach the most accurate determination of the experimental quadrupolar (and CSA) parameters, TOP processing[3] was implemented (see the inset on the right-hand side of Figure 2). This processing produces effectively "infinite" rotation spectra for the CT and ST. As the ST powder pattern is much broader than that of the corresponding CT, highly accurate CSA, $C_Q(^{23}Na)$, $\eta_Q(^{23}Na)$ parameters and Euler angles orienting both tensors are obtained by detailed fitting. We notice here that other NMR parameters ($\delta_{iso}(^1H)$ = 4.9 (H_2O) and 15.6 ppm (COOH), and $\delta_{iso}(^{13}C)$ = 164.9 (COOH) and 166.1 ppm (COO^-)) could act as pertinent indicators in the frame of variable temperature experiments and GIPAW calculations.

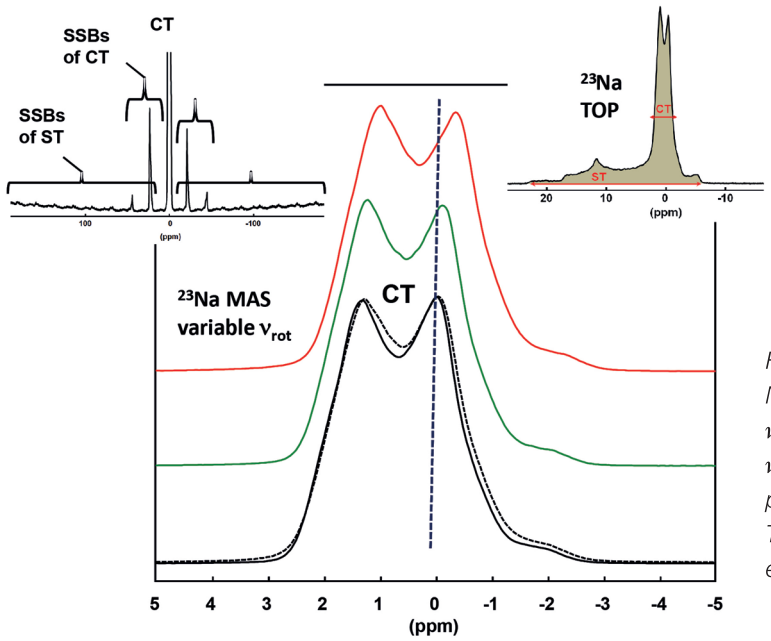

Figure 2. ^{23}Na (20.0 T) MAS spectra of $NaHC_2O_4.H_2O$. Black (solid) line: ν_{rot} = 5 kHz. Green: ν_{rot} = 10 kHz. Red: ν_{rot} = 20 kHz. Black (dashed) line: ν_{rot} = 5 kHz (back from 20 kHz). 3.2 mm MAS Bruker probe. {^{1}H} high-power decoupling (SPINAL-64). The vertical dashed line is used as a guide to estimate the shift of the ^{23}Na line vs ν_{rot}.

References

1. Harris, K. J.; Lupulescu, A.; Lucier, B. E. G.; Frydman, L.; Schurko, R. W. *J. Magn. Reson.*, **2012**, *224*, 38.
2. Nemausat, R.; Cabaret, D.; Gervais, C.; Brouder, C.; Trcera, N.; Bordage A.; Errea, I.; Mauri, F. *Phys. Rev. B*, **2015**, *92*, 144310.
3. Massiot, D.; Hiet. J.; Pellerin, N.; Fayon, F.; Deschamp, M.; Steuernagel, S.; Grandinetti, P.J. *J. Magn. Reson.*, **2006**, *181*, 310.

Mediation Mechanism of Tyrosine 185 on the Retinal Isomerization Equilibrium and the Proton Release Channel in the Seven-Transmembrane Receptor Bacteriorhodopsin

Xiaoyan Ding,[1] Xin Zhao[1] and Anthony Watts[1,2]

[1]*Shanghai Key Lab of Magnetic Resonance, East China Normal University, China*

[2]*Department of Biochemistry, University of Oxford*

Overview

Bacteriorhodopsin (bR), a member of the microbial rhodopsin family of seven-transmembrane receptors, functions as a light-driven proton pump for light energy capture in *Halobacterium salinarum*.[1] The retinal (Ret) chromophore is covalently bound to Lys216 on helix G to form a protonated Schiff base (SB).[2] In the dark, two Ret isomers, 13-cis, 15-syn Ret (bR_{cis}) and all-trans, 15-anti Ret (bR_{trans}), are thermally interconvertible with a molar ratio close to 1:1.[3-6] The *cis-trans* thermal equilibrium of the Ret chromophore occurs in many bacterial rhodopsins in their native membrane; however, the mechanism by which this equilibrium is maintained is not well described, and the direct demonstration of electrostatic coupling leading to conformational changes within proteins that explore multiple equilibria of states, is still challenging. In this study, two-dimensional (2D) magic-angle spinning solid-state NMR of specifically labeled bR, reinforced with light-induced transient absorption measurements, molecular dynamics (MD) simulations and site-directed mutagenesis was used to examine how Y185 interacts with the Ret chromophore and modulates the proton release channel through aspartic acid 212 (D212) in its natural membrane environment. We first show that Y185 both maintains the *cis-trans* isomerization thermal equilibrium of the Ret chromophore, and retains aspartic acid 212 in a favorable conformation through a hydrogen bond to produce a cascade of conformational changes associated with photoreactions with the appropriate lifetime. Removal of the phenolic hydroxyl group in the Y185F mutant shifts the *cis-trans* isomerization thermal equilibrium to a bR_{cis}-dominated state and causes a weakening of the M state, loss of the O state and elongation of the proton pump cycle time.

Results

Figure 1 shows a 2D PDSD spectra of the [U-$^{13}C_9$, ^{15}N]-Tyr and [10, 11, 14, 15-$^{13}C_4$]-Ret-labeled bR purple membrane recorded at the 850 MHz Facility at –65 °C, and superimposed ^{13}C–^{13}C correlation spectra of the [10, 11, 14, 15-$^{13}C_4$]-Ret-labelled WT-bR with Y185F mutant in the dark-adapted membrane. It is clear that coupling of Tyr185 with the retinal chromophore in the dark purple membrane has been observed for the first time. Our results show that the cis-trans thermal equilibrium of the retinal chromophore isomerization is maintained by coupling with Tyr185 through differential electrostatic interactions, and the *cis-trans* thermal isomerization equilibrium of the Ret chromophore is shifted to a new position dominated by bR_{cis}.

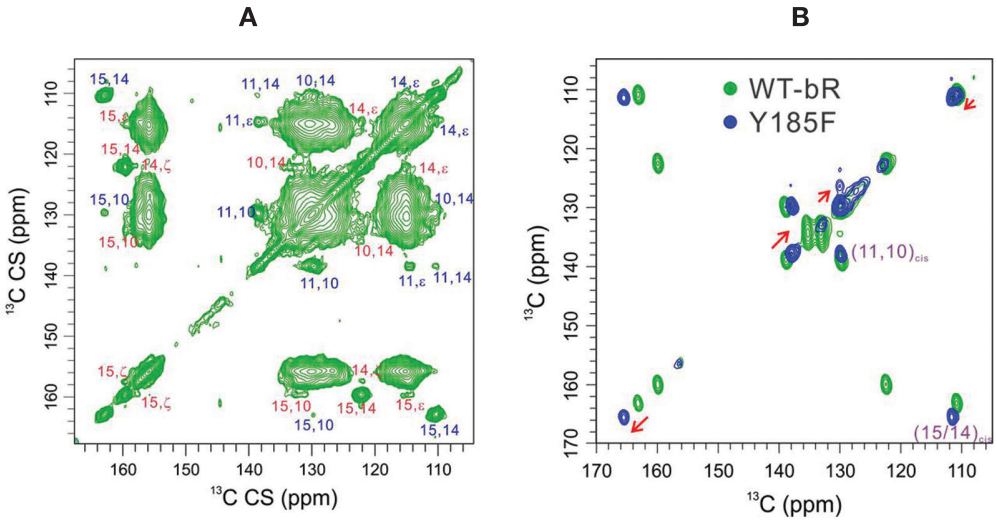

Figure 1. (A) 2D PDSD NMR spectra of the [U-$^{13}C_9$, ^{15}N]-Tyr and [10, 11, 14, 15-$^{13}C_4$]-Ret-labeled bR purple membrane. Cross-peak assignments are highlighted in blue for the correlations in bR_{cis} and red for the correlations in bR_{trans} between the aromatic ring of Tyr185 and the four labeled carbon sites of the retinal polyene chain recorded at the 850 MHz Facility at −65 °C; (B) Superimposed ^{13}C–^{13}C correlation NMR spectra of the [10, 11, 14, 15-$^{13}C_4$]-Ret-labelled WT-bR with Y185F mutant in the dark-adapted membrane on the 600 MHz spectrometer at −25 °C.

Y185 not only mediates the isomerization and binding of the Ret chromophore, but also mediates the H-bonding network around D85-D212-R82 in the proton pumping channel. Removal of the phenolic hydroxyl group in the Y185F mutant causes the guanidine group of R82 to swing upwards by approximately 3 Å and from MD to form a direct H-bond with D212 to stabilize its conformation in the inactive state, which in turn weakens the formation of the M state. Removal of the phenolic hydroxyl group in the Y185F mutant further affects the H-bonding network along the proton pumping channel. The crystal structure shows that the guanidine group of R82 needs to rotate downwards to form H-bonds with E194 and E204 to maintain the conformation for the proton release out of the extracellular side in the M state.[2] However, this rotation needs to swing over a much longer distance to establish the H-bond network with E194 and E204 to maintain the conformation required for proton release, and assist the proton release for the Y185F mutant. More time is required to cover a longer distance, which implies a weak formation and decay of the M state in the Y185F mutant, as shown in Figure 2.

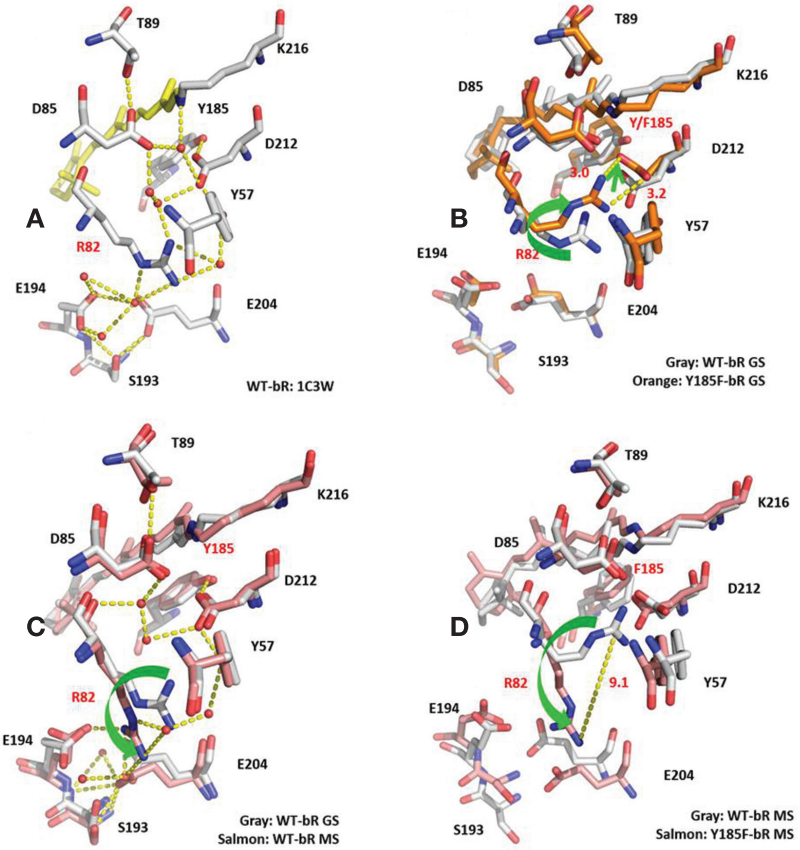

Figure 2. (A) Crystal structure of the region around Ret-D85-D212-R82 H-bonding network in the bR ground state; (B) superposition of the WT-bR and Y185F-bR structures in the ground state; (C) superposition of crystal structures of the ground state and M state; (D) superposition of the WT-bR and Y185F-bR structures in the M state.

In summary, these studies have shown that the equilibrium that is not accessible from crystal structural models, but requires NMR to define equilibrium states, has given new insights into how the retinal isomerization is coupled with the proton release channel and the bR photocycle. Our studies further demonstrate that a high field magnet (850 MHz here) is essential to provide high sensitivity for acquiring a 2D spectra of a protein in an active state in as short a time as possible, and also to resolve an inward shift of a small separated chemical shifts of the ligand in the active state, which cannot be achieved on a lower-field spectrometer.

References

1. Oesterhelt, D.; Stoeckenius, W. *Nature New Biol.* **1971**, *233*, 149.
2. Luecke, H.; Schobert, B.; Richter, H. T.; Cartailler, J. P.; Lanyi, J. K. *Science* **1999**, *286*, 255.
3. Oesterhelt, D.; Meentzen, M.; Schuhmann, L. *Eur. J. Biochem.* **1973**, *40*, 453.
4. Sperling, W.; Carl, P.; Rafferty, C. N.; Dencher, N. A. *Biophys. Struct. Mech.* **1977**, *3*, 79.
5. Stoeckenius, W.; Lozier, R. H.; Bogomolni, R. A. *Biochim. Biophys. Acta* **1979**, *505*, 215.
6. Harbison, G. S.; Smith, S. O.; Pardoen, J. A.; Winkel, C.; Lugtenburg, J.; Herzfeld, J.; Mathies, R.; Griffin, R. G. *Proc. Natl. Acad. Sci. U.S.A.* **1984**, *81*, 1706.

Heterogeneous Biocatalysts: Towards Atomic-Level Structural Characterisation using Solid-State NMR

Sabu Varghese,[1] Peter J. Halling,[2] Stephen Wimperis[1]

[1]*Department of Chemistry, Lancaster University*

[2]*Department of Pure and Applied Chemistry, University of Strathclyde*

Overview

The immobilisation of proteins and living cells on non-biological surfaces plays a central role in a wide range of important technological applications, including industrial biocatalysis, drug delivery, medical diagnosis and biosensing.[1] In particular, immobilised enzymes are widely used in diverse industrial applications including conversion of biomass to oil, synthesis of fine chemicals, pharmaceuticals, food and cosmetics.[1] Although immobilised enzymes on various organic and inorganic surfaces have been extensively characterised by different biochemical methods, the rational design of the biocatalytic system still remains a considerable challenge as very little is known about the state of the enzyme upon immobilisation. Very recently, magic angle spinning (MAS) solid-state NMR has been successfully employed to characterise a heterogeneous biocatalytic system consisting of a model enzyme (α-chymotrypsin), mesoporous silica as the support matrix, and (3-glycidyloxypropyl)trimethoxysilane (GOPS) as the covalent linker.[2] However, the state of the enzyme and its dynamics upon immobilisation are not well understood. The aim of this research work is to provide atomic-level structural and dynamical insights from the model enzyme human carbonic anhydrase II (hCA II) covalently grafted to epoxy-silica in the uniformly and selectively ^{15}N labelled (^{15}N leucine labelled, termed as ^{15}N Leu/hCA II) forms. The biophysical characterisation of the system before and after immobilisation was accomplished using a JEOL fast MAS probe (1.0 mm @ 75 kHz) at the 850 MHz NMR Facility, together with our own NMR spectrometers at Lancaster University (400, 700 MHz).

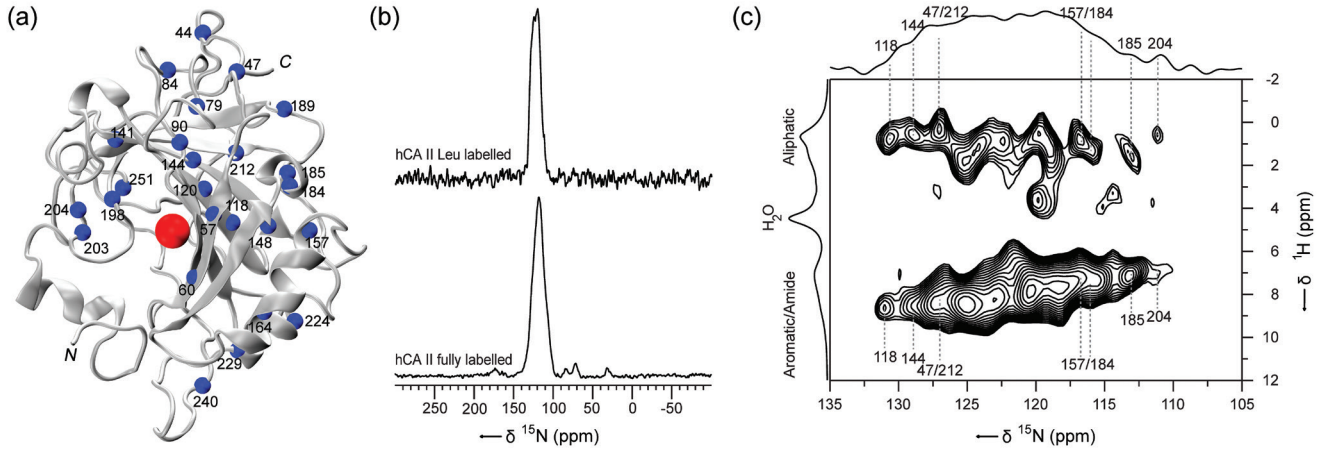

Figure 1. (a) Modified cartoon representation of the crystal structure[3] of hCA II showing the overall distribution of leucine residues (blue spheres) and the active-site zinc (red sphere). The N and C termini of the enzyme are shown in italicised letters and the leucine residues in the sequence are labelled. (b) One-dimensional ^{15}N CP MAS NMR spectra of uniformly ^{15}N labelled hCA II (bottom) and selectively ^{15}N Leu labelled hCA II (top) obtained on a B_0 = 9.4 T spectrometer at a MAS frequency of 10 kHz. (c) Two-dimensional ^{1}H-^{15}N HETCOR (HETeronuclear CORrelation) spectrum of selectively ^{15}N Leu labelled hCA II obtained at 20 T at a MAS frequency of 75 kHz. Identified Leu residues in the hCA II sequence are labelled based on the corresponding solution-state ^{1}H-^{15}N HSQC (Heteronuclear Single Quantum Coherence) NMR spectrum of the same sample.

Results

Since the size of the hCA II (30 kDa) still poses challenges for solid-state NMR and site-specific resonance assignment, the samples were selectively ^{15}N labelled for the most abundant amino acid residue leucine (Figure 1a). Prior to the study of immobilised enzyme on epoxy-silica, we successfully characterised the uniformly ^{15}N labelled hCA II and ^{15}N Leu/hCA II using one-dimensional ^{15}N and two-dimensional ^{1}H-^{15}N CPMAS HETCOR NMR experiments (Figure 1b, c). The one-dimensional spectrum of the fully labelled hCA II shows an intense signal from the backbone amide (100 to 135 ppm) in addition to the weak signals from amino acid residues containing side chain nitrogen (Lys, Arg, His). In contrast, the spectrum of ^{15}N Leu/hCA II shows mainly backbone amide signals from the leucine residues (100 to 135 ppm) and the absence of signals from amino acid residues containing side-chain nitrogens indicates the lack of isotopic scrambling. The two-dimensional ^{1}H-^{15}N HETCOR spectrum (Figure 1c) of ^{15}N Leu/hCA II obtained at higher magnetic field (B_0 = 20 T) at a MAS frequency of 75 kHz is well resolved and site-specific chemical shifts assignments could be obtained that are in good agreement with a corresponding solution-state NMR spectrum.

Figure 2 shows two-dimensional ^{1}H-^{13}C HETCOR spectra of epoxy-silica (Figure 2b) and ^{15}N Leu/hCA II immobilised on epoxy-silica (Figure 2c) acquired using a homonuclear FSLG (Frequency-Switched Lee–Goldberg)[4] decoupling scheme with a contact time of 2 ms. The spectrum of the epoxy-silica (Figure 2b) is characterised by short (one bond) and long-range (more than two bonds) cross-peaks between carbon atoms from the epoxy-silica and the protons directly bonded to the carbons (0 to 3.8 ppm); from the bulk water (4.3 ppm) and also between the hydrogen-bonded water molecules with the surface silanol groups (5.8 ppm). On the other hand, the spectrum of the ^{15}N Leu/hCA II immobilised on epoxy-silica (Figure 2c) is characterised by cross-peaks appearing from the fingerprint regions of the immobilised enzyme (red labels) in addition to the signals from the epoxy-silica (green labels) and bulk water (blue label). Successful covalent grafting of the ^{15}N Leu/hCA II on epoxy-silica is evident from the ^{1}H-^{13}C cross-peaks appearing from the carbonyl, aromatic and aliphatic groups in the protein in addition to the cross-peaks from the epoxy-silica. Based on the resonance assignments, a simplified schematic representation of the different possible silica species present on the epoxy-silica surface and also the grafting of the immobilised enzyme on epoxy-silica could be proposed (Figure 2a).

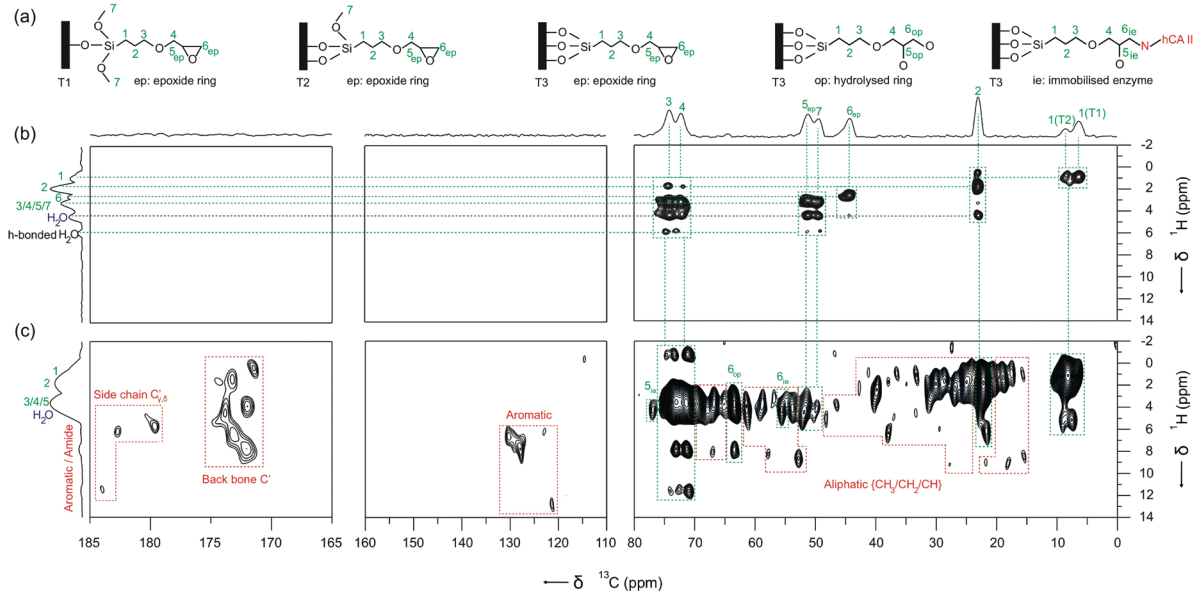

Figure 2. (a) Simplified schematic representation of epoxy-silica surface and hCA II immobilised on an epoxy-silica surface. (b, c) A two-dimensional ^{1}H-^{13}C HETCOR spectra of (b) epoxy-silica and (c) ^{15}N Leu/hCA II immobilised on epoxy-silica acquired using homonuclear FSLG decoupling scheme with a ^{1}H-^{13}C contact time of 2 ms on a B_0 = 9.4 T spectrometer at a MAS frequency of 22 kHz. Chemical shift assignments from the epoxy-silica are shown by green labels and from the fingerprint regions of the immobilised enzyme using red labels.

References

1. Guisan, J. M. *Immobilization of enzymes and cells Methods in Biotechnology* **2006**, *22*, 1.
2. Fauré, N. E.; Halling, P. J.; Wimperis, S. *J. Phys. Chem. C* **2013**, *118*, 1042.
3. Avvaru, B. S.; Kim, C. U.; Sippel, K. H.; Gruner, S. M.; Agbandje-McKenna, M.; Silverman, D. N.; McKenna, R. *Biochemistry* **2010**, *49*, 249.
4. Lee, M.; Goldburg, W. I. *Phys. Rev.* **1965**, *140*, A1261.

Measuring Intermolecular "Through-Space" Homonuclear ^{31}P-^{31}P J Couplings

Paula Sanz Camacho,[1] David McKay,[1] Daniel M. Dawson,[1] Alexandra M. Z. Slawin,[1] Jonathan R. Yates,[2] J. Derek Woollins[1] and Sharon E. Ashbrook[1]

[1]*School of Chemistry, EaStCHEM and Centre of Magnetic Resonance, University of St Andrews*

[2]*Department of Materials, University of Oxford*

Overview

Although the electron-mediated spin-spin, or J, coupling is conventionally viewed as being transmitted *via* covalent bonds, examples of J couplings between atoms that are not formally bonded but are in close proximity (generally termed "through-space" J couplings in the literature) have been reported. Heavy atoms, such as Te and Se, sterically confined in a crowded framework, (*e.g.,* in *peri*-substituted naphthalenes) have been shown to exhibit an intramolecular through-space J coupling.[1] We recently reported the measurement of a through-space heteronuclear ^{31}P-^{77}Se J coupling in a novel P-Se heterocycle (compound **1**, shown in Figure 1a).[2] In this case, the through-space nature of the coupling is unambiguous as the interaction occurs between two distinct molecules. Density functional theory (DFT) calculations of the coupling deformation density (CDD) were used to demonstrate that the through-space ^{31}P-^{77}Se coupling in **1** is mediated by the P lone pairs. Here we report an additional, and perhaps surprising, intermolecular through-space coupling in **1**,[3] this time the coupling is homonuclear, between crystallographically-equivalent (*i.e.,* with the same isotropic chemical shift) ^{31}P.

Results

While investigating the heteronuclear ^{31}P-^{77}Se J couplings in **1**, the DFT calculations also predicted a 148 Hz homonuclear ^{31}P-^{31}P J coupling, again mediated by the P lone pairs as shown by the CDD plot in Figure 1b. No such coupling was able to be observed in the ^{31}P MAS NMR spectrum (shown in Figure 1c), owing to a linewidth of ~240 Hz. However, in principle, J couplings can also be measured from the modulation of a spin echo in a "J-resolved" experiment.[4] Figure 1d shows the isotropic centreband of a two-dimensional ^{31}P homonuclear J-resolved spectrum. The outer two signals correspond to magnetically-inequivalent ^{31}P species coupled with J = 84 Hz and the central resonance corresponds to pairs of magnetically-equivalent ^{31}P, where there is no modulation of the spin echo.

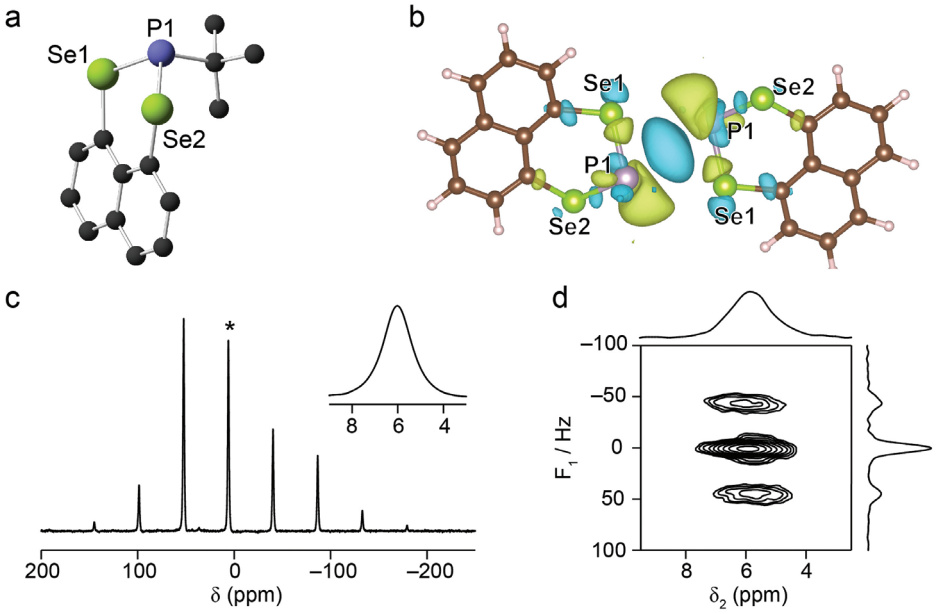

*Figure 1. (a) The crystal structure of compound **1**. (b) The CDD isosurface for the ^{31}P-^{31}P J coupling in **1**, computed from non-relativistic J-coupling calculations. (c) ^{31}P (9.4 T, 7.5 kHz MAS) NMR spectrum of **1**, with the inset showing the isotropic resonance (marked * in the main spectrum). (d) The isotropic centreband of the ^{31}P (20.0 T,10 kHz MAS) two-dimensional homonuclear J-resolved NMR spectrum of **1**.*

While the observed coupling is smaller than predicted by DFT, the interaction is temperature dependent (most likely owing to alkyl group motion), increasing by ~3 Hz per 25 K decrease in temperature, suggesting that, at 0 K, the value might be closer to that calculated (effectively for the 0 K structure).[3] However, it is perhaps even more surprising that a coupling is observed at all, given that the two coupled ^{31}P are crystallographically equivalent. It is well known that it is impossible to observe a J coupling between equivalent spins in solution and, similarly, one would expect to observe only the central (unmodulated) signal in the J-resolved spectrum. However, in the solid state, anisotropic interactions (*e.g.*, the CSA), will have the same magnitude and asymmetry for crystallographically-equivalent spins, but the interaction tensors may have different relative orientations, owing to the different physical orientation of the equivalent molecules with respect to B_0. In such cases, the anisotropic shifts would be different for each molecule, lifting any magnetic equivalence at any one instant during the rotor period, and a J coupling could then be measured.[4] However, although ^{31}P in **1** has a significant CSA, ($\Omega \approx 231$ ppm), the two coupled ^{31}P (and, therefore, their CSA tensors) are related *via* an inversion centre,[2] resulting in both crystallographic and magnetic equivalence. There is also no significant change in the J-resolved spectrum of **1** with varying magnetic field strength, which might be expected if an anisotropic interaction were responsible for lifting magnetic equivalence.[3,4]

Consideration of the larger spin system around the coupled ^{31}P, shown in Figure 2a, gives some indication of the origin of the magnetic inequivalence in **1**. Each P atom is bonded to two Se atoms (Se1 and Se2) and, at natural abundance, only 7.6% of these will be magnetically-active ^{77}Se, giving a ~27% chance that at least one Se in the two molecules will be ^{77}Se. In the presence of a ^{77}Se-containing isotopomer, the two ^{31}P will experience different J couplings to ^{77}Se, removing their magnetic equivalence. In order to determine whether this effect allows the observation of the homonuclear ^{31}P coupling in **1**, a second J-resolved experiment with rotor-synchronised Hahn-echo pulse train (RS-HEPT) decoupling[5] of ^{77}Se during t_1 was carried out. Figure 2b shows the comparison of the F_1 projections of the ^{31}P homonuclear J-resolved spectra of **1**, recorded without and with ^{77}Se decoupling, and it can be seen that removing the heteronuclear J coupling restores the magnetic equivalence, leaving only the unmodulated signal.

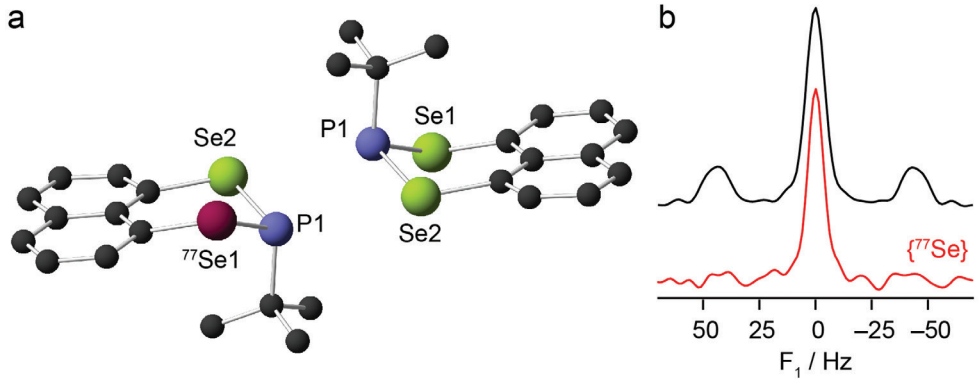

Figure 2. (a) Expansion of the structure of ***1****, with a possible ^{77}Se/^{31}P pair highlighted (see mauve labelled ^{77}Se). (b) F_1 projections of two-dimensional ^{31}P (14.1 T, 5 kHz MAS) homonuclear J-resolved NMR spectra of* ***1****, acquired with (red) and without (black) ^{77}Se decoupling.*

References

1. Kilian, P.; Knight, F. R.; Woollins, J. D. *Chem. Eur. J.* **2011**, *17*, 2302.
2. Sanz Camacho, P.; Athukorala Arachchige, K. S.; Slawin, A. M. Z.; Green, T. F. G.; Yates, J. R.; Dawson, D. M.; Woollins, J. D.; Ashbrook, S. E. *J. Am. Chem. Soc*. **2015**, *137*, 6172.
3. Sanz Camacho, P.; McKay, D.; Dawson, D. M.; Kirst, C.; Yates, J. R.; Green, T. F. G.; Cordes, D. B.; Slawin, A. M. Z.; Woollins, J. D.; Ashbrook, S. E. *Inorg*. *Chem.* **2016** (DOI 10.1021/acs.inorgchem.6b01121).
4. Duma, L.; Lai, W. C.; Carravetta, M.; Emsley, L.; Brown, S. P.; Levitt, M. H. *ChemPhysChem* **2004**, *5*, 815.
5. Griffin, J. M.; Tripon, C.; Samoson, A.; Filip, C.; Brown, S. P. *Magn. Reson. Chem.* **2007**, *S1*, 198.

Signal Improvement in MQMAS Spectra of Challenging ^{25}Mg Samples Using "FAM-N" Pulses

Henri Colaux, Daniel M. Dawson and Sharon E. Ashbrook

School of Chemistry, EaStCHEM and Centre of Magnetic Resonance, University of St Andrews

Overview

Over 75% of all NMR-active nuclei are quadrupolar (*i.e.*, with spin quantum number I > 1/2), yet their study is still more challenging than spin I = 1/2 nuclei, owing to the broadening of their resonances by the second-order quadrupolar interaction, which cannot be removed completely under magic-angle spinning (MAS). The introduction of the multiple-quantum (MQ) MAS technique[1] provided a convenient way to investigate quadrupolar nuclei through the separation of the components of the signal according to their respective quadrupolar coupling constants and isotropic chemical shifts. It has quickly become established as one of the most widely-used techniques to exploit the information provided by NMR spectroscopy of quadrupolar nuclei, and to explore local structure and disorder in solids. However, this method suffers from inherently poor sensitivity, which can lead to long acquisition times and restricts the materials able to be studied. We have recently developed an approach which uses computationally pre-optimised composite pulses, termed FAM-N, consisting of a succession of N oppositely-phased pulses, optimised independently using a program built on MatLab and SIMPSON.[2]

Natural-abundance ^{25}Mg MQMAS NMR of Forsterite

FAM-N has proven very efficient even on the most challenging samples, where experimental re-optimisation of the MQMAS pulses is difficult or impossible.[2] ^{25}Mg NMR of forsterite (α-Mg_2SiO_4) presents several difficulties, including a low gyromagnetic ratio (ν_0 = 52 MHz at B_0 = 20.0 T) and a low natural abundance (10%). Forsterite has two distinct ^{25}Mg sites that experience a strong quadrupolar interaction (C_Q = 4.3 MHz and η_Q = 0.4 for Mg 1 and C_Q = 5.0 MHz and η_Q = 0.9 for Mg 2).[3,4] Figure 1 shows a natural abundance ^{25}Mg MQMAS spectra of forsterite, acquired at 20.0 T, using a FAM-N conversion pulse with no experimental re-optimisation. In Figure 1a, the signal corresponding to Mg1 is clearly seen, but the sensitivity is not sufficient to observe the signal for Mg2 (expected between 30 and 40 ppm in δ_1). The sensitivity can be further improved by the use of a CPMG echo train[5] in acquisition, as shown in Figure 1b, where this signal starts to become apparent. From simulation it can be estimated that FAM-N is expected to give a signal improvement of ~2.2 (*i.e.*, a time saving of 11 days for the spectra in Figure 1).

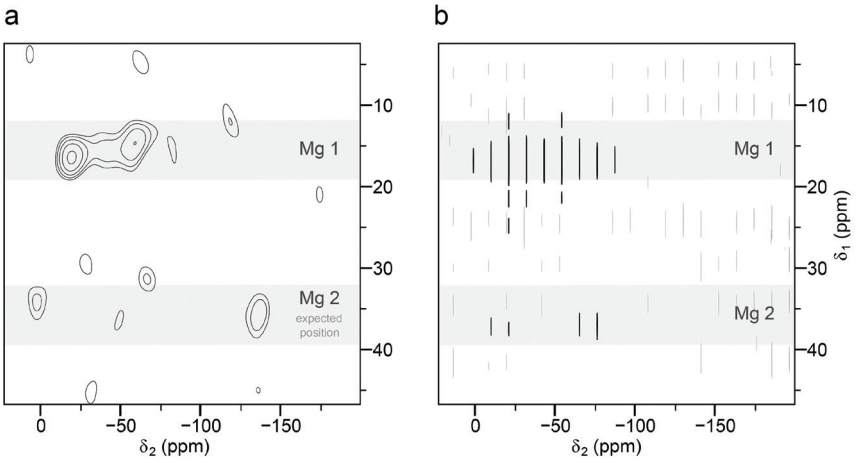

Figure 1. ^{25}Mg MQMAS spectra of forsterite (α-Mg_2SiO_4) acquired at 20.0 T using FAM-N conversion pulses. In (b), a CPMG echo train was also employed in acquisition.

References

1. Frydman, L.; Harwood, L. *J. Am. Chem. Soc.* **1995**, *117*, 5367.
2. Colaux, H.; Dawson, D. M.; Ashbrook, S. E. *J. Phys. Chem. A* **2014**, *118*, 6018.
3. Pallister, P. J.; Moudrakovski, I. L.; Ripmeester, J. A. *Phys. Chem. Chem. Phys.* **2009**, *11*, 11487.
4. Derighetti, B.; Hafner, S.; Marxer H.; Rager H. *Phys. Lett. A* **1978**, *66*, 150.
5. Larsen F. H.; Farnan, I. *J. Phys. Chem. B* **2004**, *108*, 9764.

Scientific excellence

Excellent Science (2015-2016) at the UK 850 MHz Solid-State NMR Facility

The UK 850 MHz Solid-State NMR Facility offers its users access to high magnetic field, as well as specialist equipment, including ultrafast magic angle spinning (MAS) and double rotation (DOR) probes. The instrumentation available provides substantial gains in both sensitivity and resolution, enabling NMR experiments on challenging isotopes with low receptivity or large quadrupolar couplings. The Facility supports a broad range of excellent science in the UK, from the development of novel NMR methods, through atomic-level studies of materials, pharmaceuticals and catalysts, to fundamental investigations of biological systems.

Materials

Materials research at the Facility aims to characterize disordered, heterogeneous or defect structures with technological applications as fast ion conductors, molecular sensors, catalysts or disposal systems for nuclear waste. Much of this involves measurements of quadrupolar nuclei with large quadrupole couplings, low magnetogyric ratio or low natural abundance, including ^{17}O, ^{25}Mg, ^{39}K, $^{63/65}$Cu and ^{71}Ga, which would not be feasible at lower magnetic fields. For example, during 2015 Blanc and co-workers studied Li defect chemistry in a distorted double perovskite using ^{6}Li and ^{17}O NMR combined with DFT calculations to reveal a previously unreported structure with Li ions located on two sites (pages 20-21). Ashbrook and co-workers investigated the coordination environment of CN ligands and the symmetry of Cu species using $^{63/65}$Cu NMR as part of structural studies of luminescent coordination polymers with molecular sensing applications (pages 16-17). Provis and co-workers used ^{25}Mg and ^{39}K NMR to study the immobilisation of Mg-rich Magnox sludge[1] and to assess new magnesium potassium phosphate cements.[2] Finally, in a geochemical study Ashbrook and co-workers used ^{25}Mg and ^{71}Ga NMR to study the coordination environment of Mg and trace amounts of Ga in high-pressure glasses which serve as models for natural silicate phases in magma (pages 18-19).

Case Study: Oxide Ion Conductivity in Sodium Strontium Silicate

The phase behaviour and high oxide ion conductivity of sodium strontium silicate manufactured using an unusual alkali metal substitution strategy have been controversial topics in the recent chemical literature (Singh, P.; Goodenough, J. B. *J. Am. Chem. Soc.* **2013**, *135*, 10149; Bayliss, R. D. *et al.*, *Energy Environ. Sci.* **2014**, *7*, 2999). Blanc and co-workers settled this controversy using a combination of ^{17}O and ^{23}Na NMR to explain the differences observed in previous studies and to demonstrate the absence of Na doping in $SrSiO_3$ and the presence of amorphous $Na_2O{\cdot}2SiO_2$ as the Na-containing phase (pages 22-23). The research was published in *Chemistry of Materials*.[3]

Crystallization and self assembly

The sensitivity gained at high field allows time-resolved measurements of dynamic processes, such as crystallization. For example, Harris and co-workers have developed an in-situ high-field NMR strategy for following the time evolution of crystallizing systems via a combination of solution- and solid-state NMR. This approach was recently presented at a Faraday Discussion on Nucleation[4] and during 2015 has been used to investigate mechanochemically generated polymorphs in co-crystals of α,ω-dihydroxyalkanes and urea (Zhou *et al.*, *Cryst. Growth Des.*, **2015**, *15*, 2901–2907), the role played by amorphous intermediates in two-step crystallization processes and the chemical processes that take place during cement hydration (pages 38-41). In related research (accepted for publication in *Nature Chemistry*) Carravetta and co-workers reported the preparation of the first closed-cage fullerene to encapsulate HF and recorded high-field solid-state ^{19}F MAS spectra at the Facility to investigate the dynamics of the HF molecule in the supramolecular complex (pages 28-29).

Case Study: Self Assembly in Guanosine Derivatives

The combination of high magnetic field and ultrafast sample spinning offers new possibilities for solid-state ^{1}H NMR studies of the intermolecular interactions which drive self assembly, such as hydrogen bonding and π-π interactions. During 2015 Brown and co-workers studied the ribbon-like self-assembly of guanosine-based derivatives in the solid state, as well as the incorporation of drugs into guanosine-quartet borate hydrogels (pages 24-25). Some of these results were published in *Crystal Growth and Design* in 2015.[5]

New NMR methodologies

The state-of-the-art instrumentation available at the Facility allows researchers to develop new NMR methods which take advantage of specialist hardware. For example, during 2015 Titman and co-workers designed new experiments for measuring ^{19}F chemical shift anisotropies (CSAs) with "ultrafast" MAS at rates up to 80 kHz.[6] A major focus of the new methods developed at the Facility involves acquisition of challenging isotopes with low receptivity and large quadrupolar broadening, often demonstrating the feasibility of such measurements for the first time. For example, Smith and co-workers developed new polarization transfer approaches to quadrupolar nuclei and applied these to ^{87}Sr measurements on model systems (pages 48-49). In related work Ashbrook and co-workers (page 56) invented new methods for signal enhancement in quadrupolar nuclei and demonstrated these on the low receptivity ^{25}Mg nucleus, studying a natural abundance sample of the mineral forsterite.

Case study: New NMR Methods for ^{14}N Signal Enhancement

Despite its high natural abundance and the ubiquity of nitrogen in materials, pharmaceuticals and biologcal systems, the utility of the spin-1 ^{14}N isotope in NMR studies is limited by its large quadrupolar interaction. One approach to ^{14}N NMR relies on the detection of the so-called overtone transition, a normally forbidden double-quantum transition, with direct detection at twice the Larmor frequency. Carravetta and co-workers have designed a novel MAS method for the transfer of polarization from ^{1}H to the ^{14}N overtone using symmetry-based recoupling sequences that overcome many of the limitations of previous adiabatic approaches used for static samples.[7]

Biomaterials

Understanding complex biological structures requires detailed information about the molecular assembly of the component materials. Solid-state NMR, especially at the high magnetic field available at the Facility, is proving a powerful technique for unravelling the molecular interactions which are essential to the biological function of, for example, bone or plant cell walls. Duer and co-workers (pages 32-33) have studied octacalcium phosphate ($Ca_8H_2(PO_4)_6.5H_2O$) as a model for the disordered interface between the thin ordered platelets in bone mineral. They characterized double hydrid salts of octacalcium phosphate with a range of organic acids by ^{43}Ca MAS, 3Q MAS and DOR using both natural abundance and ^{43}Ca-enriched samples, in order to gain a better understanding of pathological phases in bone mineral. This work is part of ongoing solid-state NMR research into bone mineralization which was recently summarized in the *Journal of Magnetic Resonance*.[8]

Case Study: Plant Cell Wall Recalcitrance

Dupree and co-workers (pages 34-35) have made use of the improved resolution obtained at high magnetic field to investigate cell wall architecture in never-dried mature stems from the model plant *Arabidopsis* grown in air containing ^{13}C-enriched CO_2. The aim of this study (recently published as a *Nature Communication*[9]) was to understand the molecular basis of plant cell wall recalcitrance which hinders the use of plant biomass for renewable energy by inhibiting the conversion of lignocellulose into fermentable sugars. Both wild-type *Arabidopsis* and cellulose-defective mutants were investigated using multi-dimensional ^{13}C NMR, and the plant enzymes required for cellulose synthesis were determined. This is significant because pilot biofuel production processes involve the use of energy-intensive pre-treatments and the addition of large amounts of enzymes.

Protein Structure and Dynamics

In addition to the above, and outside of the EPSRC remit, experiments at the Facility have been used to study the binding of amyloidosis inhibitors to amyloid fibrils (pages 14-17), the structure of proteins bound to F-actin (pages 46-47), and the isomerization of the retinal chromophore in the light-driven proton pump bacteriorhodopsin (pages 50-51). Finally, new NMR relaxation methods for studying the structure and dynamics of proteins have been developed at the Facility (pages 42-43) and recently published as an *Angewandte Chemie* Very Important Paper.[10]

References

1) Gardner, L. J.; Bernal, S. A.; Walling, S. A.; Corkhill, C. L.; Provis, J. L.; Hyatt, N. C., *Cement Concrete Res*. **2015**, *74*, 78–87.

2) Walling, S. A.; Kinoshita, H.; Bernal, S. A.; Collier, N. C.; Provis, J. L., *Dalton Trans.* **2015**, *44*, 8126–8137.

3) Inglis, K. K.; Corley, J. P.; Florian, P.; Cabana, J.; Bayliss, R. D.; Blanc, F., *Chem. Mater.* **2016**, *28*, 3850–3861.

4) Hughes, C. E.; Williams, P. A.; Keast, V. L.; Charalampopoulos, V. G.; Edwards-Gau, G. R.; Harris, K. D. M., *Faraday Discuss.* **2015**, *179*, 115–140.

5) Reddy G. N. M.; Marsh, A.; Davis, J. T.; Masiero, S.; Brown, S. P., *Cryst. Growth Des.* **2015**, *15*, 5945–5954.

6) Martini, F.; Miah, H. K.; Iuga, D.; Geppi, M.; Titman, J. J., *J. Magn. Reson.* **2015**, *259*, 102–107.

7) Haies, I. M.; Jarvis, J. A.; Bentley, H.; Heinmaa, I.; Kuprov, I.; Williamson, P. T. F.; Carravetta, M., *Phys. Chem. Chem. Phys.* **2015**, *17*, 6577–6587.

8) Duer, M. J., *J. Magn. Reson.* **2015**, *253*, 98–110.

9) Zhang, Y.; Nikolovski, N.; Sorieul, M.; Vellosillo, T.; McFarlane, H. E.; Dupree, R.; Kesten, C.; Schneider, R.; Driemeier, C.; Lathe, R.; Lampugnani, E.; Yu, X.; Ivakov, A.; Doblin, M. S.; Mortimer, J. C.; Brown, S. P.; Persson, S.; Dupree, P., *Nature Commun.* **2016**, *7*, 11656.

10) Lamley, J. M.; Öster, C.; Stevens, R. A.; Lewandowski, J. R., *Angew. Chem. Int. Ed. Engl.* **2015**, 54, 15374–15378.

Improvements

"The evaluation questionnaires speak to the high degree of satisfaction associated with the use of the Facility..."

The Facility continues to endeavour to provide the best possible experimental set-up so as to allow users to obtain very high quality data at the 850 MHz solid-state NMR spectrometer. For example, a recent improvement is the development of a protocol for inserting and spinning rotors at low temperatures (below –60° C), essential for biological samples initially activated at low temperature for which the temperature must be kept low to preserve the activated state. The evaluation questionnaires (see page 8) speak to the high degree of satisfaction associated with the use of the Facility – nevertheless, users are encouraged to make suggestions for improvements, either directly to the Facility Manager, or via the questionnaires.

As described in the user reports, new pulse programs continue to be implemented by the Facility Manager and/or by users, notably a Repetitive Double Frequency Sweep (RDFS) for enhancing the signal of half-integer quadrupolar nuclei, which gave a signal enhancement of ~5 for e.g. ^{17}O and ^{43}Ca, and interleaved acquisition for relaxation time measurements.

For the operation of the Facility as an EPSRC-funded (with partial support from BBSRC) mid-range facility under contract funding from January 2015, there have been changes to the management structure, notably the creation of an Oversight Committee whose membership comprises the three members of the external advisory board, two user representatives (at least one of whom is an early career researcher) as well as the director and deputy director who represent the Facility Executive (previously called the National Management Committee under grant funding). The Oversight Committee is chaired by a NMR spectroscopist working in UK industry, Dr Stephen Byard from Arcinova.

In years four and five of contract funding (2018-2019), direct funding via the contract will only be provided at 80% of cost, with the remaining 20% to come from academic users requesting funding on grants (from RCUK and other agencies) as well as paid-for industrial access. To facilitate the former, a form has been created on the Facility website whereby, prior to submitting an application, users provide basic information (number of days requested in which time-allocation periods, type of experiment(s) to be carried out and probe(s) to be used). When a user follows this procedure and secures funding (at the daily rate of £941 +VAT), time will be allocated independent of the time allocation procedure (this will continue to run for the remaining available days).

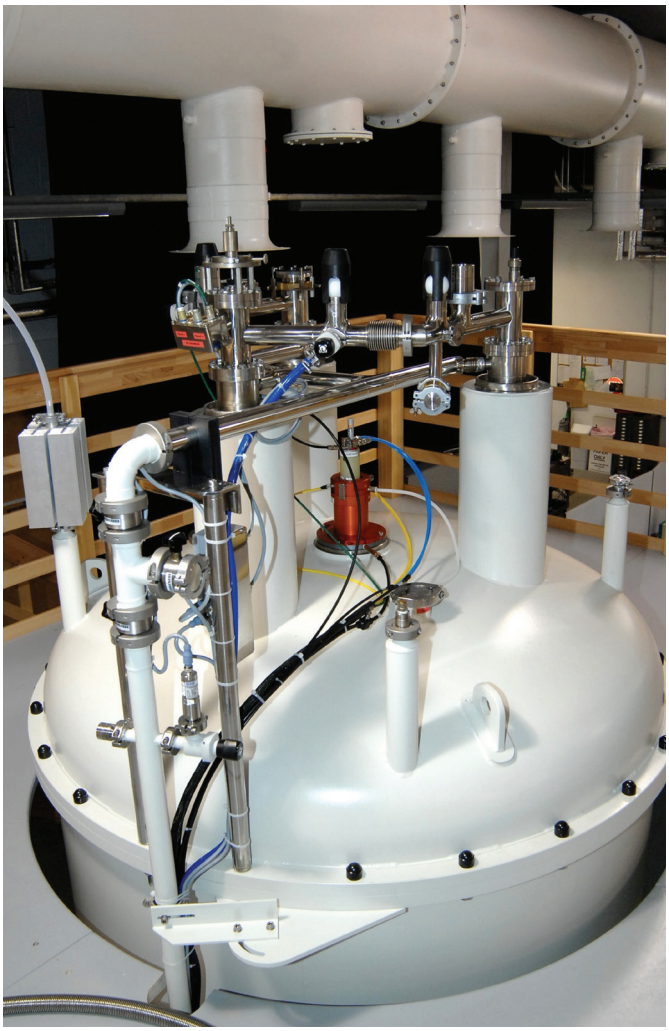

The new three plus two years funding also included provision for hardware purchases, notably new magic-angle spinning probes. Following a tender process, two 4 mm MAS probes are on order; one which will enable data to be acquired at up to 300° C compared with an achievable 180° C at present, the other optimised for low-gamma nuclei, a popular area for study using the Facility. The Facility Executive also hopes to place an order soon for a state-of-the-art 100+ kHz MAS probe, with discussions with vendors ongoing.

Impact

Broader Impact of the UK 850 MHz Solid-State NMR Facility on the Research Landscape in the UK.

Since starting operation in February 2010, the UK 850 MHz Solid-State NMR Facility has hosted research projects from more than 48 Principal Investigators originating from 23 UK institutions. One anonymous EPSRC reviewer on the recent 2014 funding extension noted that the Facility "has now become an essential part of the NMR landscape in the UK."

Despite providing a platform for the NMR community, the use of the Facility is not limited to the NMR community within the UK. Increasingly, PIs from a broad spectrum of disciplines including the materials and biological sciences community are frequently non-NMR specialists; this is strong evidence for the wider impact of both the Facility and NMR more generally on the scientific community within the UK. Examples from 2015 include the groups of Darton (Keele), Dupree (Cambridge), Gibson (Aberdeen), and Morris and Woollins (St Andrews) – see the Scientific Excellence section.

The broad spectrum of research now supported by the Facility is beginning to address some of the major challenges faced by society. In the biological sciences, the group of Antzutkin has used the 850 MHz Facility to study the binding of possible inhibitors of amyloid fibril formation to model proteins related to Alzheimer's disease. The Facility is also contributing to the development of new biofuels, supporting research by Dupree and co-workers who are investigating the development of plant cell walls (see, for example, **http://www.isaaa.org/kc/cropbiotechupdate/article/default.asp?ID=14488**). Wimperis, Halling and co-workers are using the Facility to study structure and function in heterogeneous biocatalysts, which are widely used in the pharmaceutical, food and biofuel industries. In materials science, the group of Harris are studying the curing of cement at the 850 MHz Facility.

"The broad spectrum of research now supported by the Facility is beginning to address some of the major challenges faced by society."

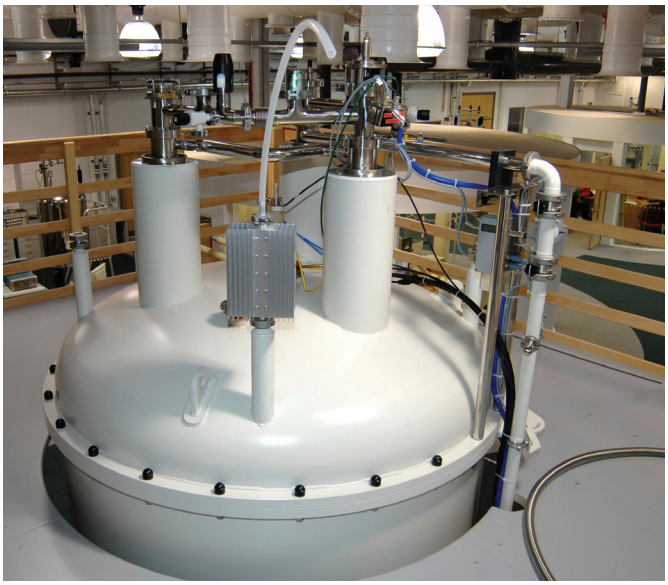

The Facility plays a major role in the training of PhD students from NMR research groups across the UK. A total of 19 visited the Facility during 2015, gaining valuable experience in the use of specialist equipment (some not available elsewhere in the UK) such as the ultrafast-MAS probes (1.0- and 1.3-mm rotor diameter) and the double-rotation (DOR) probe, as well as the general protocols involved in working at an away-from-home laboratory.

The 5th Annual Symposium was held in March 2015 and attracted more than 60 attendees from academia and industry. This meeting has become a fixture in the UK solid-state NMR calendar, providing a showcase for the best research to come out of the Facility and a forum for discussions about the future direction of NMR in the UK. Indeed, the role of this meeting in creating a community "feel" for the UK's solid-state NMR spectroscopists cannot be overstated.

Strategic fit

"As a solid-state NMR Facility, it stands comparison with other leading facilities throughout the World..."

The current strategic landscape in engineering and physical sciences (EPS) continues to reflect the objectives enunciated in EPSRC's shaping capability exercise. The key points made in last year's report still apply such that the 850 MHz Solid-State NMR Facility can readily demonstrate how it plays to key parts of the shaping capability strategy, namely of quality, importance and capacity. The underpinning quality of any work has to be of really top rank international standing. Much of physical science is underpinned by the quality of the infrastructure available; for a technique such as NMR, that plays a characterisation role, this is of primary importance to the health of a wide range of its sub-disciplines. For techniques such as this to be most effective, the community needs to have access to genuinely leading-edge instrumentation backed up by a first class environment that includes academic and technical expertise. The 850 MHz Facility demonstrably fulfils this role providing unique capability for solid-state NMR within the UK, both in the strength of the magnetic field, as well as the range of probes and experiments that the Facility can provide. As a solid-state NMR Facility, it stands comparison with other leading facilities throughout the world, hence clearly playing into this element of the EPS strategy. There is a question of how sustainable the position of having only one such high field instrument can continue to be and allow the UK to remain internationally leading in solid-state NMR. There is no doubt as to the importance to the user community and hence the user need, being readily demonstrated by the consistent significant oversubscription rate for time requested on the spectrometer. The quality of the research that has been carried out is indicated by the quality of the publications that have been produced, which has also been highlighted in the report from the Oversight Committee that includes the independent International Advisory Board.

In the context of the eight great technologies areas, commercial and wider societal challenges have been highlighted: research carried out at the Facility has played into at least four of these eight, namely energy storage, advanced materials, regenerative medicine and synthetic biology. Looking at a more fine grained level with the research fields identified in the EPSRC portfolio, several of the areas designated as 'grow', such as catalysis, require NMR as a key characterisation approach. Investigations using the 850 MHz Facility to tackle societal challenges have included a similar range of materials-based challenges such as biomaterials for bone replacement, novel battery materials and pharmaceutical products, which underpin some key areas of several high priority challenges. Industrial links continue through joint projects including CASE awards as well as the first directly industrially-funded work for a UK pharmaceutical company. EPSRC's refreshed strategy in 2014 identified the importance of providing the vital foundations that stimulate further investigation in bioscience, medicine and environmental sciences; several of the NMR approaches developed using the Facility play directly into this role.

Beyond the core scientific elements of the EPSRC strategy, other areas identified include reforming the provision of equipment with a national prioritisation of needs. Operation of the 850 MHz Facility commenced prior to these concepts becoming fully developed. However, the subsequent detailed consultation and prioritisation exercise around NMR in 2013 very clearly identified the 'pyramidal' model of access to NMR for the physical sciences community. The 850 MHz instrument remains at the apex of national infrastructure and is run very much as a shared capital item, 365/24/7. This approach and philosophy has found more resonance as work on the equipment sharing agenda has gathered pace over the last few years, in particular as new approaches have been developed for capital investment and equipment sharing following the 2010 comprehensive spending review. With the need for increased efficiency becoming ever more important, especially as capital funding becomes squeezed, asset sharing especially of high value capital investments is essential; the 850 MHz spectrometer plays strongly into this agenda. The time allocation mechanism and the highly skilled and experienced Facility Manager have added to the efficient use of the Facility. Under the new contract, the Facility has committed to investigating its sustainability, particularly of the recurrent funding, through targeting a mixture of funding streams, notably for years four and five. In the spirit of equipment sharing, the contribution to the costs by BBSRC is a good example of cross Research Council sharing of assets. The learning in developing the 850 MHz Facility should provide a basis for future cross-Council thinking in developing the 1.2 GHz Facility announced in the Capital Investment Roadmap in December 2014, noting the further publishing in March 2015 by the UK NMR community of "A UK-wide cross-disciplinary integrated infrastructure for NMR spectroscopy".

Crystallized ^{13}C,^{15}N labeled MLF peptide for solid state NMR method development

- ✓ Crystalline form.
- ✓ Outstanding SNR and resolution.
- ✓ Highly favorable relaxation times.

N-formyl-methionyl-leucyl-phenylalanine (fMLF) is a formylated tripeptide produced by certain types of bacteria. Also known as the chemotactic bacterial peptide, the fMLF peptide is a strong leukocyte chemoattractant which interacts with the human N-formyl peptide receptor (FPR) and the N-formyl peptide receptor-1 (FPRL1). fMLF peptide is a well-characterized peptide which has been widely used to develop solid state NMR methods.

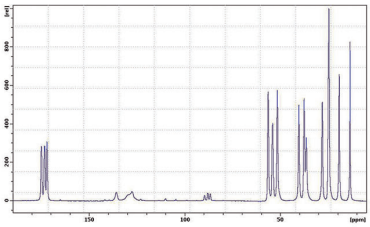

^{1}H-^{13}C CP NMR spectrum of ^{13}C, ^{15}N labeled fMLF. Experience recorded at 700 MHz (^{1}H), T= 265 K, MAS= 15 kHz.

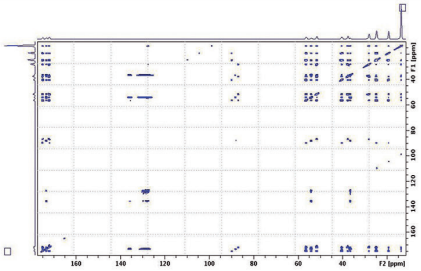

Shanghai NMR spectrum of ^{13}C, ^{15}N labeled fMLF. Experience recorded at 700 MHz (^{1}H), T= 265 K, MAS= 15 kHz, mixing time: 50 ms.

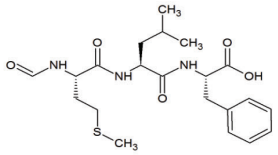

Since 20 years, CortecNet is known as one of the most reliable supplier of NMR consumables and stable isotope enriched products. CortecNet is composed of a team of analytical engineers capable to understand and fulfill all your needs. Over the years, CortecNet has developed a strong professional network including thousands of academic labs and industrial companies all around the world.

CortecNet S.A.S
15/17, rue des Tilleuls
78960 Voisins-Le-Bretonneux, France
Tél : 33 (0)1 30 12 11 31 - 33 (0)1 30 43 86 54
Email : pcorcos@cortecnet.com
www.cortecnet.com

cortecnet
INNOVATION ACCELERATOR IN LIFE SCIENCE

CortecNet Corp.
160 Parkside Avenue
Brooklyn, NY, 11226, USA
Tel: (347) 404-6810 - Fax: (415) 230-5796
Email : pcorcos@cortecnet.com
www.cortecnet.com/us

JEOL

NMR Spectrometer ZETA

JNM-ECZS Series - Next Generation NMR Spectrometer

- ***STS (Smart Transceiver System)***
  High performance in a compact size using digital circuit technology and the latest high frequency technology
- ***High stability measurements from lock feedback circuitry***
  Providing digital control of the interlock between lock frequency and the shim controller
- ***High order shim control yields high magnetic field homogeneity***
- ***Enhanced S/N without the helium - new nitrogen SuperCool cryogenic probe™***
- ***Highly stable temperature control system***
  Rapid and stable operation of attachments
- ***Improved functionality and unique design***
  Designed for ease of use with improved spectrometer functionality
- ***Compact design, high performance NMR spectrometer***

www.jeol.com

CPMAS at 111 kHz
New Applications and New Horizons

111 kHz CPMAS 0.7 mm Probe

During the last year magic angle spinning at very high spinning rates (> 100 kHz) opened new possibilities and application fields in solid-state NMR, notably enabling the study of fully protonated systems in very small quantities with ^{1}H detection. Following the first determinations on microcrystalline model samples, the capabilities of very fast MAS rates have been demonstrated on a number of systems of increasing complexity and variable aggregation states, from sedimented nucleocapsids to membrane proteins.

In addition to applications in biological systems, studies of systems with highly anisotropic features (e.g. paramagnetic environments) can benefit dramatically if studied using very fast MAS rates.

Applications and Results

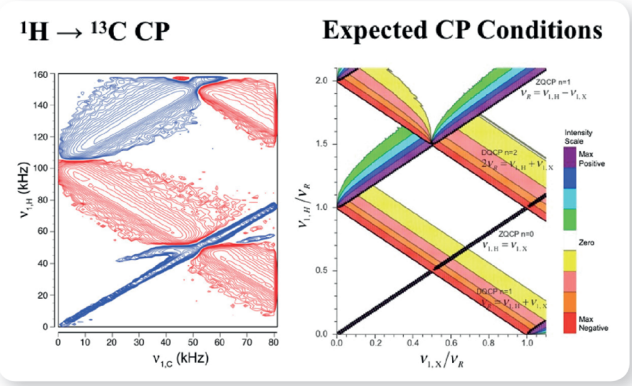

Fig. 1 CP ^{13}C-^{1}H matching conditions under ultra fast MAS. The theoretical expected ZQ and DQ transfers can nicely be seen in the experimental data. Data courtesy of Guido Pintacuda, ENS Lyon.

Ultra fast MAS rates at approximately 100 kHz enable new matching regimes for CP Hartman-Hahn conditions. Here the "traditional" Zero-Quantum (ZQ) CP-transfer is no longer the only and main CP-transfer; the Double-Quantum (DQ) CP-transfer becomes equally efficient and important. Figure 1 shows a theoretical matching profile for both CP-conditions side by side with experimental data. This demonstrates how the different ZQ/DQ conditions evolve and how important it is to avoid regimes where both transfer types overlap, since in these regions the efficiency is dramatically reduced.

Biological Systems

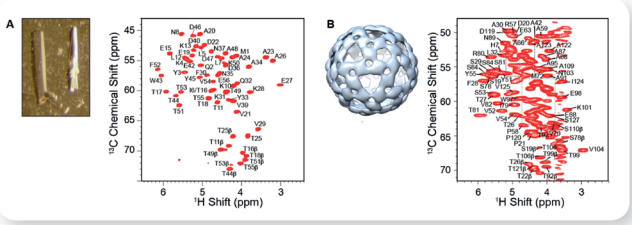

Fig. 2 ^{1}H detected proton-carbon correlation spectra for different types of biological systems studied without the need of deuteration.[1] The left side shows a Cα-Hα dipolar correlation of microcrystalline GB1, while the right picture shows the same correlation acquired on a sedimented icosahedral nucleocapsid. Data courtesy of Guido Pintacuda, ENS Lyon.

Figure 2 shows a recent example using ultra fast MAS rates for investigating complex biological systems. At >100 kHz MAS, sensitive and resolved ^{1}H-detecetd correlations can be acquired, without the need of any deuteration, on fully-protonated systems, from microcrystalline models (e.g. GB1) to more heterogeneous targets (e.g. sedimented nucleocapsids). These correlations open the way to fast backbone and side-chain resonance assignment, and allow expedite measurement of inter-proton distances for structure calculations.

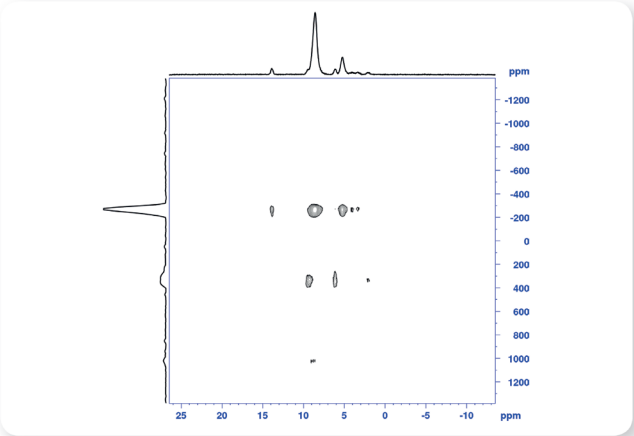

Fig. 3 Inverse detected ^{1}H^{14}N correlation as an HMQC type experiment.[2] You can see correlation peaks from various protons to ^{14}N. This can help to elucidate e.g. pharmaceutical compounds. Data recorded in collaboration with Dinu Iuga, Facility Manager at the UK 850 MHz Solid-State NMR Facility at the University of Warwick.

Figure 3 shows another example where solid-state NMR benefits from ultra fast MAS in combination with very strong excitation fields.

Here a proton detected HMQC type ^{1}H-^{14}N correlation spectrum shows the structure connectivity in a dipeptide sample without the need of ^{15}N enrichment.

^{14}N is especially challenging, since it has a fairly high quadrupolar moment and is a low gamma nucleus. These features tend to prohibit efficient solid-state NMR experiments involving ^{14}N due to sensitivity and low available RF-fields. Here the small diameter combined with very fast rotation enables the detection of highly resolved NMR spectra, even under these difficult conditions.

Acknowledgements

We thank Guido Pintacuda (ENS Lyon) and his group and also Dinu Iuga (High Field Laboratory Warwick) for sharing their inspiring ideas, spectra and figures.

1. Pintacuda et al .., submitted
2. Andrew S. Tatton et al. Probing intermolecular interactions and nitrogen protonation in pharmaceuticals by novel ^{15}N edited and 2D ^{14}N-^{1}H solid state NMR, CrystEngComm (2012) DOI 10.1039/c2ce06547a

Summary

- 111 kHz probe brings new applications and insights into the field of solid-state NMR.
- MAS rates >100 kHz can give detailed insights even in complex samples.
- New handling tools provide straightforward sample packing.

Design by Mustard: www.mustardhot.com

Advantage West Midlands
www.advantagewm.co.uk

BBSRC
bioscience for the future

EPSRC
Engineering and Physical Sciences Research Council

investing in your future
European Regional Development Fund
European Union

Dr Dinu Iuga (Facility Manager)
Department of Physics
University of Warwick
Coventry CV4 7AL

T +44 (0) 24 761 50814
F +44 (0) 24 761 50897
E D.Iuga@warwick.ac.uk
W http://go.warwick.ac.uk/850mhz/

UNIVERSITY OF CAMBRIDGE

Lancaster University

The University of Nottingham
UNITED KINGDOM · CHINA · MALAYSIA

UNIVERSITY OF Southampton

University of St Andrews

WARWICK